SLOW INACTIVATION OF SODIUM CHANNELS: STRUCTURAL CLUES AND

DISEASE ASSOCIATIONS

APPROVED BY SUPERVISORY COMMITTEE

Steve Cannon, M.D., Ph.D.

Ilya Bezprozvanny, Ph.D.

Paul Blount, Ph.D.

Rolf Joho, Ph.D.

DEDICATION

SLOW INACTIVATION OF SODIUM CHANNELS: STRUCTURAL CLUES AND

DISEASE ASSOCIATIONS

by

JADON RAY WEBB

DISSERTATION

Presented to the Faculty of the Division of Basic Science

The University of Texas Southwestern Medical Center at Dallas

In Partial Fulfillment of the Requirements

For the Degree of

DOCTOR OF PHILOSOPHY

The University of Texas Southwestern Medical Center at Dallas

Dallas, Texas

June, 2007

SLOW INACTIVATION OF SODIUM CHANNELS: STRUCTURAL CLUES AND

DISEASE ASSOCIATIONS

JADON RAY WEBB, Ph.D.

The University of Texas Southwestern Medical Center at Dallas, 2007

STEVE CANNON, M.D./Ph.D.

ABSTRACT

Voltage gated sodium channels underlie the rapid upstroke of action potentials in electrically excitable mammalian tissues. A cardinal feature of Na^+ channels is their ability to rapidly inactivate to a refractory state during membrane depolarization, in a process known as 'fast inactivation'. During sustained membrane depolarization or prolonged busts of discharges, channels can further inactivate to non-conducting states collectively referred to as 'slow inactivation'.

Fast inactivation occurs by occlusion of the inner pore by the intracellular III-IV Loop, and defects in fast inactivation gating are known to underlie certain forms of myotonia, periodic paralysis, epilepsy, and cardiac arrhythmias. The mechanism of slow inactivation and its relevance to human disease, on the other hand, are much less understood. The primary aim of this thesis was to characterize the mechanism of sodium channel slow inactivation, and also to further define its role in disease.

In Chapter 1, an overview of sodium channel structure and gating is provided as background for understanding the rational and interpretation of the experimental studies.

The experiments in Chapter 2 characterized the gating of a sodium channel mutation (P1158S) associated with temperature-sensitive periodic paralysis. This disease mutation caused a robust defect in slow inactivation, in accordance with an emerging model that associates defective slow inactivation with increased susceptibility to paralytic attacks. Additionally, the slow inactivation gating defects were elicited by cold temperature, analogous to the temperature-dependent provocation of paralysis. This finding further strengthens the association between defective slow inactivation gating and a specific disease phenotype.

Chapter 3 explores the interaction of the sodium channel β1 subunit and slow inactivation, which is incompletely characterized especially in mammalian

cell expression systems. I found that co-expression of wild-type β1 significantly depolarized the voltage-dependence of steady-state slow inactivation and also reduced the number of channels occupying the slow state (I_S) after a long depolarizing conditioning pulse, but did not affect the kinetics of slow inactivation.. To understand which region(s) of β1 are important for modulation of slow inactivation, two mutant constructs were tested. A point mutation in the extracellular N-terminus associated with epilepsy (C121W) disrupts a critical disulfide bond in an Ig-like fold and abolished the ability of β1 to modulate slow inactivation. Conversely, truncation of the short cytoplasmic C-terminus did not alter the effects of β1 on slow inactivation. These observations parallel the structure-function relations that have been established for β1 modulation of fast inactivation. Interestingly, however, I used a mutant fast-inactivation deficient α subunit to show that the β1 effect on slow inactivation was independent of coupling to fast inactivation.

In Chapter 4, the interaction of slow inactivation and alkali metal cations is explored. External cations have been shown to influence slow inactivation, but little is known about the location and mechanism of this interaction. To address this, I examined the interaction of Group IA alkali metal cations with slow inactivation in rat Nav1.4 channels expressed in HEK293t cells. Slow inactivation was significantly impeded by external, but not internal Na^+ and Li^+

cations in the buffer solutions. External K^+, Rb^+, and Cs^+, on the other hand, caused little effect compared to sucrose (cation-free) buffer. Cation effects on slow inactivation were found to be very low affinity and were not dependent on the ability of cations to permeate deep into the channel. Indeed, Na^+ interaction occurred at a shallow apparent electrical distance (δ) of 0.15 relative to the outside of the channel, and was affected by mutagenesis in the outer pore. Overall, these results suggest that external cations impede slow inactivation at a highly selective interaction site located in the external entrance of the pore region, external to the channel selectivity filter.

Finally, in Chapter 6, the results of these experiments are summarized, and future directions are proposed.

TABLE OF CONTENTS

PRIOR PUBLICATIONS

Braha O, Webb J, Gu LQ, Kim K, Bayley H. Carriers versus adapters in stochastic

sensing. *Chemphyschem*. 2005 May;6(5):889-92.

List of figures

LIST OF TABLES

LIST OF DEFINITIONS

Nav – voltage-gated sodium channel

SI – Slow inactivation

FI – Fast inactivation

I_M – Intermediate Inactivation

I_S – Slow Inactivation

I_{US} – Ultraslow Inactivation

msec – millisecond

s – second

Nav1.4 – skeletal muscle sodium channel isoform

Nav1.5 – heart muscle sodium channel isoform

CHAPTER 1.   INTRODUCTION

1.1   Sodium channel overview

Voltage-gated sodium channels are heteromeric integral membrane protein complexes that underlie the rapid upstroke of the action potential in electrically excitable mammalian tissues [1]. In quiescent cells Na^+ channels are closed and do not contribute substantially toward setting the resting potential. The activation of Na^+ channels is steeply voltage dependent, and in response to modest depolarization channels rapidly open in a fraction of a millisecond. The inward flow of Na^+ ions through these channels further drives membrane depolarization but is self-limiting, because sodium channels inactivate at depolarized potentials and will not be available to open until reset by membrane hyperpolarization, in a process termed recovery from inactivation.

The inactivation of Na^+ channels is a major feature of their intrinsic biophysical behavior and is a major determinant of cellular excitability. Inactivation is more than an all-or-none loss of availability and has many complex features that have been conceptualized as multiple inactivated states. The rapid inactivation that was observed as current decay in the first voltage-clamp recordings of Na^+ currents [2] limits the maximal firing rate due to the time required for recovery (1 – 5 msec), and is termed fast inactivation [3].

After prolonged depolarization lasting seconds to minutes or following a long burst of high-frequency discharges, Na^+ channels can also become "slow inactivated", as defined

experimentally by the similarly long periods of time (hundreds of msec to tens of seconds) required for channels to recover [4]. In fact, the time course of such recovery may show multiple exponential components, which has led to the notion that there are multiple slow-inactivated states [4-6]. The physiological importance of slow inactivation has recently been highlighted by the discovery that impaired slow inactivation increases the susceptibility to depolarization-induced attacks of periodic paralysis [7]. Slow inactivation is a universal property shared by all voltage-gated Na^+ channels, and yet in comparison to other aspects of Na^+ channel gating relatively little is known about its underlying molecular mechanism. For example, the mechanism of fast inactivation is generally accepted to arise from occlusion of the inner mouth of the channel by the intracellular III-IV Loop, in a "hinged-lid" mechanism [8]. The mechanism of slow inactivation, on the other hand, appears to be much more complicated and is far less understood. This thesis is directed at characterizing the attributes of slow inactivation, in an effort to gain insight into the mechanism.

This introductory chapter provides a summary of Na^+ channel gating behavior and reviews the current concepts on the mechanisms that may underlie these changes in the ability of ions to permeate the pore of the channel. The focus will be on slow inactivation, as this background will lay the foundation for understanding the experiments conducted in Chapters 2 through 4.

1.2 *Kinetics of sodium channel gating*

The availability of the ion conducting pore to allow passage of cations through the sodium channel is governed by three voltage-dependent gating events: (1) activation, which rapidly opens the channels in response to membrane depolarization; (2) fast inactivation, which causes the rapid termination of ion flow during depolarization; and (3) slow inactivation, which causes a more sustained termination of ion flow after periods of prolonged depolarization.

Upon membrane depolarization, sodium channels open within a fraction of a millisecond to a highly conductive state, and are said to become 'activated'. The underlying changes in the sodium channel that lead to this activated state are one of the most intensely studied features of sodium channels, and kinetic models to describe this process are now fairly well established. Early work by Hodgkin and Huxley [9] found that upon depolarization, the increase in channel conductance over time showed a small initial time delay followed by a sigmoidal rise to full conductance within hundreds of microseconds. This delayed opening and sigmoidal rise in conductance implies that the pathway from a resting to open channel is a multi-step process. A reasonably accurate approximation of this initial opening behavior can be achieved by viewing channel activation as a sequential transition through three independent closed states before the channel finally opens [9].

While channels activate in response to membrane depolarization, they also simultaneously start to enter into a non-conducting state (fast inactivation) that develops

with a single exponential time constant on the order of milliseconds. An example trace of sodium current in voltage clamp is shown in Figure 1.1, which illustrates the lack of current in the closed (C) state, rapid activation to a peak current, and the decline and loss of current as channels partition into the fast inactivated (I) state. Rapid entry into the fast inactivated state accounts for the short, self-limiting nature of current flux through Na^+ channels during a membrane depolarization event such as an action potential. Channels that enter into this fast inactivated state are no longer immediately available to return to the closed and ready state upon repolarization, but must first recover from this refractory state for several milliseconds at hyperpolarized membrane potentials.
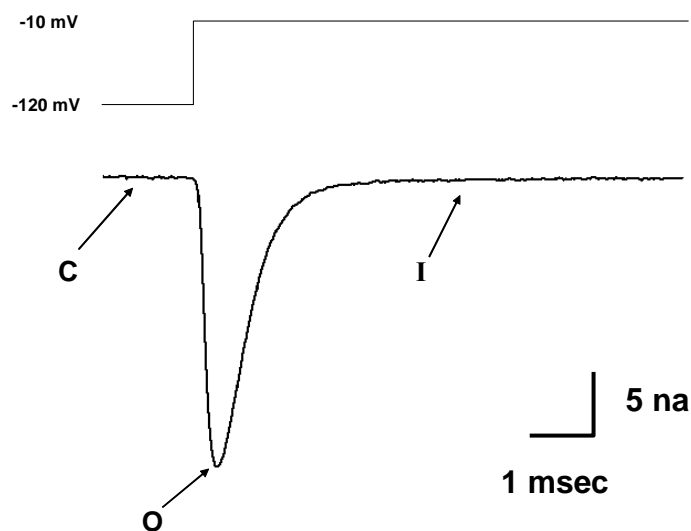
Figure 1.1 Example sodium current trace, showing channels initially in the closed, non-conducting state (C) while held at a hyperpolarized (-120 mV) potential. Upon membrane depolarization to -10 mV, channels rapidly transit into the open (O) or activated state through which current can pass. With continued depolarization, peak current declines as channels enter into the non-conducting fast inactivated state (I) from which no further current can be elicited.

Fast inactivation is voltage dependent, and channels partition into the fast inactivated state in response to membrane voltage as predicted by a Boltzmann function. The voltage at which half of the channels are fast inactivated is at approximately –50 mV in neurons, and is more hyperpolarized in skeletal muscle (–65 mV). Notably, fast inactivation can occur at considerably more hyperpolarized potentials than channel activation (which typically tends to occur above –40mV), implying that channels can fast inactivate either from the closed (resting) or open (activated) states. In other words, channels do not have to open first before they can inactivate.

In practice, activation and fast inactivation are sometimes treated as independent, Markovian events [9], but a variety of experiments suggest some degree of coupling between the two states. For instance, fast inactivation does not appear to possess sufficient gating charge by itself to account for its steep voltage sensitivity [10]. Instead, it is thought that fast inactivation derives at least some of its voltage-dependence from activation since changes to the activation-associated S4 voltage sensors can profoundly influence the voltage-dependent behavior of fast inactivation. Conversely, fast inactivation is known to immobilize the activation S4 voltage sensors, further indicating interaction between the two gating events.

In addition to fast inactivation, during periods of prolonged membrane depolarization channels can also enter into other long-lived non-conducting states collectively termed 'slow inactivation'. Because fast and slow inactivation are both non-conducting states, special experimental protocols are needed to measure slow inactivation in the background of functioning fast inactivation. The section below provides a brief

overview of how slow inactivation can be observed experimentally, followed by further discussion of the kinetics of slow inactivation gating.

1.3 Experimental Measurement of Slow Inactivation

Upon sustained membrane depolarization, fast inactivation causes the initial rapid and complete termination of ionic current, which obscures observation of the development of any additional slower non-conducting states. The time courses of recovery from fast and slow inactivation are very different, however, and this fact is routinely exploited in experimental pulse protocols to separate the two states. An example of the extreme difference in recovery behavior between fast and slow inactivation is shown by the whole cell recordings of Na^+ currents from human Nav1.4 channels (skeletal muscle isoform) expressed in HEK cells in Figure 1.2 A (below, next page). Current recovery after a short (30 msec) conditioning pulse is very rapid, indicating that channels exclusively populated the fast inactivated state. In Figure 1.2 B, the same cell was subjected to a conditioning pulse for a much longer period of time (30,000 msec), and current now recovers with a much slower time constant, indicative of recovery from slow inactivation. Note that in Figure 1.2 B channels also recovered from fast inactivation as in 1.2 A, but observation of this fast recovery was masked by the presence of slow inactivation, which is also a non-conducting state. Intermediate length conditioning pulses in which only part of the channels are able to slow inactivate would

show bi-exponential recovery, reflecting recovery from both the fast and slow states (see Figure 1.3).

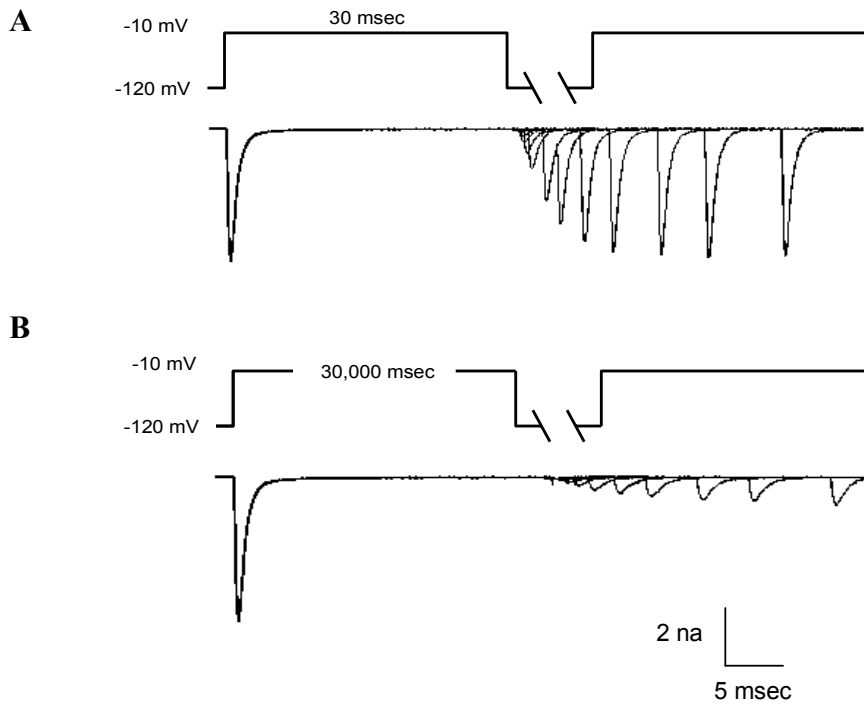**Figure 1.2   Recovery of sodium current after short and long depolarizing pre-pulses. Recovery after a 30msec pre-pulse (A) is rapid with a τ recovery of several milliseconds, indicative of recovery from fast inactivation.   Recovery after a much longer 30,000 msec pre-pulse (B) is much slower, on the order of hundreds of milliseconds.   This suggests substantial entry to slow inactivation.**
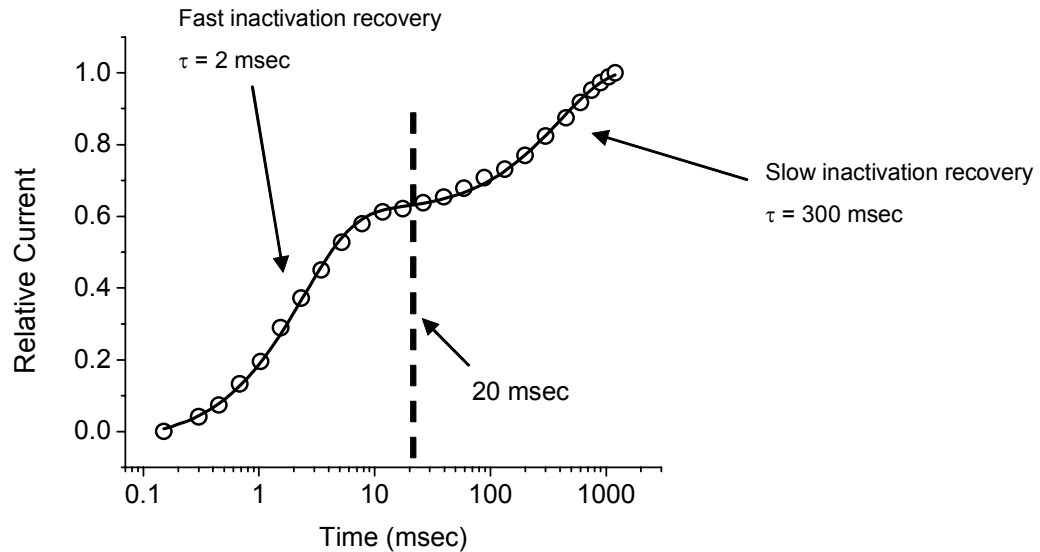
Figure 1.3 Example graph of recovery of sodium current at -120 mV, illustrating the very distinct recovery time constants of fast and slow inactivation. Typical pulse protocols that measure slow inactivation apply a 20 msec (dotted line) recovery gap immediately after the depolarizing conditioning pre-pulse. As seen in the figure, this 20 msec gap allows nearly complete recovery from fast inactivation, while largely preserving slow inactivation. A test pulse applied after this 20 msec gap, then, will accurately estimate the amount of current reduction caused by slow inactivation.

Figure 1.3 shows an example of the bi-exponential recovery from channels that are completely fast inactivated, and partly slow inactivated. To obtain this kind of data, a depolarizing conditioning pulse is applied for several seconds to shift channels into fast and slow inactivated states. Each data point represents the peak Na$^+$ current elicited by a test pulse to -10 mV after variable time of recovery at -120 mV. These current levels are plotted as the relative current in relationship to a control response measured by response observed in the absence of a preceding conditioning pulse. Two recovery time courses are readily apparent, representing recovery from fast and slow inactivation. The two components are well separated, which allows an unambiguous bi-exponential fit to

extract the time constants and relative amplitudes of both components of recovery. In this example, ~45% of channels recover with a time course slower than 20 msec, which represents the fraction of channels in the slow inactivated state (~45% in Figure 1.5). This figure highlights the basis for using a temporal cut-off to distinguish the fraction of channels that were slow inactivated. The first component of recovery at –120 mV is complete by 20 msec and reflects the fraction of channels that were not slow inactivated. In practice, the degree of slow inactivation is defined as the fraction of channels that fail to recover within a 20 msec recovery interval at –120 mV. This basic assay is applied in a wide variety of voltage protocols in which the conditioning pulse is varied to examine the voltage and time-dependence of slow inactivation. The other commonly used slow inactivation protocol is to vary the duration (or voltage) of the recovery gap between the conditioning and test pulses in order to measure the full time course of recovery. This latter measure provides a more detailed view of the inactivated status of the channels and is the basis for concluding that there is more than one slow inactivated state

1.4 Kinetics of Slow Inactivation

The rate of entry to slow inactivation is well approximated by a monoexponential time course. Recovery, however, usually shows multiple kinetic components as seen in Fig 1.4. Another striking feature of slow inactivation seen in Figure 1.4 is that, in contrast to fast inactivation, it is usually incomplete even after long depolarizations.

Entry to Slow Inactivation   Recovery from Slow Inactivation
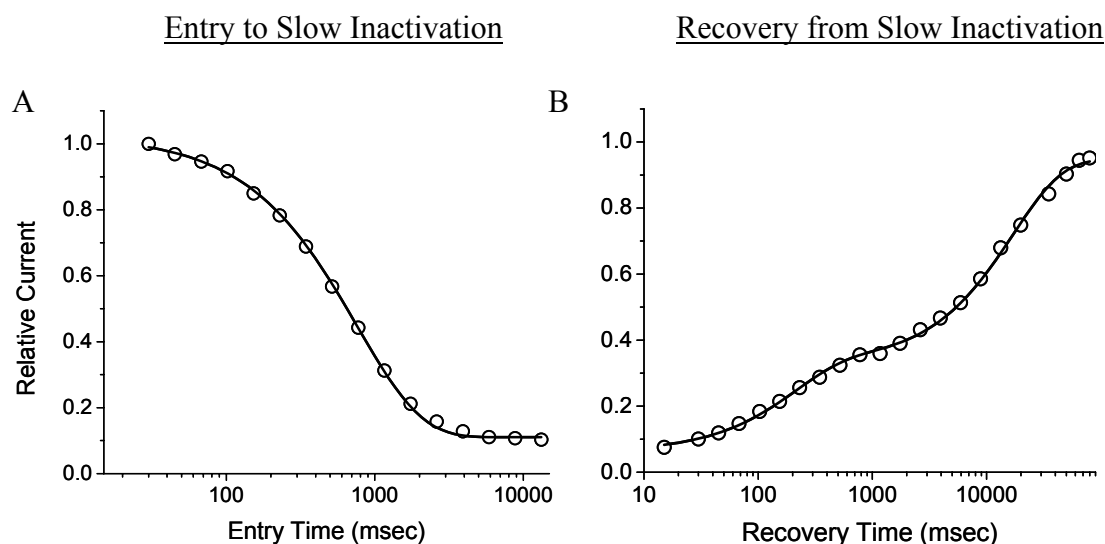
Figure 1.4   Graphs of entry to and recovery from slow inactivation.   Entry to slow inactivation (A) shows a monoexponential time course, while recovery (B) shows at least two components.   Because of the specialized pulse protocols used to measure slow inactivation (see text), fast inactivation did not significantly affect either (A) or (B), and is not shown.

Slow inactivation, like activation and fast inactivation, is voltage-dependent, with steady-state levels approximated well by a Boltzmann function in response to the applied membrane voltage. The voltage midpoint ($V_{1/2}$) of steady state slow inactivation is more hyperpolarized (~15 mV) than for activation. This implies that slow inactivation, like fast inactivation, can occur from either closed or open channels. Fast inactivation is also not an obligatory step in the pathway to slow inactivation, as demonstrated by the presence of robust slow inactivation from channels in which fast inactivation is completely destroyed by proteolytic enzymes [11, 12].

The extent of slow inactivation interaction with other channel gating events is still poorly understood. The most compelling evidence thus far suggests that fast inactivation weakly couples to slow inactivation [13, 14]. The primary evidence for this came from observations that slow inactivation typically occurs around two-fold faster and is much

more complete when fast inactivation is completely disrupted. This has led to speculation that fast and slow inactivation are actually antagonistic, or negatively coupled to each other. But this story of negative coupling is far from conclusive, since different methods of disrupting fast inactivation can produce highly variable degrees of effects on slow inactivation. What we do know for certain, however, is that fast and slow inactivation are not mutually exclusive states. Channels can slow inactivate from closed, open, or fast inactivated channels, and conversely the fast gate can recover freely in slow inactivated channels [15]. Any coupling or competition between fast and slow inactivation, then, is only partial at best. The question of coupling between fast and slow inactivation is further addressed in Chapters 3 and 4, where evidence supports the independence of these forms of gating, and further argues that interaction between them is weak, if at all.

To summarize this section, we now know that channels can fast and slow inactivate from both the closed and open channel conformations, and that fast and slow inactivation are distinct kinetic events that can occur both in the presence or absence of each other. While all of these gating events show significant independence from each other, evidence continues to accumulate showing at least some degree of coupling, such as that observed between fast and slow inactivation.

1.5   ***Structure of the Sodium Channel***

A major goal in the field of ion channel biophysics is to resolve the atomic structure of a channel complex, and from this, to gain insights on the possible conformational changes that mechanistically underlie the fundamental properties of ion channels as reflected by permeation and gating. To date, the structure of the voltage-gated Na^+ channel has not been determined at the atomic level. Nevertheless, we can make analogies to other channels whose structures have been determined (K^+ channels) or draw upon other types of experimental data, such as mutagenesis, accessibility of sentinel residues for covalent modification, or fluorescence resonance energy transfer to gain insights on channel structure and function.

The primary amino acid sequence of sodium channels has been known since 1984 [16]. Modeling of the hydrophobicity and alpha-helical tendencies of the amino acids in this sequence, as well comparison to other ion channels suggests that the canonical sodium channel has four internal homologous repeat domains, each with six transmembrane segments and arranged symmetrically around a central ion conducting pore. (Figure 1.5). This large glycoprotein of about 260 kD, termed the α-subunit, is capable of forming a functional sodium-selective pore with voltage dependent activation, and fast and slow inactivation. Nine of these α-subunit isoforms have been identified, each possessing unique gating characteristics and expressed at varying levels in the different cell types. A family of at least four smaller single-transmembrane accessory β-subunits co-assemble with the α-subunit either covalently (β2, β4) or non-covalently (β1,β3). These subunits are comprised of a large extracellular I_g-fold domain that may be

important for localizing the channel by interacting with the extracellular matrix, and a small intracellular tail.
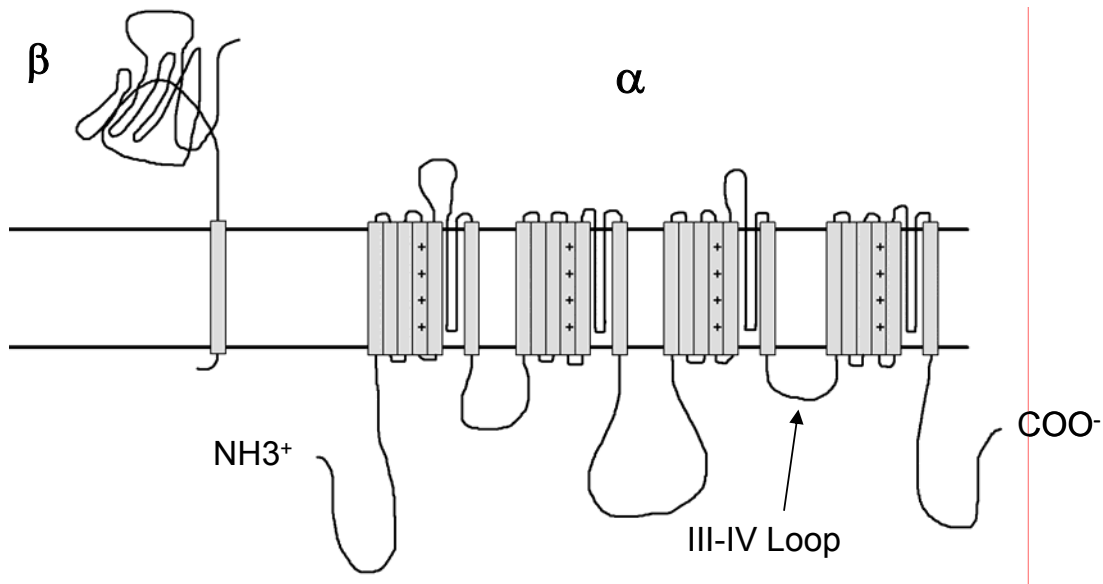
Figure 1.5 Transmembrane topology of the sodium channel α and β subunits.

Specific functions for the various components of the sodium channel α-subunit have been elucidated. For instance, the four domains are connected by three large intracellular loops, and these loops have been shown to be crucial for channel gating (fast inactivation), for mediating regulation of the channel by phosphorylation [17], and for associating with various cytoskeletal components [18]. The fourth transmembrane segment (termed the 'S4 voltage sensor') contains 6 to 8 positively charged residues (arginine or lysine at every third position), and is believed to underlie much of the voltage sensitivity of channel gating. Abundant evidence suggests that the S5 and S6 segments, as well as the external loop that connects them, form the selectivity filter and permeation pathway of the channel. This was made clear from comparison of this region to known K^+ channel structures [19], from locating residues that interacted with pore blocking

drugs [20], and from mutagenesis studies in the S5-S6 Loop that dramatically altered the selectivity of the channel for monovalent and divalent cations [21]. The S5-S6 segments and their adjoining linker also appear to be critically important for slow inactivation gating, and the evidence for that is discussed in more detail below.

1.6　　　　*Structure-Function Relationships for Activation and Fast Inactivation*

Channel activation is tightly coupled to movement in the S4 voltage-sensors. The source of the non-linear charge displacement (gating charge movement) associated with activation has been firmly established to reside in the basic residues of the S4 segments. The location of the activation gate itself, however, is considerably less well established. In K^+ channels, rotation of the S6 segments has provided a plausible explanation for a gate or constriction to ion flow that forms an activation gate at the cytoplasmic end of this transmembrane segment [22]. The mechanism by which S4 movement is coupled to motion of the activation gate, however, is still not clearly defined. By analogy to K^+ channels, the activation gate of the sodium channel is probably located on the intracellular aspect of the selectivity filter, as suggested by experiments showing that closure of the activation gate can trap cationic compounds within the inner vestibule of the channel [23].

The first insights on the localization for fast inactivation of Na^+ channels were gained from internal treatment of the axoplasm with proteases which dramatically disrupted fast inactivation [11]. This data implicated a cytoplasmic domain of the

channel. The next major advance came around 10 years later when expression studies in the oocyte demonstrated a loss of inactivation by disruption of the ~50 amino acid cytoplasmic loop between domains III and IV [24, 25]. Further refinements using site-directed mutagenesis revealed that a short stretch of hydrophobic residues (IFM) near the middle of this loop is critical for stabilizing fast inactivation and perhaps acts like a latch on a hinged-lid over the inner mouth of the channel to prevent ionic conduction [26].

Additional experiments now argue that the mechanism of fast inactivation involves other regions of the channel besides the III-IV and its docking site. For instance, toxins that bind to the Domain IV S4 voltage sensor on the external face of the channel can severely inhibit fast inactivation [27]. This suggests that immobilization of a voltage sensor can prevent conformational changes needed for closure of the III-IV loop over the inner channel mouth.

Despite the fact that fast inactivation is relatively well understood, some fundamental questions about its mechanism still remain. Mutations deep in the inner pore of the channel [28], as well as at the very shallow inner mouth entrance [29, 30] can profoundly affect fast inactivation. The widely varying locations of these inner pore residues raises questions about where the "receptor" for the hinged lid is actually located, although the clearest evidence is increasingly pointing to the mouth entrance as the most likely docking site [31]. Work remains, then, to define exactly where and how the III-IV Loop moves to block ionic current.

1.7   *Structural Aspects and Mechanism of Slow Inactivation*

A more comprehensive introduction to the mechanism of slow inactivation is presented below, since this is the primary interest for this thesis. First, a review of how slow inactivation was initially discovered will be presented, followed by what is currently known about where and how slow inactivation occurs. Finally in this section, the role of slow inactivation in both normal physiology and disease will be discussed.

1.7.1 Discovery of SI

The possibility of a much slower sodium channel inactivation process was proposed as early as 1958, shortly after the discovery of fast inactivation [32]. A key feature in this process of discovery was the recognition that more than one type of inactivation could be discerned experimentally by observing the time course of recovery from inactivation after prolonged periods of depolarization (see Figure 1.4, above). In 1964, Narahashi observed a voltage-dependent change in Na^+ conductance in response to varying the holding voltage that had a time course on the order of 1 sec, which was hundreds of times longer than the classical fast inactivation time course [33]. The first detailed evidence for slow inactivation, however, was presented by Adelman and Palti in 1969 [34], when they showed that after very long depolarizing conditioning pulses in squid giant axon, sodium channel peak currents recovered with three distinct time constants. The first time constant was the familiar fast inactivation 'τ_h' which recovered on the order of a few milliseconds. The second time constant recovered over several hundred milliseconds,

while the third recovered only after hyperpolarizing the cell for many seconds (details of the multiple slow inactivated states are discussed below in Section 1.7.2). In their work, they noticed that populating the two slower inactivated states did not interfere with the kinetic behavior of the fast inactivation, and they proposed that these longer states represented distinct Na^+ current recovery processes, rather than variations of fast inactivation. Notably, these slower recovery processes were clearly affected by the external K^+ ion concentration in their preparations, and so they proposed that these slower recovery processes might reflect pharmacological changes caused by K^+ on the sodium channel. This aspect of slow inactivation has essentially been ignored for the past 35 years, and is now re-examined in my work as an opportunity to gain insight on the mechanism of slow inactivation (Chapter 4).

Within the next few years, Rudy [35] and Schauf et al [36] also observed sodium currents with very slow recovery time courses in axons of the worm *Myxicola*. Schauf et al found that these slow changes in channel availability were strongly dependent on the membrane voltage of the cell, and were independent of $[K^+]$ in their preparation. They were the first to clearly argue that slow inactivation was not simply a byproduct or regulatory artifact of bath K^+ ion changes, but were instead likely to be intrinsic voltage-dependent gating mechanisms. For the first time, these slower recovery processes were collectively termed 'slow inactivation'.

Since then, numerous studies have confirmed that slow inactivation is a voltage-dependent gating process [37]. Moreover, it is a universal feature of all voltage-gated sodium channels from any tissues or species.

1.7.2   *Multiple Slow Inactivation States?*

One complication in studying slow inactivation has been the question of whether there are one or multiple slow inactivated states.   Since the discovery of slow inactivation, it has been clear that the time course of recovery exhibits at least two slow components in most [38] (but not all [37]) experimental preparations.   The fastest component of recovery occurs within a few msec at -120 mV and represents recovery from fast inactivation.   Many protocols designed to measure slow inactivation do not show the temporal progression of this component since the shortest recovery interval in these protocols is typically 20 msec.   Recovery from slow inactivation will often show more than one time course. The recovery of the first component has a time constant on the order of several hundred milliseconds at -120 mV, and has been termed 'intermediate inactivation' (I_M). I_M is considered to be one component of slow inactivation, and is the faster of the two recovery components shown earlier in Figure 1.4 (recall again that recovery from fast inactivation occurred before the first test pulse in Fig. 1.4).   The slowest recovery time constant commonly observed represents what is variably termed 'slow inactivation' (I_S) or 'ultraslow inactivation' (I_{US}), where recovery occurs on a time scale of many seconds [39].

Other unusual slow inactivated states have appeared in the background of certain sodium channel mutations in the pore region or S6 segments.   Unfortunately, these very slow component(s) have also been confusingly termed ultraslow inactivation by some

authors [40]. These states, however, are minimal to absent in the wild-type channels and so may not represent normal physiological processes.

One hindrance to understanding which component(s) of slow inactivated are present in any given sodium channel recording is the lack of consensus on the parameters of the pulse protocols used to study slow inactivation. Each laboratory uses its own operational definition of the recovery gap duration and voltage used to separate fast from slow inactivated components. Therefore, the kinetic behavior of the slow inactivation states often varies between authors.

While two slowly recovering components (I_M and I_S) are readily apparent in most preparations, it is not certain whether other slow inactivation states might also exist that are not easily resolved from observing recovery of ionic current. For instance, it is theoretically possible that numerous distinct slow inactivation states exist that have time courses similar to what is macroscopically observed as either 'I_M' or 'I_S'. In support of this, one group [41] observed that the recovery time course of slow inactivation varied with the length of the conditioning pre-pulse. To explain this, they proposed a fractal, non-Markovian model of slow inactivation in which longer pre-pulses drive channels into a continuum of states with increasingly longer recovery times. This view, however, is controversial and contrasts to numerous other studies that clearly identify one or two distinct kinetic components of slow inactivation (see Fig 1.2 for an example) that do not substantially change with pre-pulse duration. Whatever the case, while it is not certain how many slow inactivation states might exist, it does seem fairly clear that there is more than one.

1.7.3   Mechanism of Slow Inactivation– a Pore Region Phenomenon?

Determining the location of the various activation and inactivation gates of ion channels has proven to be a long and evolving process, and most of the progress in understanding channel gating structures has come from K^+ channels.   The best understood example is K^+ channel fast inactivation, which arises from inner pore occlusion by an N-terminal ball-and-chain type mechanism [42]. K^+ channels additionally exhibit a much slower form of inactivation, termed 'C-type' inactivation [43], which appears to occur by collapse of the outer pore at or above the selectivity filter [44, 45].   Analogously, Na^+ channels also display both fast and slow forms of inactivation, with Na^+ channel fast inactivation also resulting from inner pore occlusion by a moving cytoplasmic structure.   It is tempting, then, to also compare the mechanism of K^+ channel C-type inactivation to Na^+ channel slow inactivation, and several groups have done so to guide them in their investigation [13, 46].

Some of the first insights into the mechanism of sodium channel slow inactivation was achieved in 1978, when Rudy [11] and Starkus et al [12] showed that slow inactivation remained (and could even be enhanced) by complete removal of fast inactivation through exposure of the cytoplasmic face of the channel to proteolytic enzymes. Later work by Vedantham and Cannon [15] showed that slow inactivation did not affect movement of the fast inactivation gate and that the fast and slow inactivation states can co-exist, further proving that the fast and slow inactivation mechanisms are

distinct. Numerous additional studies have since identified regions of the channel that impact slow inactivation, although the overall mechanism(s) largely remain a mystery.

While a variety of regions and structures in the sodium channel have been implicated for their contribution to slow inactivation, a clear role for the pore region has emerged from many complimentary studies. The pore region of the sodium channel can be structurally divided into inner and outer regions, separated by the selectivity filter comprised of D E K A residues contributed by the pore loops from domains I-IV. The inner and outer pore regions each have unique and important features in relation to slow inactivation, and thus each will be considered separately below.

The outer pore of the Na^+ channel is comprised of the four extracellular P-loops connecting the S5 and S6 transmembrane segments (S5-S6 Linkers). These loops invaginate into the membrane and come into close proximity to each other at a tight constriction point in the center of the channel, forming the region of ion selectivity, which includes the DEKA selectivity filter (see Figure 1.6, below for a diagram). Connected to the S5-S6 linkers are the S6 transmembrane segments, which are shown as the kinked lines in Figure 1.6 (the S5 segments that attach to the other end of the S5-S6 linkers are omitted in the figure). The kinked nature of the S6 segments has been proposed by analogy to the atomic structure determined for K channels and allows them to come together at the inner vestibule to form another area of tight constriction, an area which may act as the activation gate.
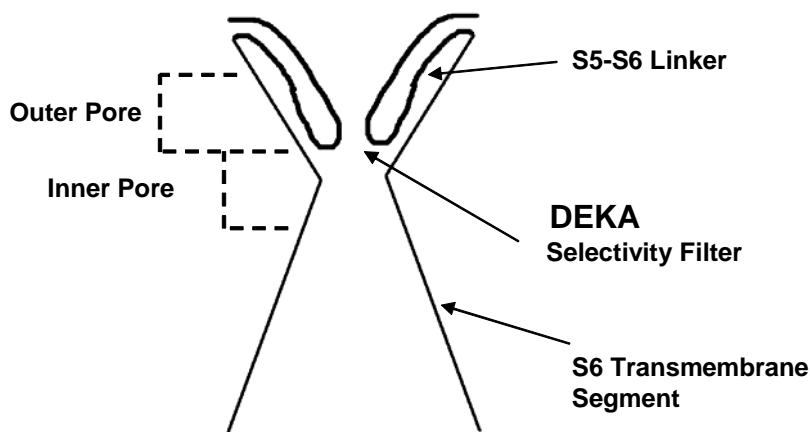
Figure 1.6 Cutaway diagram of the sodium channel pore region. The S5-S6 Pore Loops form the outer pore region of ion conduction, and mediate ion selectivity at the DEKA selectivity filter. The S6 segments kink inward to form the narrow inner pore region just below the outer pore.

1.7.4   *Inner Pore and Slow Inactivation*

The S6 transmembrane segments appear to line the inner portion of the ion permeation pathway [1, 47-49], and numerous site-directed mutagenesis studies have identified residues in the S6 segments that are especially important for slow inactivation [50-57]. For instance, mutations to residue V787 in the middle of Domain II S6 dramatically enhance slow inactivation [58]. Systematic mutagenesis of the DI and DIV S6 segments further revealed that a large number of additional residues in the inner pore S6 segments significantly modulate slow inactivation [29]. Curiously, the most commonly observed change to slow inactivation from this scanning mutagenesis in the S6 segments is enhancement, as demonstrated by faster rate of entry, greater extent of

slow inactivation at steady-state, leftward (hyperpolarized) shift of voltage dependence, and slower recovery. Initially, it would seem more likely that a series of essentially random mutations along a region of the channel would tend to disrupt a finely-tuned channel gating process, as is the case for fast inactivation. But since most mutations enhance slow inactivation, this may suggest that slow inactivation actually represents a very stable low energy ground state (perhaps a sort of collapse) that the channel must be finely tuned to prevent.

The importance of the inner pore for slow inactivation is also demonstrated by pharmacologic studies. The most dramatic example is the effect of the frog toxin batrachotoxin (BTX) [59]. BTX binding to the channel can completely eliminate all forms of fast and slow inactivation, such that the channel will remain open indefinitely if depolarized. BTX binding is the only known agent or method that can completely disrupt slow inactivation. BTX is a rigid planar molecule, and is known to bind to the S6 segments high up in the inner pore [60], just below the selectivity filter. This binding site likely corresponds to the kinked region of the S6 segments, shown in Figure 1.6. Tanguy and Yeh confirmed prior reports that BTX preferentially modifies open (activated) and not closed channels [59], perhaps suggesting that the inner pore activation gate can prevent access to the internal binding site. More importantly for this discussion, they also showed that channels which had been depolarized for a very long period of time (with fast inactivation enzymatically removed) could still be modified, albeit at a 500-fold slower rate. Since prolonged depolarization builds up significant levels of slow inactivation, they interpreted this to mean that BTX can still modify slow inactivated channels, though at a slow rate. This would imply, then, that BTX can still access the

inner pore binding site in slow inactivated channels. This interpretation has several limitations, however. For one, slow inactivation is typically incomplete even after long depolarizations, and so this 500-fold slower reaction rate may well represent BTX modification of the few channels that transiently escape slow inactivation during depolarization. Also, it was not known which of the two slow inactivated states (I_M or I_S) were present during BTX modification, and so no comments can be made about how each specific slow inactivation state interacts with BTX. But in spite of these problems, it is still reasonable to glean from this study that slow inactivation does cause significant reduction of BTX binding ability to its inner pore binding site. This in turn suggests that the S6 inner pore region must move and/or collapse in some way during this gating process. We cannot know from this, however, whether slow inactivation causes subtle movements in the inner pore that alter the BTX binding site, or whether large scale collapse somewhere in the inner pore prevents toxin access to its binding site.

Lidocaine and its derivatives are another set of pharmacological tools that have been used to explore the importance of the inner pore for slow inactivation, although interpretation of this data has been problematic. These local anesthetics are used to treat localized pain and other cellular excitability disorders, and they accomplish this primarily by blocking voltage-gated sodium channels [61]. The lidocaine binding site in sodium channels is believed, like BTX, to be located in the S6-lined inner pore region, just below the selectivity filter [62]. A key feature of the local anesthetics noted early on was their state-dependent block with increased affinity ($20 - 100$ fold) for depolarized channels [63]. One report suggested that lidocaine binding ability was reduced in the I_S state [5] and may have also been altered by I_M, perhaps analogous to the reduction of BTX

binding in this region during slow inactivation. A major complication of this particular study, however, was that state-dependent lidocaine binding was measured in frog oocytes expressing α-subunit with no β1 subunit. This is problematic because sodium channel gating in oocytes behaves very abnormally in the absence of co-expressed β1 subunit, making it difficult to know whether wild-type channel gating mechanisms are preserved, and whether the mechanistic interpretations of these lidocaine binding experiments have any relevance to the wild-type channels.

Another study [63] examining the behavior of the inner pore and lidocaine binding during ultraslow inactivation of channels with a point mutation in the pore found that lidocaine could prevent entry to slow inactivation in a manner consistent with a foot-in-the-door. In other words, lidocaine binding to the inner pore might prevent a collapse or movement in this region that is necessary for slow inactivation to occur. But interpretation of this should still be limited, since the way in which lidocaine reaches its binding site is not clear. It is known that lidocaine can traverse the cell membrane, and appears to be able to access the inner pore from the external side of the channel through an unknown pathway, at least in some channel isoforms [62]. Also, the form of slow inactivation they studied was unusual, in that it was only clearly observable in channels with mutations in the selectivity filter. It is not clear from this study, then, exactly what kind of slow gating event was actually being observed.

Another pharmacological tool to probe inner pore and its relationship to slow inactivation is tetraethylammonium (TEA). O-Leary and Horn [64] showed that internal TEA blocks Nav1.5 sodium channels at an apparent electrical distance (from the inside) of 0.43, which implies deep binding within the inner pore. Furue et al. later found that

applying 20-30 mM internal TEA to the sodium channel did not affect the time course or relative amplitudes of I_M or I_S [39]. These data suggest that TEA does not act as a foot-in-the-door to impede slow inactivation even though it can bind deep within the inner pore. While this implies that the inner pore does not collapse during slow inactivation, it is also possible that the slow gate shuts at an internal site not accessible to TEA, or that TEA is simply not able to keep an inner pore collapse from occurring.

Vedantham and Cannon attempted to directly answer the question of possible inner pore collapse during slow inactivation by measuring access of a pore-facing cysteine in DIV S6 (V1583C) to the modifying reagent MTS-EA [65]. They found that site V1583 was readily accessible in open channels, but that it became inaccessible during slow inactivation. MTS-EA, however, is known to cross membranes and hydrophobic protein boundaries [66], and they observed that MTS-EA could access V1583C when applied from either side of the membrane. This behavior suggests that MTS-EA was indeed crossing unknown boundaries to reach this inner pore site, thereby obscuring any interpretation of how slow inactivation might impede aqueous access to the site. Despite this problem, the obvious change of residue accessibility still does at a minimum suggest movement of the S6 region during slow inactivation, even though it does not address the question of a large-scale inner pore collapse.

I attempted to revisit this issue of inner pore closure by testing inner pore residue accessibility to a 'cleaner' MTS reagent, MTS-ET, which has a fixed positive charge and does not cross membranes or other hydrophobic pathways [66]. Similarly to Vedantham and Cannon [65], I used a high speed perfusion system to test how rapidly MTS-ET could react with engineered cysteines facing the inner pore before and after slow inactivation,

to see if access is impeded by the onset of slow inactivation. Unfortunately, I discovered that at the required high concentrations (2 - 4 mM) and long exposure times (seconds to minutes), MTS-ET robustly interacts with wild-type channels to block current, and this rate of reaction is similar to that of the mutant channels with the engineered cysteines. Because of this, no reliable conclusions could be drawn from the MTS-ET experiments, and the question of inner pore-facing residue accessibility changes during slow inactivation remains open.

Overall, mutagenesis and pharmacologic data suggests that the S6 inner pore region is involved in slow inactivation, and that significant conformational changes occur here during it. But thus far, it is not at all clear exactly what kind of changes take place, and whether some kind of gate actually shuts over or collapses the inner pore, or whether the conformational changes are more subtle.

1.7.5   Outer pore and Slow Inactivation

As mentioned previously, comparison of K^+ and Na^+ channel slow inactivation has led to the notion that Na^+ channel slow inactivation, like K^+ channels, might involve some form of collapse in the outer pore of the channel. Accumulating evidence supports the hypothesis that the outer pore is indeed critical for slow inactivation, but the fine details of exactly how the outer pore participates is not yet clear.

A role for the outer pore in slow inactivation gating was demonstrated by chimeric substitutions between two sodium channel isoforms (Nav1.4 and Nav1.5) with large

differences in slow inactivation. Slow inactivation is typically much more complete in the Nav1.4 isoform than in Nav1.5 [67]. Taking advantage of this difference, O-Reilly et al swapped the outer pore loops of these two isoforms. Measurement of slow inactivation in these chimeric channels showed that all four P-loops, and especially those from DI and DII, had an influence on slow inactivation. Follow-up studies [68] took this a step further and found that a specific residue in the DII S5-S6 linker (V754 in skeletal muscle) could by itself convert Nav1.4-type slow inactivation gating behavior into the much different Nav1.5-type. Other point mutations in the outer pore region similarly caused dramatic changes to slow inactivation. For instance, Balser et al found that mutations at a residue in the S5-S6 Linker from Domain I (W402) can virtually eliminate entry to the I_M state, and also significantly alter the kinetics of the I_S state [5, 13]. Mutations in some of the charged outer pore residues similarly caused clear effects on slow inactivation [69].

Another approach to studying the contribution of the outer pore to slow inactivation has been to examine the ability of engineered cytseines in the outer pore to form disulfide cross-bridges either in the resting state or when the channel is slow inactivated. These studies showed that cross linking between a wide variety of residues in the outer pore changes considerably during intermediate slow inactivation (I_M) [70]. Conversely, 'fusing' certain residues together by cross-linking was shown to slow or prevent entrance into slow inactivation [46]. This suggests that large movements must occur in the outer pore in order for the channel to slow inactivate.

To establish a mechanistic link between these outer pore movements and the propensity to slow inactivate, much attention has been focused on the contribution of the electrostatic environment in the pore. The outer pore region contains a number of

negatively charged resides, and this highly negative environment has been proposed to antagonize slow inactivation. Several groups showed that neutralization by point mutagenesis of negative charges in the outermost rim of the outer pore produced clear enhancement of slow inactivation. For instance, charge neutralization in two residues from the outer pore 'EEDD' ring of charge caused a dramatic 25-fold slowing of recovery from slow inactivation, suggesting that the slow inactivated state was significantly stabilized [71]. Charge neutralization mutations down in the selectivity filter itself also affected SI, rendering the channel much more susceptible to entry into an ultra-slow inactivated state [40, 72, 73]. From the mutagenesis data, it was reasoned [71] that perhaps the negative charges in the outer pore repel each other to keep the outer pore open, which would prevent entry to slow inactivation and to hasten recovery from it. In this view, slow inactivation is seen as being a collapse or at least a constriction in the outer pore, analogous to K^+ channel C-type inactivation.

Struyk and Cannon directly investigated this possibility of outer pore collapse by engineering cysteines into multiple outer pore residues and testing accessibility of MTS-ET to these cysteines after being slow inactivated [74]. They showed that these reagents were fully capable of traversing deep into the outer pore during the slow inactivated state, in stark contrast to the clear loss of cysteine accessibility in the outer pore of K^+ channels during C-type inactivation [75]. Such results imply that the sodium channel outer pore does not undergo large-scale collapse during slow inactivation. Struyk and Cannon, however, were only able to measure accessibility changes down to one helical turn above the selectivity filter, and not at the selectivity filter itself, leaving collapse in this lower region an open question. Ong et al [76] measured the accessibility of cysteine residues at

or just below selectivity filter to external MTS reagents, and they observed that accessibility was slightly enhanced by depolarizing conditions that favor slow inactivation. While this might suggest subtle conformational changes in the selectivity filter during slow inactivation, only the reagent MTS-EA was able to react with these cysteines (MTS-ET had no effect). This is problematic, again, because MTS-EA is known to cross various hydrophobic barriers and so may interact with the channel via unknown pathways that would obscure a clean interpretation. Overall, then, the cysteine accessibility studies have been quite useful in defining behavior of the outer pore during slow inactivation, but they still leave open the question of collapse or other significant conformational changes at or below the DEKA selectivity filter.

From all of these experiments, it is becoming clear that the outer pore moves significantly during slow inactivation, but does not undergo wholesale collapse as in K^+ channels. Tikhonov recently attempted to synthesize these observations, and has proposed a novel model in which the outer pore does not collapse at all during slow inactivation, but may in fact open even wider during it [77]. In other words, slow inactivation may cause the outer pore to open wider than it normally would be during rest. In this model, it was suggested that the negative charges in the outer pore electrostatically repulse each other and that this repulsion predisposes the channel towards this ultra-wide pore opening associated with slow inactivation. Pore-loop movements associated with this ultra-wide opening event of the outer pore are proposed to pivot and allosterically cause constriction of structures deeper in the pore (perhaps below the selectivity filter), thereby rendering the channel impermeable (slow inactivated). The basis for this model rests in large part on the observation that the outer

pore likely does not collapse during slow inactivation. It also attempts to explain the observation that external cations can impede slow inactivation. In this model, external positively charged ions are thought to partially neutralize the negative charge in the outer pore, and so their presence would reduce the repulsive driving force that predisposes the channel to slow inactivation. One major limitation of this model, however, is that we currently know very little about where or how cations interact with slow inactivation.

Several studies on the effects of alkali metal cations on K^+ channel gating found that certain cations act as a foot-in-the-door at the selectivity filter to impede entry to C-type inactivation [78, 79]. Such data have been instrumental in establishing the outer pore region as the locus for the C-type gate. In Na^+ channels, Adelman and Palti first showed in 1969 that the relative concentrations of external Na^+ and K^+ influenced the degree of slow inactivation, with higher Na tending to impede slow inactivation [4]. Other studies [70, 80] have since confirmed that extracellular Na^+ impedes slow inactivation relative to certain other cations. It has largely been assumed that this cation interaction occurs in the outer pore region, perhaps again reflecting a bias towards analogy to K^+ channels. But the observations of this cation effect have been variable, and have thus far lacked the mechanistic insights gained from studying the effects of external cations on K^+ channel C-type inactivation. For example, it is still not at all clear where or how cations interact with the Na^+ channel to modulate slow inactivation. A large portion of the work presented in this thesis is directed at increasing our understanding of the interaction of cations with sodium channel slow inactivation. My findings clearly show an interaction between specific external cations and slow inactivation. Moreover, these data show for the first time that this interaction occurs in the outer pore region, above the selectivity

filter. The details of these findings are elaborated further in the discussion section in Chapter 4.

In summary, there is evidence that both the inner pore S6 region and outer pore S5-S6 P-loops are integral to slow inactivation. Both of these pore regions are in close contact, and so it is highly likely that slow inactivation is the result of concerted interactions between these two regions.

1.8   *Physiological Relevance of Slow Inactivation*

Experimentally, slow inactivation is observed under rather extreme conditions of prolonged depolarization, which raises the question of the relevance of slow inactivation to sodium channel function under physiological conditions. An early clue to the importance of slow inactivation was the observation that it is highly conserved and occurs in every sodium channel isoform examined, in species ranging from cockroaches to humans. Almost all of the many calcium and potassium channel subtypes similarly show forms of slowly inactivating gating processes, implying that the ability of an ion channel to inactivate on a slow time scale is important.

Numerous studies of endogenously expressed sodium channel in their native tissue have since confirmed that sodium channel slow inactivation is prominent under many physiological conditions and that disruption of this gating mechanism can result in pathological cellular excitability, and so deserves careful attention. Since its discovery, slow inactivation was proposed to play a role in long-term modulation of Na^+ channel

availability. One of the first examples of this was in *Myxicola* sea worms. A prominent behavior of *Myxicola* is its ability to withdraw into its shell upon contact from an outside stimulus. This behavior slowly adapts to a constant stimulus, such that the worm withdraws less over time. Electrically, this withdrawal behavior begins as a rapid burst of action potentials that slowly decreases in frequency. In 1981, Rudy [81] showed that this spike frequency adaptation could be accounted for by a reduction in Na^+ channel availability, and that the time course of this reduction paralleled the entry rate to sodium channel slow inactivation. Rudy proposed that this adaptive response in *Myxicola* must be primarily due to loss of available sodium channels coming from a buildup of slow inactivation. Although only a few channels entered the slow inactivated state during each short action potential, recovery from slow inactivation is very slow, and so a long train of action potentials (such as during the sustained stimulus) can lead to significant cumulative trapping into this state. This work was among the first to clearly characterize a physiological role for slow inactivation.

Shortly after the characterization in *Myxicola*, slow inactivation was confirmed in skeletal muscle by Collins et al in 1982 [82]. Subsequent work in skeletal muscle revealed that slow inactivation is prominent under normal physiological conditions [83-85]. It was estimated from these studies that 50% or more channels may be slow inactivated at normal membrane resting potentials (V_{rest}). Since V_{rest} lies at the steep midpoint of the sigmoidal-shaped steady-state slow inactivation curve. Consequently, small changes in V_{rest} can dramatically affect the level of slow inactivation. This, in turn, will affect the number of available channels, and hence, overall cellular excitability. Another important point to note is that the voltage midpoint of steady-state slow

inactivation in muscle (-108 mV) was ~30 mV hyperpolarized relative to fast inactivation (-78 mV), and the steepness of the voltage dependencies were approximately the same. Since typical muscle V_{rest} is between -90 and -100 mV, this implies that a large proportion of Nav1.4 channels in skeletal muscle are slow inactivated state, meaning that slow inactivation is more important for determining channel availability at rest. This relationship is reversed in some cell expression systems, however, such that the midpoint of steady-state slow inactivation is more depolarized than for slow inactivation [50, 86].

In skeletal muscle, a clear link is now being established between defects in slow inactivation and human disease [50]. Defects in skeletal muscle sodium channel slow inactivation increase the susceptibility to depolarization-induced loss of muscle excitability, arising from persistent sodium currents conducted by mutant channels with impaired fast inactivation. In Chapter 2, this disease link is examined for a novel disease mutation, P1158S, which was found in a patient that was susceptible to these attacks of muscle periodic paralysis.

In the mammalian CNS, slow inactivation was found to be prominent in neocortical pyramidal cells [87]. As in *Myxicola*, the adaptation of spike firing rates was proposed to be heavily influenced by the degree of slow inactivation. Because of this, defects in slow inactivation could lead to aberrant spike firing influence and possibly epilepsy [88], however, this is not yet certain.

Slow inactivation is also observed in heart ventricular cells [39, 89-91], albeit less prominently than in muscle or neuronal Na channels, and has been proposed to serve as a natural anti-arrhythmic mechanism. Defects in slow inactivation have correspondingly

been linked to diseases such as Brugada syndrome, which predisposes the patient to dangerous arrhythmias [92].

1.9 Conclusion

Sodium channel slow inactivation is fundamentally important for controlling long term Na^+ channel availability, and is relevant to normal physiology. The extent of this effect, however, is not fully known, and is an area of ongoing research. In Chapter 2, I characterize a novel mutation in the sodium channel associated with periodic paralysis, and examine the role that defects in slow inactivation may play in the disease pathology.

In spite of its importance, the mechanism of slow inactivation is still quite unclear, and difficult work remains ahead to understand where and how it occurs. To that end, as the main focus of this thesis I examine how the β1 subunit and alkali metal cations interact with slow inactivation in Chapters 3 and 4, with the hope that this information will help augment our understanding of this mysterious gating process.

1. Catterall, W.A., *From ionic currents to molecular mechanisms: the structure and function of voltage-gated sodium channels.* Neuron, 2000. **26**(1): p. 13-25.

2. Hodgkin, A.L. and A.F. Huxley, *Currents carried by sodium and potassium ions through the membrane of the giant axon of Loligo.* J Physiol, 1952. **116**(4): p. 449-72.

3. Rojas, E. and B. Rudy, *Destruction of the sodium conductance inactivation by a specific protease in perfused nerve fibres from Loligo.* J Physiol, 1976. **262**(2): p. 501-31.

4. Adelman, W.J., Jr. and Y. Palti, *The effects of external potassium and long duration voltage conditioning on the amplitude of sodium currents in the giant axon of the squid, Loligo pealei.* J Gen Physiol, 1969. **54**(5): p. 589-606.

5. Kambouris, N.G., et al., *Mechanistic link between lidocaine block and inactivation probed by outer pore mutations in the rat micro1 skeletal muscle sodium channel.* J Physiol, 1998. **512 (Pt 3)**: p. 693-705.

6. Cummins, T.R. and F.J. Sigworth, *Impaired slow inactivation in mutant sodium channels.* Biophys J, 1996. **71**(1): p. 227-36.

7. Cannon, S.C., *Pathomechanisms in channelopathies of skeletal muscle and brain.* Annu Rev Neurosci, 2006. **29**: p. 387-415.

8. Patton, D.E., et al., *Amino acid residues required for fast Na(+)-channel inactivation: charge neutralizations and deletions in the III-IV linker.* Proc Natl Acad Sci U S A, 1992. **89**(22): p. 10905-9.

9. Hodgkin, A.L. and A.F. Huxley, *A quantitative description of membrane current and its application to conduction and excitation in nerve.* J Physiol, 1952. **117**(4): p. 500-44.

10. Armstrong, C.M., *Sodium channels and gating currents.* Physiol Rev, 1981. **61**(3): p. 644-83.

11. Rudy, B., *Slow inactivation of the sodium conductance in squid giant axons. Pronase resistance.* J Physiol, 1978. **283**: p. 1-21.

12. Starkus, J.G. and P. Shrager, *Modification of slow sodium inactivation in nerve after internal perfusion with trypsin.* Am J Physiol, 1978. **235**(5): p. C238-44.

13. Balser, J.R., et al., *External pore residue mediates slow inactivation in mu 1 rat skeletal muscle sodium channels.* J Physiol, 1996. **494 (Pt 2)**: p. 431-42.

14. Nuss, H.B., et al., *Coupling between fast and slow inactivation revealed by analysis of a point mutation (F1304Q) in mu 1 rat skeletal muscle sodium channels.* J Physiol, 1996. **494 (Pt 2)**: p. 411-29.

15. Vedantham, V. and S.C. Cannon, *Slow inactivation does not affect movement of the fast inactivation gate in voltage-gated Na+ channels.* J Gen Physiol, 1998. **111**(1): p. 83-93.

16. Noda, M., et al., *Primary structure of Electrophorus electricus sodium channel deduced from cDNA sequence.* Nature, 1984. **312**(5990): p. 121-7.

17. Murphy, B.J., et al., *Identification of the sites of selective phosphorylation and dephosphorylation of the rat brain Na+ channel alpha subunit by cAMP-dependent protein kinase and phosphoprotein phosphatases.* J Biol Chem, 1993. **268**(36): p. 27355-62.

18. Bouzidi, M., et al., *Interaction of the Nav1.2a subunit of the voltage-dependent sodium channel with nodal ankyrinG. In vitro mapping of the interacting domains and association in synaptosomes.* J Biol Chem, 2002. **277**(32): p. 28996-9004.

19. Lipkind, G.M. and H.A. Fozzard, *KcsA crystal structure as framework for a molecular model of the Na(+) channel pore.* Biochemistry, 2000. **39**(28): p. 8161-70.

20. Backx, P.H., et al., *Molecular localization of an ion-binding site within the pore of mammalian sodium channels.* Science, 1992. **257**(5067): p. 248-51.

21. Heinemann, S.H., et al., *Calcium channel characteristics conferred on the sodium channel by single mutations.* Nature, 1992. **356**(6368): p. 441-3.

22. Yellen, G., *The moving parts of voltage-gated ion channels.* Q Rev Biophys, 1998. **31**(3): p. 239-95.

23. Yeh, J.Z. and J. Tanguy, *Na channel activation gate modulates slow recovery from use-dependent block by local anesthetics in squid giant axons.* Biophys J, 1985. **47**(5): p. 685-94.

24. Stuhmer, W., et al., *Structural parts involved in activation and inactivation of the sodium channel.* Nature, 1989. **339**(6226): p. 597-603.

25. Vassilev, P., T. Scheuer, and W.A. Catterall, *Inhibition of inactivation of single sodium channels by a site-directed antibody.* Proc Natl Acad Sci U S A, 1989. **86**(20): p. 8147-51.

26. West, J.W., et al., *A cluster of hydrophobic amino acid residues required for fast Na(+)-channel inactivation.* Proc Natl Acad Sci U S A, 1992. **89**(22): p. 10910-4.

27. Rogers, J.C., et al., *Molecular determinants of high affinity binding of alpha-scorpion toxin and sea anemone toxin in the S3-S4 extracellular loop in domain IV of the Na+ channel alpha subunit.* J Biol Chem, 1996. **271**(27): p. 15950-62.

28. McPhee, J.C., et al., *A critical role for transmembrane segment IVS6 of the sodium channel alpha subunit in fast inactivation.* J Biol Chem, 1995. **270**(20): p. 12025-34.

29. Wang, S.Y., et al., *Tryptophan scanning of D1S6 and D4S6 C-termini in voltage-gated sodium channels.* Biophys J, 2003. **85**(2): p. 911-20.

30. Popa, M.O., et al., *Cooperative effect of S4-S5 loops in domains D3 and D4 on fast inactivation of the Na+ channel.* J Physiol, 2004. **561**(Pt 1): p. 39-51.

31. McPhee, J.C., et al., *A critical role for the S4-S5 intracellular loop in domain IV of the sodium channel alpha-subunit in fast inactivation.* J Biol Chem, 1998. **273**(2): p. 1121-9.

32. Cole, K.S., *Effects of polarization on membrane ion currents.* Abstracts of the Biophysical Society 2nd Annual Meeting., 1958.

33. Narashashi, T., *Restoration of Action Potential by Anodal Polarization in Lobster Giant Axons.* J Cell Physiol, 1964. **64**: p. 73-96.

34. Adelman, W.J., Jr. and Y. Palti, *The influence of external potassium on the inactivation of sodium currents in the giant axon of the squid, Loligo pealei.* J Gen Physiol, 1969. **53**(6): p. 685-703.

35. Rudy, B., *Proceedings: Slow recovery of the inactivation of sodium conductance in Myxicola giant axons.* J Physiol, 1975. **249**(1): p. 22P-24P.

36. Schauf, C.L., T.L. Pencek, and F.A. Davis, *Slow sodium inactivation in Myxicola axons. Evidence for a second inactive state.* Biophys J, 1976. **16**(7): p. 771-8.

37. Brismar, T., *Slow mechanism for sodium permeability inactivation in myelinated nerve fibre of Xenopus laevis.* J Physiol, 1977. **270**(2): p. 283-97.

38. Fox, J.M., *Ultra-slow inactivation of the ionic currents through the membrane of myelinated nerve.* Biochim Biophys Acta, 1976. **426**(2): p. 232-44.

39. Furue, T., et al., *Characteristics of two slow inactivation mechanisms and their influence on the sodium channel activity of frog ventricular myocytes.* Pflugers Arch, 1998. **436**(5): p. 631-8.

40. Hilber, K., et al., *The selectivity filter of the voltage-gated sodium channel is involved in channel activation.* J Biol Chem, 2001. **276**(30): p. 27831-9.

41. Toib, A., V. Lyakhov, and S. Marom, *Interaction between duration of activity and time course of recovery from slow inactivation in mammalian brain Na+ channels.* J Neurosci, 1998. **18**(5): p. 1893-903.

42. Demo, S.D. and G. Yellen, *The inactivation gate of the Shaker K+ channel behaves like an open-channel blocker.* Neuron, 1991. **7**(5): p. 743-53.

43. Hoshi, T., W.N. Zagotta, and R.W. Aldrich, *Two types of inactivation in Shaker K+ channels: effects of alterations in the carboxy-terminal region.* Neuron, 1991. **7**(4): p. 547-56.

44. Kiss, L., J. LoTurco, and S.J. Korn, *Contribution of the selectivity filter to inactivation in potassium channels.* Biophys J, 1999. **76**(1 Pt 1): p. 253-63.

45. Eghbali, M., et al., *External pore collapse as an inactivation mechanism for Kv4.3 K+ channels.* J Membr Biol, 2002. **188**(1): p. 73-86.

46. Xiong, W., et al., *Molecular motions of the outer ring of charge of the sodium channel: do they couple to slow inactivation?* J Gen Physiol, 2003. **122**(3): p. 323-32.

47. Ragsdale, D.S., et al., *Molecular determinants of state-dependent block of Na+ channels by local anesthetics.* Science, 1994. **265**(5179): p. 1724-8.

48. Sunami, A., et al., *Accessibility of mid-segment domain IV S6 residues of the voltage-gated Na+ channel to methanethiosulfonate reagents.* J Physiol, 2004. **561**(Pt 2): p. 403-13.

49. Fozzard, H.A. and D.A. Hanck, *Structure and function of voltage-dependent sodium channels: comparison of brain II and cardiac isoforms.* Physiol Rev, 1996. **76**(3): p. 887-926.

50. Hayward, L.J., R.H. Brown, Jr., and S.C. Cannon, *Slow inactivation differs among mutant Na channels associated with myotonia and periodic paralysis.* Biophys J, 1997. **72**(3): p. 1204-19.

51. Wright, S.N., S.Y. Wang, and G.K. Wang, *Lysine point mutations in Na+ channel D4-S6 reduce inactivated channel block by local anesthetics.* Mol Pharmacol, 1998. **54**(4): p. 733-9.

52. Takahashi, M.P. and S.C. Cannon, *Enhanced slow inactivation by V445M: a sodium channel mutation associated with myotonia.* Biophys J, 1999. **76**(2): p. 861-8.

53. Wang, S.Y. and G.K. Wang, *A mutation in segment I-S6 alters slow inactivation of sodium channels.* Biophys J, 1997. **72**(4): p. 1633-40.

54. McNulty, M.M., et al., *An inner pore residue (Asn406) in the Nav1.5 channel controls slow inactivation and enhances mibefradil block to T-type Ca2+ channel levels.* Mol Pharmacol, 2006. **70**(5): p. 1514-23.

55.   Kondratiev, A. and G.F. Tomaselli, *Altered gating and local anesthetic block mediated by residues in the I-S6 and II-S6 transmembrane segments of voltage-dependent Na+ channels.* Mol Pharmacol, 2003. **64**(3): p. 741-52.

56.   Nau, C., S.Y. Wang, and G.K. Wang, *Point mutations at L1280 in Nav1.4 channel D3-S6 modulate binding affinity and stereoselectivity of bupivacaine enantiomers.* Mol Pharmacol, 2003. **63**(6): p. 1398-406.

57.   Wang, S.Y., C. Russell, and G.K. Wang, *Tryptophan substitution of a putative D4S6 gating hinge alters slow inactivation in cardiac sodium channels.* Biophys J, 2005. **88**(6): p. 3991-9.

58.   O'Reilly, J.P., S.Y. Wang, and G.K. Wang, *Residue-specific effects on slow inactivation at V787 in D2-S6 of Na(v)1.4 sodium channels.* Biophys J, 2001. **81**(4): p. 2100-11.

59.   Tanguy, J. and J.Z. Yeh, *BTX modification of Na channels in squid axons. I. State dependence of BTX action.* J Gen Physiol, 1991. **97**(3): p. 499-519.

60.   Nau, C. and G.K. Wang, *Interactions of local anesthetics with voltage-gated Na+ channels.* J Membr Biol, 2004. **201**(1): p. 1-8.

61.   Carroll, I., *Intravenous lidocaine for neuropathic pain: diagnostic utility and therapeutic efficacy.* Curr Pain Headache Rep, 2007. **11**(1): p. 20-4.

62.   Fozzard, H.A., P.J. Lee, and G.M. Lipkind, *Mechanism of local anesthetic drug action on voltage-gated sodium channels.* Curr Pharm Des, 2005. **11**(21): p. 2671-86.

63.   Sandtner, W., et al., *Lidocaine: a foot in the door of the inner vestibule prevents ultra-slow inactivation of a voltage-gated sodium channel.* Mol Pharmacol, 2004. **66**(3): p. 648-57.

64.   O'Leary, M.E. and R. Horn, *Internal block of human heart sodium channels by symmetrical tetra-alkylammoniums.* J Gen Physiol, 1994. **104**(3): p. 507-22.

65.   Vedantham, V. and S.C. Cannon, *Rapid and slow voltage-dependent conformational changes in segment IVS6 of voltage-gated Na(+) channels.* Biophys J, 2000. **78**(6): p. 2943-58.

66.   Holmgren, M., et al., *On the use of thiol-modifying agents to determine channel topology.* Neuropharmacology, 1996. **35**(7): p. 797-804.

67.   Richmond, J.E., et al., *Slow inactivation in human cardiac sodium channels.* Biophys J, 1998. **74**(6): p. 2945-52.

68.   Vilin, Y.Y., E. Fujimoto, and P.C. Ruben, *A single residue differentiates between human cardiac and skeletal muscle Na+ channel slow inactivation.* Biophys J, 2001. **80**(5): p. 2221-30.

69.   Zhang, Z., et al., *A negatively charged residue in the outer mouth of rat sodium channel determines the gating kinetics of the channel.* Am J Physiol Cell Physiol, 2003. **284**(5): p. C1247-54.

70.   Benitah, J.P., et al., *Molecular dynamics of the sodium channel pore vary with gating: interactions between P-segment motions and inactivation.* J Neurosci, 1999. **19**(5): p. 1577-85.

71.   Xiong, W., et al., *A conserved ring of charge in mammalian Na+ channels: a molecular regulator of the outer pore conformation during slow inactivation.* J Physiol, 2006. **576**(Pt 3): p. 739-54.

72. Hilber, K., et al., *Selectivity filter residues contribute unequally to pore stabilization in voltage-gated sodium channels.* Biochemistry, 2005. **44**(42): p. 13874-82.

73. Todt, H., et al., *Ultra-slow inactivation in mu1 Na+ channels is produced by a structural rearrangement of the outer vestibule.* Biophys J, 1999. **76**(3): p. 1335-45.

74. Struyk, A.F. and S.C. Cannon, *Slow inactivation does not block the aqueous accessibility to the outer pore of voltage-gated Na channels.* J Gen Physiol, 2002. **120**(4): p. 509-16.

75. Liu, Y., M.E. Jurman, and G. Yellen, *Dynamic rearrangement of the outer mouth of a K+ channel during gating.* Neuron, 1996. **16**(4): p. 859-67.

76. Ong, B.H., G.F. Tomaselli, and J.R. Balser, *A structural rearrangement in the sodium channel pore linked to slow inactivation and use dependence.* J Gen Physiol, 2000. **116**(5): p. 653-62.

77. Tikhonov, B.S.Z., *Molecular Modeling of Slow Inactivation and State-Dependent Drug Binding in Sodium Channels.* Biophysical Society Abstract, 2007.

78. Molina, A., A.G. Castellano, and J. Lopez-Barneo, *Pore mutations in Shaker K+ channels distinguish between the sites of tetraethylammonium blockade and C-type inactivation.* J Physiol, 1997. **499 (Pt 2)**: p. 361-7.

79. Lopez-Barneo, J., et al., *Effects of external cations and mutations in the pore region on C-type inactivation of Shaker potassium channels.* Receptors Channels, 1993. **1**(1): p. 61-71.

80. Townsend, C. and R. Horn, *Effect of alkali metal cations on slow inactivation of cardiac Na+ channels.* J Gen Physiol, 1997. **110**(1): p. 23-33.

81. Rudy, B., *Inactivation in Myxicola giant axons responsible for slow and accumulative adaptation phenomena.* J Physiol, 1981. **312**: p. 531-49.

82. Collins, C.A., E. Rojas, and B.A. Suarez-Isla, *Activation and inactivation characteristics of the sodium permeability in muscle fibres from Rana temporaria.* J Physiol, 1982. **324**: p. 297-318.

83. Ruff, R.L., L. Simoncini, and W. Stuhmer, *Slow sodium channel inactivation in mammalian muscle: a possible role in regulating excitability.* Muscle Nerve, 1988. **11**(5): p. 502-10.

84. Ruff, R.L., L. Simoncini, and W. Stuhmer, *Comparison between slow sodium channel inactivation in rat slow- and fast-twitch muscle.* J Physiol, 1987. **383**: p. 339-48.

85. Simoncini, L. and W. Stuhmer, *Slow sodium channel inactivation in rat fast-twitch muscle.* J Physiol, 1987. **383**: p. 327-37.

86. Featherstone, D.E., J.E. Richmond, and P.C. Ruben, *Interaction between fast and slow inactivation in Skm1 sodium channels.* Biophys J, 1996. **71**(6): p. 3098-109.

87. Fleidervish, I.A., A. Friedman, and M.J. Gutnick, *Slow inactivation of Na+ current and slow cumulative spike adaptation in mouse and guinea-pig neocortical neurones in slices.* J Physiol, 1996. **493 (Pt 1)**: p. 83-97.

88. Barela, A.J., et al., *An epilepsy mutation in the sodium channel SCN1A that decreases channel excitability.* J Neurosci, 2006. **26**(10): p. 2714-23.

89.   Clarkson, C.W., T. Matsubara, and L.M. Hondeghem, *Slow inactivation of Vmax in guinea pig ventricular myocardium.* Am J Physiol, 1984. **247**(4 Pt 2): p. H645-54.

90.   Saikawa, T. and E. Carmeliet, *Slow recovery of the maximal rate of rise (Vmax) of the action potential in sheep cardiac Purkinje fibers.* Pflugers Arch, 1982. **394**(1): p. 90-3.

91.   Payet, M.D., *Effect of lidocaine on fast and slow inactivation of sodium current in rat ventricular cells.* J Pharmacol Exp Ther, 1982. **223**(1): p. 235-40.

92.   Wang, D.W., et al., *Enhanced Na(+) channel intermediate inactivation in Brugada syndrome.* Circ Res, 2000. **87**(8): p. E37-43.

CHAPTER 2

TEMPERATURE DEPENDENT DEFECTS OF SODIUM CHANNEL SLOW INACTIVATION FOR AN ATYPICAL FORM OF PERIODIC PARALYSIS PLUS MYOTONIA.

Jadon Webb and Stephen C. Cannon

(Adapted from a paper submission to *Journal of Neurology*)

2.1   Abstract

Background: Missense mutations of the skeletal muscle voltage-gated sodium channel (Nav1.4) are an established cause of several clinically distinct forms of periodic paralysis and myotonia. The mechanistic basis for the phenotypic variability of these allelic disorders of muscle excitability remains unknown. An atypical phenotype with cold-induced hypokalemic paralysis and myotonia at warm temperatures was reported to segregate with the P1158S mutation. *Objective*: This study extends the functional characterization of the P1158S mutation and tests the specific hypothesis that impairment of Na channel slow inactivation is a common feature of periodic paralysis. *Methods*: Mutant Nav1.4 channels (P1158S) were transiently expressed in HEK cells and

characterized by voltage-clamp studies of Na currents. *Results*: Wildtype and P1158S channels displayed comparable behavior at 37 $^{\circ}$C, but upon cooling to 25 $^{\circ}$C mutant channels activated at more negative potentials and slow inactivation was destabilized. *Conclusions*: Consistent with other Nav1.4 mutations associated with a paralytic phenotype, the P1158S mutation disrupts slow inactivation. The unique temperature sensitivity of the channel defect may contribute to the unusual clinical phenotype.

2.2   *Introduction*

Missense mutations in the voltage-gated sodium channel of skeletal muscle (Nav1.4) have been shown to cause a variety of clinical disorders in which the derangement of muscle excitability is manifest as myotonia or periodic paralysis [1, 2]. The spectrum of disorders includes those with myotonia only (potassium aggravated myotonia - PAM), myotonia plus periodic paralysis (paramyotonia congenita - PMC and hyperkalemic periodic paralysis - HyperPP) or only attacks of paralysis (hypokalemic periodic paralysis type 2 – HypoPP-2). The mechanistic basis for the phenotypic variability in this group of allelic disorders of Nav1.4 is not fully established and is of great importance for understanding the regulation of skeletal muscle excitability and for developing improved approaches for the clinical management of these disorders.

The occurrence of atypical clinical presentations provides an opportunity to gain additional insights into these genotype – phenotype associations. Sugiura and colleagues described an unusual syndrome of myotonia during warm weather for which the predominate feature changed in cold weather to periodic paralysis without myotonia [3].

The phenotype was inherited as a dominant trait in a large Japanese family with affected members in 5 generations and was associated with a missense mutation in Nav1.4 for which proline 1158 was replaced by serine (P1158S). Unlike the classical presentation of PMC, the myotonia was not aggravated by repeated muscular activity and the paralytic attacks were associated with hypokalemia. Myotonia is not a feature of HypoPP, and when present is considered a basis for excluding this diagnosis [4]. The unusual clinical presentation with P1158S is of additional interest in light of the recent discovery that loss-of-function mutations in Nav1.4 may cause HypoPP [5-7]; whereas gain-of-function changes are associated with HyperPP, PMC, and PAM [1].

Sugiura tested the functional consequences for P1158S and reported a novel temperature dependent enhancement of mutant channel activation, manifest as a 10 mV leftward (hyperpolarized) shift in the voltage dependence of activation upon cooling from 32 $^{\circ}$C to 22 $^{\circ}$C [8]. Slow inactivation gating was not examined for P1158S in this initial study. Abnormalities in slow inactivation of Nav1.4 have been shown to predispose affected muscle to depolarization-induced attacks of periodic paralysis, but without increased risk for myotonia. Moreover, disrupted slow inactivation is associated with weakness in the HyperPP-PMC complex [9, 10] whereas enhanced slow inactivation is implicated in attacks of weakness for HypoPP type 2 [6]. Because the clinical phenotype associated with P1158S has unusual features of both PMC and HypoPP, I re-examined the functional consequences of P1158S, particularly with regard to slow inactivation.

2.3   *Methods*.

2.3.1 Site-directed mutagenesis. The cDNA for the human skeletal muscle sodium channel (Nav1.4) was provided in the mammalian expression construct pRc/CMV-hSkM1 by Prof. A. L. George, Jr. [11]. The P1158S missense mutation was introduced with the QuikChange[TM] site-directed mutagenesis kit (Stratagene, La Jolla, CA), and was confirmed by sequencing both strands in the regions flanking site 1158.

2.3.2 Sodium channel expression. Transient expression of skeletal muscle sodium channels in human embryonic kidney (HEK) cells and was performed as described previously [12]. Briefly, normal WT or mutant sodium channel Nav1.4 plasmid (0.25 μg/35-mm dish) was cotransfected with the human β_1 accessory subunit [13] at threefold molar excess over Nav1.4, and with a CD8 marker (0.15 μg/35-mm dish) using the calcium phosphate method. After 36 to 72 hours, HEK cells were trypsinized and passaged to 12-mm round glass coverslips for electrophysiological recording. Individual transfection-positive cells were identified by labeling with anti-CD8 antibody cross-linked to microbeads (Dynal, Great Neck, NY) [14].

2.3.3 Whole-cell recording. Na^+ currents were recorded using conventional whole-cell voltage-clamp techniques as described previously [12]. Current was measured with an Axopatch 200A amplifier (Axon Instruments, Foster City, CA), filtered at 5 kHz and digitally sampled at 100 kHz using pClamp 9.0 (Axon Instruments). The pipette (internal) solution contained 105 mM CsF, 35 mM NaCl, 10 mM EGTA, and 10 mM Cs-

HEPES (pH 7.4). Fluoride was used in the pipette to prolong seal stability. The bath solution contained 140 mM NaCl, 4 mM KCl, 2 mM $CaCl_2$, 1 mM $MgCl_2$, 2.5 mM glucose, and 10 mM Na-HEPES (pH 7.4). Recordings were made in a temperature-controlled chamber that was regulated to either 25°C or 37 ^{o}C . Analysis was restricted to cells with maximal peak Na current amplitudes between 0.5 - 15 nA to minimize the effects of endogenous background currents or series resistance artifacts. A stabilization period of 10 minutes was employed after establishing whole-cell access to allow for the leftward (hyperpolarizaed) shift in channel gating that occurs with whole-cell recordings. In addition, the sequence of applying different voltage protocols was kept constant so that characterization of each gating feature was determined at approximately the same time after establishing whole-cell access.

2.3.4 Data analysis. Sodium currents were analyzed with ClampFit 9.0 (Axon Instruments), and parameter estimation for fits of the reduced data was performed with Origin 1.6 (Microcal, Northhampton, MA). The steady-state voltage dependence of activation and inactivation was quantified by fitting the relative peak current to a Boltzmann function with a characteristic midpoint ($V_{1/2}$) and slope factor (k): $I/I_{max} = 1/[1 + \exp((V-V_{1/2})/k)]$. Kinetic data for entry to slow inactivation were fit to a single-exponential decay, whereas adequate fits for recovery required a double-exponential function with two time constants. Symbols with error bars indicate mean $\pm$ SEM in all figures.

2.4   *Results.*

Although the primary question to be addressed in this study was whether slow inactivation was affected by the P1158S mutation, we also examined activation and fast inactivation to confirm the mutation-dependent changes with cooling reported by Sugiura *et al*. [8].   The expression levels of the wild-type Nav1.4 (WT) and P1158S mutant channels were comparable, as reflected by the mean peak current elicited at -10 mV (3.78 nA $\pm$ .71, n = 11 for WT, 4.01 nA $\pm$ .85, n = 10 for P1158S).   In agreement with the report by Sugiura *et al*. [8], I observed a temperature-dependent shift in the voltage the voltage dependence of activation for mutant channels. No difference in activation was detectable at 37 $^{\circ}$C (midpoint of the conductance-voltage relation was -39.4 mV $\pm$ 1.5, n = 5 for WT; and -39.0 mV $\pm$ 1.8, n = 5 for P1158S). Upon cooling to 25 $^{\circ}$C, activation of P1158S mutant channels was shifted -5 mV (hyperpolarized) relative to WT (-26.7 mV $\pm$ 1.5, n = 6 for WT compared to -31.9 mV $\pm$ 1.9, n = 7 for P1158S, p = 0.045; (Figure 1).

Fast inactivation was not substantially affected by the P1158S mutation. At the provocative temperature of 25 $^{\circ}$C, the voltage dependence of fast inactivation was comparable for WT and P1158S channels (midpoint of fast inactivation -73.1 mV $\pm$ 1.1, n = 7 for WT and -74.9 mV $\pm$ 1.6, n = 9 for P1158S, p = 0.39), and I did not detect the -5 mV shift reported previously [8]. The rate of fast inactivation was slower for P1158S channels (time constant at strongly depolarized voltages > 40 mV was 0.11 msec $\pm$ 0.002 for WT and 0.14 msec $\pm$ 0.007 for P1158S). While this 1.3-fold slowing is a robust observation (p < 0.005) and comparable to the observations reported by Sugiura et al. [8], the functional consequence on muscle fiber excitability is expected to be negligible since

impairment in the speed of fast inactivation on the order of 3- to 5-fold is required to create susceptibility to myotonia [15, 16]. Overall, we agree with Sugiura and colleagues [8] that the most important alteration of fast gating properties for P1158S mutant channels is a hyperpolarized shift of activation at cool temperatures that is absent at warmer (37 $^{\circ}$C) temperatures.

Slow inactivation was studied with paired-pulse voltage protocols. In the first conditioning pulse, a prolonged step of depolarization was applied to induce slow inactivation. The cell was then briefly hyperpolarized (20 ms at -120 mV) to remove fast inactivation, and the extent of slow inactivation was measured as the peak Na current amplitude elicited by a second test pulse, relative to the maximal response recorded in the absence of a conditioning pulse. The onset of slow inactivation was measured as the relative decrement in the peak available Na current (Figure 2A) produced by conditioning the cell at 0 mV for varying durations (from 10 ms to 15 s). At 25 $^{\circ}$C, the maximal extent of slow inactivation was reduced for the P1158S mutant, as shown by the higher amplitude of the relative current for the longest conditioning pulse durations (fraction not slow inactivated by 15 sec was 0.19 ± 0.012 for WT and 0.27 ± 0.012 for P1158S, $p <$ 0.0005). The kinetics of slow inactivation onset was quantified by fitting the data with a single exponential to determine the time constant of entry (curves in Figure 2A). The entry time course did not differ between WT (720 ± 47 msec) and P1158S mutants (810 ± 70 msec; $p = 0.38$). At 37 $^{\circ}$C the onset of slow inactivation was much more rapid as expected (notice the time axis in Figure 2A, left), but again there was no difference the rate of onset for slow inactivation for WT compared to mutant channels. In addition, at

37 $^{\circ}$C the difference in the maximal extent of slow inactivation between WT and P1158S channels was reduced.

Recovery from slow inactivation was measured after a conditioning pulse to 0 mV for 30 s at 25 $^{\circ}$C and 2 s at 37 $^{\circ}$C. The cell was then returned to the recovery potential (− 120 mV), and a series of brief test pulses (-10 mV for 3 ms) were applied after recovering for 1, 2, 4… ms and extending to 30 s (Figure 2B, top). Recovery was monitored as amplitude of the peak current relative to a control response elicited without a conditioning step depolarization. Figure 2B (left) shows the recovery data for the P1158S at 25 $^{\circ}$C were shifted upward, which was due to the greater fraction of mutant channels resistant to slow inactivation at the end of the conditioning pulse (asymptote for short recovery intervals at the bottom left of the graph: 0.19 ± 0.02, n = 4 for P1185S versus 0.065 ± 0.005, n = 4 for WT; p = 0.0018). The time course of slow recovery, however, was indistinguishable between P1158S and WT, and contained two exponential components, Tau_1 = 97 ms (~ 80% of channels that were slow-inactivated) and Tau_2 = 2.8 s (~20%). At 37 $^{\circ}$C, all aspects of recovery from slow inactivation were identical for P1158S and WT channels as shown by the superposition of data in Figure 3B (right).

The voltage-dependence of slow inactivation at steady-state was measured by application of long-duration conditioning pulses (2 sec at 37 $^{\circ}$C or 15 sec at 25 $^{\circ}$C) at voltages ranging from -120 to 0 mV, in 10 mV steps. A repolarizing step to -120 mV for 20 ms was applied to enable recovery from fast inactivation, followed by a test pulse to -10 mV to measure the available peak Na current. At 25 $^{\circ}$C, the maximal extent of slow inactivation at strongly depolarized potentials was reduced for P1158S (larger remaining

relative current in Figure 3 left; WT 0.14 ± 0.010 and P1158S 0.24 ± 0.013; $p < 0.0005$).

In addition, the voltage-dependence of slow inactivation was mildly shifted toward more

depolarized potentials for the P1158S mutant (half inactivated at -63.2 ± 0.38 mV for WT

and -60.5 ± 0.46 mV for P1158S, $p < 0.005$). At 37 ^{o}C, however, the voltage dependence

of slow inactivation was comparable for WT and P1158S (Figure 3, right), and none of

the parameter values were statistically different for the two fitted curves ($p > 0.05$).

2.5   *Discussion*.

Mutations of Nav1.4 have been associated with a spectrum of allelic disorders of

muscle excitability that span a range of phenotypes including myotonia, periodic

paralysis (both hyperkalemic and hypokalemic), and congenital myasthenic syndrome

[1]. For any given mutation, however, the phenotype is fairly consistent among affected

members in a family or even between unrelated families. This genotype – phenotype

correlation has led to the notion that specific types of biophysical defects in mutant

Nav1.4 channels produce myotonia, for example, whereas other defects lead to paralysis.

One of the most consistent associations to emerge from this analysis is that Nav1.4

mutations that disrupt slow inactivation increase the susceptibility to periodic paralysis

due to sarcolemmal depolarization and loss of excitability [9, 10, 17]. In fact, for every

Nav1.4 mutation in which voltage-clamp studies have identified a defect of slow

inactivation, periodic paralysis is a prominent feature of the clinical phenotype (Figure 4).

The reverse is not true; not all mutations associated with periodic paralysis have a recognized defect in slow inactivation. The present study now establishes that P1158S also has impaired slow inactivation. Moreover, a pattern is emerging wherein all of the paralysis-associated mutations that disrupt slow inactivation are at the cytoplasmic end of the 5th or 6th transmembrane segments in domains II or IV, and now III (Figure 4), which are predicted to be the inner vestibule of the ion-conducting pore. The severity of the defect is comparable to that observed for other Nav1.4 mutations in hyperkalemic periodic paralysis, and has been shown by computer simulation to be sufficient to increase the susceptibility to depolarization-induced loss of excitability [18]. A hyperpolarized shift of activation, as observed for P1158S channels, also contributes to the aberrant persistent Na current that depolarizes an affected fiber. These two gain-of-function defects will act synergistically to increase the propensity for attacks of periodic paralysis.

The classification of the clinical phenotype observed in patients with the P1158S mutation was problematic [3]. The concurrence of myotonia and periodic paralysis suggested either paramyotonia congenita or hyperkalemic periodic paralysis, and the presence of myotonia would be considered by most experts to be an exclusionary criterion for hypokalemic periodic paralysis [19]. However, the venous potassium was low during several spontaneous attacks of weakness and daily K supplementation (16 mEq) alleviated the attacks of weakness. Myotonia was prominent during warm summer months and was reduced in winter during which attacks of paralysis were more common. Paradoxical aggravation of myotonia with repeated effort, i.e. paramyotonia, was not present. The unusual temperature sensitivity of the gating defect in P1158S mutant

channels may account for the atypical clinical phenotype. Furthermore, we propose that

P1158S should be classified as a variant of the PMC-HyperPP complex because P1158S

channels share overlap in the biophysical profile of the gating defects in this group rather

than HypoPP. More specifically, the gating defects reported for Nav1.4 in HypoPP Type

2 all share the common feature of loss-of-function changes due to enhanced inactivation

(either fast or slow) [5, 6]. Conversely, Nav1.4 mutations in the PMC-HyperPP complex

all have gain-of-function changes due to either impaired inactivation or enhanced

activation. P1158S causes gain-of-function changes and we propose the following

mechanism for the unusual clinical phenotype. Myotonia at warm temperatures must

arise from residual enhancement of activation (left shift of voltage dependence) or the

small persistent current reported by Sugiura et al. [8], either of which has been shown by

computer simulation to promote myotonic discharges, whereas simulations of disrupted

slow inactivation do not. With cooling, the leftward shift of activation becomes more

pronounced (Figure 1) slow inactivation becomes impaired (Figures 2 and 3), and

together these defects synergistically increase the risk of a persistent Na current that gives

rise to stable depolarization of the resting potential and loss of excitability with paralysis.

Mechanistically, the critical feature is the aggravation of the gain-of-function defects by

cooling. This scenario is consistent with computer simulations that have demonstrated a

transition from normal excitability to myotonia, to periodic paralysis as the severity of Na

channel gain-of-function defects is gradually increased [20].

Slow inactivation is cumbersome to study experimentally, which has probably

contributed to the scarcity of any published studies on the temperature sensitivity of this

gating process [21]. In this context, it is notable that the temperature sensitivity for the

66

midpoint in the voltage dependence of slow inactivation is surprisingly much greater than for that of fast inactivation, even for WT channels. For the 12 $^{\circ}$C temperature change used in these studies, the midpoint of slow inactivation of WT channels shifted by 15.8 mV whereas fast inactivation shifted by only 2.7 mV. While the temperature sensitivity for the voltage dependence of slow inactivation may be large in absolute terms, it is the relative difference between WT and P1158S channels at 25 $^{\circ}$C that we propose is responsible for producing the increased susceptibility to periodic paralysis.

2.6 *References*

1. Cannon, S.C., *Pathomechanisms in channelopathies of skeletal muscle and brain.* Annu Rev Neurosci, 2006. **29**: p. 387-415.

2. Lehmann-Horn, F. and K. Jurkat-Rott, *Voltage-gated ion channels and hereditary disease.* Physiol Rev, 1999. **79**(4): p. 1317-72.

3. Sugiura, Y., et al., *Temperature-sensitive sodium channelopathy with heat-induced myotonia and cold-induced paralysis.* Neurology, 2000. **54**(11): p. 2179-81.

4. Gasser, T., et al., *EFNS Task Force on Molecular Diagnosis of Neurologic Disorders: guidelines for the molecular diagnosis of inherited neurologic diseases. Second of two parts.* Eur J Neurol, 2001. **8**(5): p. 407-24.

5. Jurkat-Rott, K., et al., *Voltage-sensor sodium channel mutations cause hypokalemic periodic paralysis type 2 by enhanced inactivation and reduced current.* Proc Natl Acad Sci U S A, 2000. **97**(17): p. 9549-54.

6. Struyk, A.F., et al., *The human skeletal muscle Na channel mutation R669H associated with hypokalemic periodic paralysis enhances slow inactivation.* J Neurosci, 2000. **20**(23): p. 8610-7.

7. Carle, T., et al., *Gating defects of a novel Na+ channel mutant causing hypokalemic periodic paralysis.* Biochem Biophys Res Commun, 2006. **348**(2): p. 653-61.

8. Sugiura, Y., et al., *Cold induces shifts of voltage dependence in mutant SCN4A, causing hypokalemic periodic paralysis.* Neurology, 2003. **61**(7): p. 914-8.

9. Cummins, T.R. and F.J. Sigworth, *Impaired slow inactivation in mutant sodium channels.* Biophysical Journal, 1996. **71**: p. 227-236.

10. Hayward, L.J., G.M. Sandoval, and S.C. Cannon, *Defective slow inactivation of sodium channels contributes to familial periodic paralysis.* Neurology, 1999. **52**(7): p. 1447-53.

11. Chahine, M., et al., *Functional expression and properties of the human skeletal muscle sodium channel.* Pflugers Archiv - European Journal of Physiology, 1994. **427**(1-2): p. 136-42.

12. Hayward, L.J., R.H. Brown, Jr., and S.C. Cannon, *Inactivation defects caused by myotonia-associated mutations in the sodium channel III-IV linker.* Journal of General Physiology, 1996. **107**(5): p. 559-576.

13. McClatchey, A.I., et al., *The cloning and expression of a sodium channel beta 1-subunit cDNA from human brain.* Human Molecular Genetics, 1993. **2**(6): p. 745-9.

14. Jurman, M.E., et al., *Visual identification of individual transfected cells for electrophysiology using antibody-coated beads.* Biotechniques, 1994. **17**: p. 874-881.

15. Green, D., A. George, and S. Cannon, *Human sodium channel gating defects caused by missense mutations in S6 segments associated with myotonia: S804F and V1293I.* Journal of Physiology, 1998. **510**: p. 685-694.

16. Yang, N., et al., *Sodium channel mutations in paramyotonia congenita exhibit similar biophysical phenotypes in vitro.* Proceedings of the National Academy of Sciences of the United States of America, 1994. **91**(26): p. 12785-9.

17.   Bendahhou, S., et al., *Impairment of slow inactivation as a common mechanism for periodic paralysis in DIIS4-S5.* Neurology, 2002. **58**(8): p. 1266-72.

18.   Hayward, L.J., R.H. Brown, Jr., and S.C. Cannon, *Slow inactivation differs among mutant Na channels associated with myotonia and periodic paralysis.* Biophysical Journal, 1997. **72**: p. 1204-1219.

19.   Lehmann-Horn, F., R. Rüdel, and K. Jurkat-Rott, *Nondystrophic myotonias and periodic paralyses*, in *Myology*, A.G. Engel and C. Franzini-Armstrong, Editors. 2004, McGraw-Hill: New York. p. 1257-1300.

20.   Cannon, S.C., R.H. Brown, Jr., and D.P. Corey, *Theoretical reconstruction of myotonia and paralysis caused by incomplete inactivation of sodium channels.* Biophysical Journal, 1993. **65**(1): p. 270-88.

21.   Ruff, R.L., *Effects of temperature on slow and fast inactivation of rat skeletal muscle Na(+) channels.* Am J Physiol, 1999. **277**(5 Pt 1): p. C937-47.
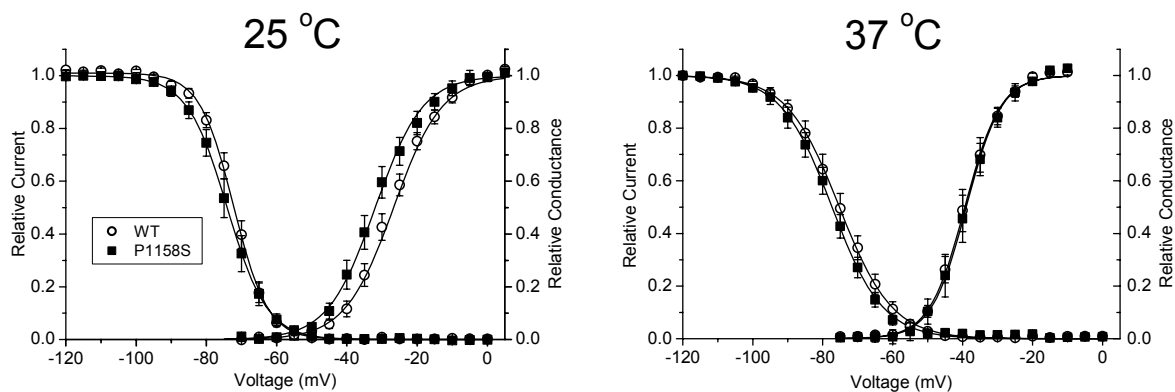
3.7 *Figures*

FIGURE 1 Voltage dependence of activation and fast inactivation. Activation was shifted -5 mV for P1158S mutants at 25 $^{\circ}$C, but was indistinguishable for WT and P1158S at 37 $^{\circ}$C (right-hand curves in each plot). The voltage dependence of fast inactivation was comparable for WT and P1158S channels at both temperatures (left-hand curves in each plot).
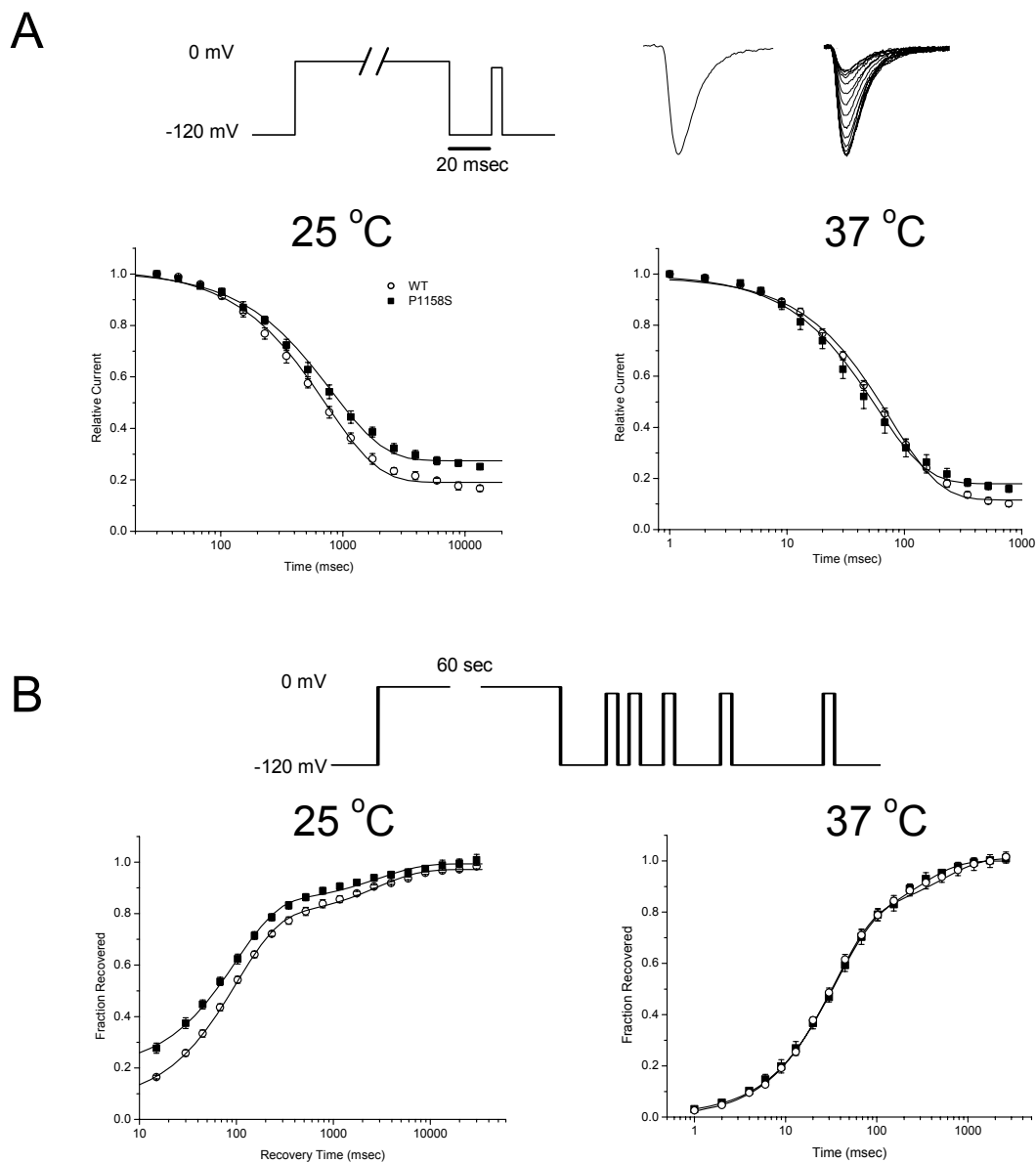
FIGURE 2 Kinetics of sodium channel slow inactivation. (A) Onset of slow inactivation was measured by applying a conditioning pulse to 0 mV of varying duration, followed by a brief hyperpolarization to -120 mV for 20 msec to allow recovery from fast inactivation, and then application of a test depolarization to measure the fractional recovery (pulse protocol, top). Sodium currents (traces at top) show the maximum

current elicited in the absence of a conditioning depolarization (left), and a superposition of traces recorded after progressively longer conditioning pulses, which results in smaller peak currents. Plots show the decrement in relative current as slow inactivation ensues with longer duration conditioning pulses (logarithmic scale). Entry to slow inactivation is comparable for P1158S and WT channels at 37 °C, but is less complete for P1158S mutants at 25 °C. (B) Recovery from slow inactivation was monitored by brief test depolarizations after a prolonged conditioning pulse (30 s at 25 °C or 2 sec at 37 °C) to maximally slow inactivate channels (top). At 25 °C, recovery of P1158S channels precedes that of WT, primarily because the extent of slow inactivation was less complete for P1158S (larger fractional recovery at the shortest recovery times).
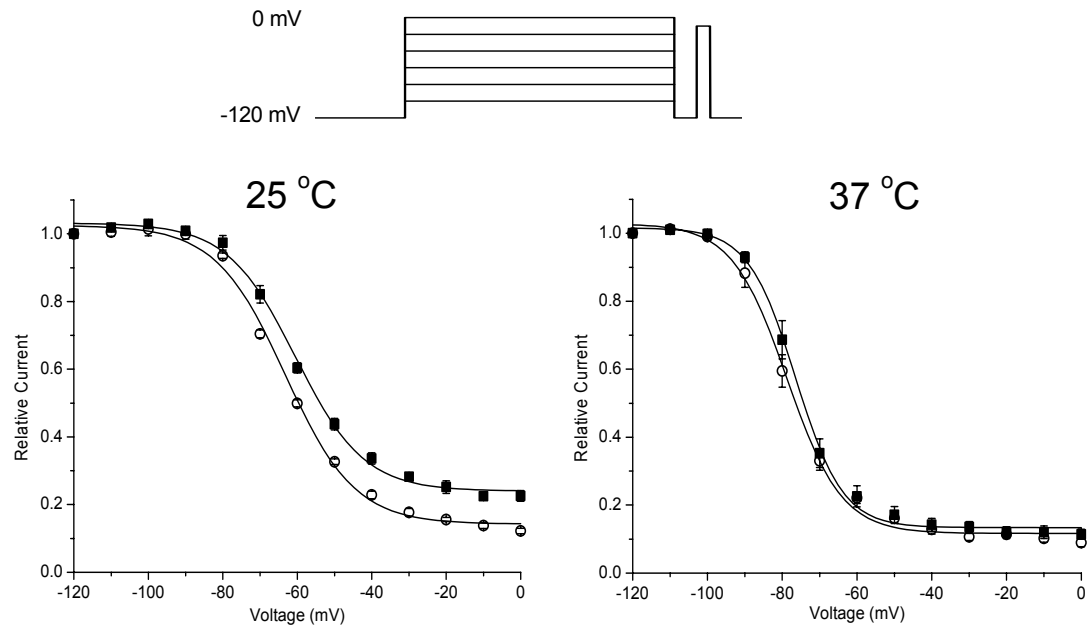
FIGURE 3 Voltage dependence of steady-state slow inactivation. Relative available current decreased with progressively more positive conditioning pulses (inset at top) that caused a larger fraction of channels to become slow inactivated. At 25 °C, the voltage dependence of slow inactivation is shifted toward more positive potentials and the extent of slow inactivation at strongly depolarized potentials is reduced (larger available relative current).
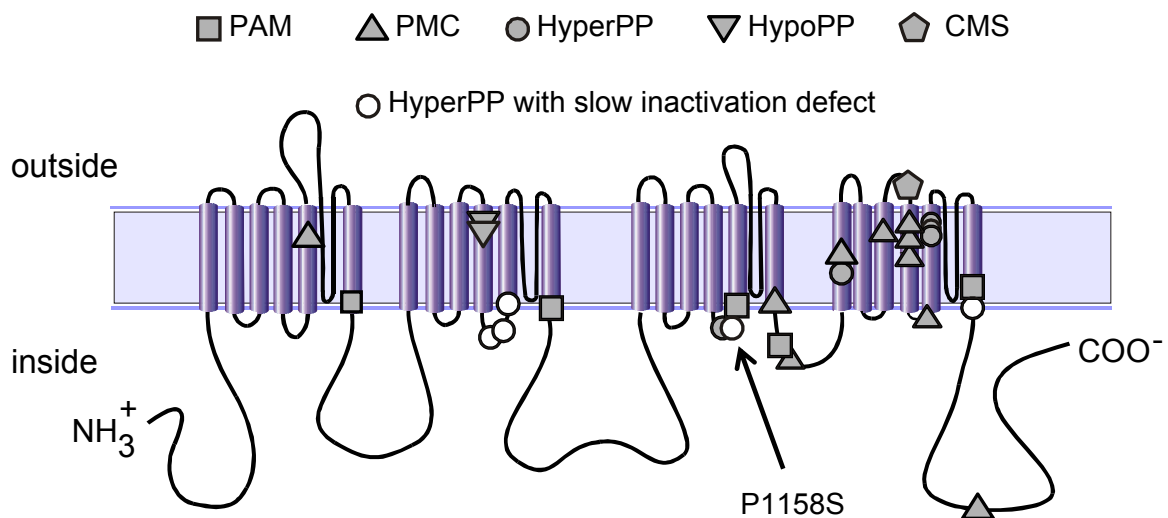
FIGURE 4 Membrane-spanning model for Nav1.4 topology and location of missense mutations associated with hyperkalemic periodic paralysis (HyperPP), paramyotonia congenita (PMC), potassium aggravated myotonia (PAM), hypokalemic periodic paralysis type 2 (HypoPP-2), or congenital myasthenic syndrome (CMS). Mutations previously known to disrupt slow inactivation are highlighted and are all associated with HyperPP.

CHAPTER 3

CO-EXPRESSION OF THE B1 SUBUNIT IMPEDES SODIUM CHANNEL SLOW INACTIVATION, INDEPENDENT OF COUPLING TO FAST INACTIVATION.

Jadon Webb, Fen-fen Wu, and Stephen C. Cannon

(Adapted from a paper being submitted to *Biophysical Journal*)

3.1 Abstract

In response to sustained depolarization or prolonged bursts of activity in spiking cells, sodium channels enter long-lived non-conducting states from which recovery at hyperpolarized potentials occurs over hundreds of milliseconds to seconds. The molecular basis for this slow inactivation remains unknown, although many functional domains of the channel have been implicated. Expression studies in Xenopus oocytes have suggested a role for the accessory $\beta 1$ subunit in slow inactivation, but the effect has been variable. Moreover, a role for the $\beta 1$ subunit on slow inactivation has not been fully characterized in mammalian cells. We examined the effects of the $\beta 1$ subunit on slow inactivation of skeletal muscle (Nav1.4) sodium channels expressed in HEK cells. Co-expression of the $\beta 1$ subunit impeded slow inactivation such that the voltage dependence right shifted (depolarized) and fewer channels occupied the I_S slow

inactivated state. Mutational studies showed that this effect was independent of the negative coupling between fast and slow inactivation. The β1 mutation in the extracellular Ig-like domain associated with epilepsy, C121W, abolished this effect on slow inactivation, which may contribute to the increased risk of seizures.

3.2   Introduction

Slow inactivation is a universal feature of voltage-gated Na channels wherein after a sustained depolarization recovery from inactivation occurs over hundreds of msec to seconds [1]. Slow inactivation is functionally important for setting the fractional availability of channels in response to sustained shifts in the resting potential or for regulating cellular excitability in response to prolonged bursts of action potentials [2]. Moreover, defects in slow inactivation contribute to the pathogenesis of human disorders affecting skeletal muscle, heart, and brain [3]. These observations have stimulated many investigations to gain some understanding of the molecular mechanism underlying this slow gating process, but as of yet no structural details or conceptual models have emerged that provide a firm understanding of the conformational changes that cause slow inactivation. The challenge has been that perturbations at many different domains of the channel affect slow inactivation, including the outer vestibule of the pore [4], selectivity filter [5, 6], inner vestibule, S6 segments [7], and voltage sensor domains [8]. Another complexity is that several distinct kinetic components of slow inactivation may be revealed, depending of the specific voltage protocol.

The objective of this study was to clarify the role of the accessory β1 subunit on slow inactivation, and thereby add to the growing knowledgebase that will shape the development of a

mechanistic understanding. The β1 subunit is expressed in brain, peripheral nerve, skeletal muscle, and possibly heart where it forms a non-covalent association with the pore-forming α subunit [9]. The β1 subunit is a single-pass transmembrane protein with an extracellular amino terminus that forms an Ig-like domain important for interacting with cell adhesion molecules and extracellular matrix, and a short intracellular carboxyl tail. The α subunit alone is capable of forming functional voltage-gated Na channels. Co-expression of the β1 subunit increases cell surface expression levels and modulates channel gating. The effect of β1 is most prominent in the Xenopus oocyte expression system, where channels comprised of the α subunit alone have a markedly decreased rate of whole-cell current decay during a test depolarization (~ 5-fold slower than for native channels in mammalian cells), and co-expression of α and β1 subunits results in heteromeric channels that inactivate with fast kinetics comparable to that observed in mammalian cells [10]. The oocyte system has been used to examine the effect of β1 subunit co-expression on slow inactivation, but the results have been conflicting with some reports of enhancement [6] whereas others have reported disruption of slow inactivation [4, 11]. Moreover, the interpretation is limited by the anomalously slow gating of fast inactivation, which has an uncertain relation to slow inactivation.

We have examined the effect of β1 subunit on slow inactivation of human skeletal muscle sodium channels (Nav1.4 α subunit) transiently expressed in a mammalian cell line (HEK293). Co-expression of the β1 subunit mildly impeded slow inactivation, as revealed by enhanced recovery and a depolarized shift in voltage dependence. Additional studies with mutated Nav1.4 α subunits show this effect is independent of the negative coupling between fast and slow inactivation. The β1 subunit mutation associated with generalized epilepsy and febrile seizures (C121W at a critical disulfide link in the extracellular Ig-like domain [12]) abolished the

Webb et al.

modulatory effect on slow inactivation and thereby may be another important gating defect in the pathogenesis of epilepsy.

3.3   Materials and Methods

3.3.1 Construction of plasmids.   The cDNA for the human sodium channel α-subunit (Nav1.4) was kindly provided by A.L. George in plasmid pRc/CMV-hSkM1 [13]. The human sodium channel $\beta1$ subunit cDNA [14] was subcloned into the EcoR1 site of the mammalian expression plasmid pcDNA3.1(+) (Invitrogen, Carlsbad, CA). The C-terminal deletion of the $\beta1$ subunit ($\beta1$/CTdel, deletion of amino acids 185-218) was generated as described previously [10]. Site-directed mutagenesis was performed according to the manufacturer's protocol (QuikChange^{TM} Stratagene, La Jolla, CA) to generate the N-terminal cysteine to tryptophan missense mutation in the $\beta1$ subunit ($\beta1$/C121W) and the domain III-IV loop mutation F1311C in Nav1.4 (α/F1311C). The mutated constructs were sequenced in both directions to confirm the presence of the mutation and to ensure that no other mutations were introduced during the site-directed mutagenesis.

3.3.2 Expression of sodium channels.   Human embryonic kidney cells (HEK293) were transiently transfected with various combinations of α and $\beta1$ subunits, using the calcium phosphate method [15]   Briefly, α-subunit containing plasmid (either wild-type or mutant α/F1311C) at a concentration of 0.2 μg per 35-mm dish was co-transfected with four-fold molar excess $\beta1$-subunit plasmid (wild-type or mutant), as well as a CD8 marker (0.2 μg per 35-mm

dish). After 24–72 hours, cells were trypsinized and passaged to 12-mm round glass cover slips for electrophysiological recording. Individual transfection-positive cells were identified by labeling with anti-CD8 antibody cross-linked to gold microbeads [16] (Dynal, Great Neck, NY).

3.3.3 Whole-cell recording. Na^+ currents were measured with standard whole-cell recording techniques as previously described [15]. Recordings were made with an Axopatch 200A amplifier controlled by pClamp 9.0 (Molecular Devices, Sunnyvale, CA). The output was filtered at 5 kHz and digitally sampled at 50 kHz using a DigiData 1200 Series interface (Molecular Devices). More than 70% of the series resistance was compensated by the analog circuitry of the amplifier and leakage conductance was corrected by digital scaling and subtraction of passive current elicited by hyperpolarizing voltage steps applied from the holding potential. To minimize the effects of small endogenous currents and avoid residual effects from series resistance, only cells with peak currents between 0.5 nA and 15 nA at −10 mV were included. After initially establishing whole-cell access, we often observed an increase in the size of the peak current, as well as a leftward shift in the voltage dependence of activation and fast inactivation. To standardize responses across cells, we waited at least 10 min after gaining whole-cell access before recording.

Patch electrodes were fabricated from borosilicate capillary tubes with a multi-stage puller (Sutter, Novato, CA). The shank of the pipette was coated with Sylgard and the tip was heat-polished to a final tip resistance (in bath solution) of 0.5–1.5 MΩ. The pipette (internal) solution contained (mM): CsF 105, NaCl 35, EGTA 5, and Cs-HEPES 10 (pH 7.4). Fluoride was used in the pipette to prolong seal stability. The bath solution contained (mM): NaCl 140, KCl 4, $CaCl_2$ 2, $MgCl_2$ 1, glucose 2.5, and Na-HEPES 10 (pH 7.4). [2-(Trimethylammonium)

ethyl]methanethiosulfonate Bromide (MTS-ET) (Toronto Research Chemicals, North York, Ontario, Canada) was kept dry in small aliquots and diluted to 500 μM in internal pipette solution immediately before use. Recordings were made at room temperature (24–28°C).

3.3.4 Data analysis. Analysis of raw current traces was performed manually off-line using Clampfit 9.0 (Molecular Devices). Reduced data were then analyzed and plotted in Origin 6.1 (Microcal, Northampton, MA). The voltage-dependence of steady-state slow inactivation was fitted to a Boltzmann function plus a non-zero pedestal (I_0) calculated as $I/I_{PEAK} = (1 − I_0)/[1 + \exp((V − V_{1/2})/k)] + I_0$, where $V_{1/2}$ is the half-maximum voltage and k is the slope factor. The time constant of entry to fast inactivation was measured as the monoexponential decay of currents elicited at −10 mV, as measured between 90% and 10% of the peak current. Data from a series of peak currents undergoing entry to slow inactivation were fit with a monoexponential decay to determine the time constant. Recovery from slow inactivation showed two components, and was fit with a biexponential function. Symbols with error bars indicate means ± S.E.M. Statistical significance was determined by the Student's unpaired t-test with p-values noted in the text.

3.4 Results

While the primary objective of this study was to test for the influence of β1 subunit on slow inactivation of sodium channels expressed in mammalian cells, we also characterized fast gating behavior to explicitly define how accessory subunit expression or mutations in the β1

subunit affected activation and fast inactivation in the HEK cell expression system, which may secondarily influence slow inactivation gating [17, 18].

3.4.1 Activation and fast inactivation. Robust sodium currents with comparable maximal peak current amplitudes were observed in HEK cells transfected with the α subunit only, $\alpha + \beta 1$, or α + either of the two mutant $\beta 1$ subunit constructs (Figure 1A). The voltage dependence of activation was not appreciably affected by coexpression of wild-type or mutant $\beta 1$ subunits, as shown by the superposition of the peak current – voltage data in Figure 1 B.

The kinetics of entry to fast inactivation from the open state was determined by fitting the current decay elicited by step depolarizations from -120 mV to between -40 and +75 mV with a monoexponential time course. Time constants (τ_h) were similar for the Nav1.4 α-subunit expressed alone or coexpressed with WT or mutant $\beta 1$ subunits (Figure 1C). Recovery from fast inactivation was determined by a two-pulse protocol. A 30-msec conditioning pulse to 0 mV was applied to fully fast inactivate channels, followed by a recovery gap to -120 mV for a variable duration, and finally a test pulse to -10 mV to assay availability as the peak Na current. Recovery of the peak Na current as a function of gap duration was fit with a monoexponential function. Recovery time constants at -120 mV were indistinguishable between HEK cells transfected with α-subunit alone or cotransfected with WT $\beta 1$, $\beta 1$/CTdel, or $\beta 1$/C121W (Table 1).

The voltage-dependence of steady-state fast inactivation was measured as the relative peak current elicited after 300 msec conditioning pulses to voltages ranging from -120 to -50 mV. Data were fit with a Boltzmann function for each cell individually and the sets of parameter values for each channel type were compared to WT (Figure 2 and Table 1). Coexpression of WT

β1 or the C-terminal deletion construct (β1/CTdel) both caused a small +5.5 mV ($p < 0.005$) depolarized shift in the half-inactivation voltage ($V_{1/2}$). Co-transfection of the β1 N-terminal mutant (β1/C121W) yielded $V_{1/2}$ results intermediate to α-subunit alone and α + β1. In addition, the slope factor (k) was reduced compared to α + β1 WT ($p < 0.05$).

These data show that channels containing WT β1 and the C-terminal deletion construct β1/CTdel have similar fast inactivation gating behavior, as has been reported in the oocyte expression system where the effects are more prominent [10]; whereas mutation of the extracellular N-terminus disrupts β1 function and results in gating properties more similar to currents observed when the α-subunit alone is expressed [10, 12, 19]. Because transfection of all three β1 subunit constructs (WT, β1/CTdel, β1/C121W) produced a detectable change of fast inactivation, we conclude each of these constructs was expressed and formed heteromeric complexes with the α-subunit at the plasma membrane. This result implies we can test for modulatory effects on slow inactivation for all three β1 subunit constructs, rather than being limited by a null. Finally, these data also show that the effect of exogenously transfected β1 expression is detectable, despite the possible contribution from a low level expression of endogenous β1a splice variants in HEK cells [20].

3.4.2 Steady-state slow inactivation. The voltage-dependence of steady-state slow inactivation was measured using a series of 30-s conditioning pulses to voltages ranging from –120 to 0 mV. Each conditioning pulse was followed by a 20-msec gap at –120 mV to allow full recovery from fast inactivation (time constant ~2 msec, Table 1) before a test depolarization was applied to measure slow inactivation as the reduction in peak current (Fig. 3 *A*). Peak currents elicited by the test pulse were normalized to the maximum available current elicited from a

holding potential of –120 mV. The voltage-dependence measured for a series of conditioning depolarizations was then fit with a Boltzmann function with a non-zero pedestal. Voltage of half-inactivation ($V_{1/2}$) for steady-state slow inactivation was depolarized (right-shifted, Fig. 3) by +10.5 mV upon coexpression of WT β1 ($p < 0.005$). Co-transfection of the β1 C-terminal deletion (β1/CTdel) yielded results similar to WT β1, whereas co-transfection of the N-terminal β1 mutant (β1/C121W) produced channels with a voltage dependence similar to that when the α-subunit alone was expressed. The slope factor (k) was not significantly affected by any condition tested: α $V_{1/2}$ = –61.4 ± 2.1 mV, k = 12.3 ± 1.0 mV, n = 5; α + β1 $V_{1/2}$ = –50.9 ± 0.8 mV, k = 11.7 ± 0.39 mV, n = 5; α + β1/C121W $V_{1/2}$ = –59.0 ± 1.3 mV, k = 12.1 ± 0.82, n = 5; α + β1/CTdel $V_{1/2}$ = –52.9 ± 1.7 mV, k = 11.7 ± 0.51 mV, n = 5. The maximal extent of slow inactivation, I_o as measured at a conditioning voltage of 0 mV, was not statistically different among the various β1 subunit constructs: α 0.076 ± 0.013; α + β1/C121W 0.098 ± 0.0097; α + β1 0.064 ± 0.0051; α + β1/CTdel 0.11 ± 0.014.

3.4.3 Entry to slow inactivation.   The rate of entry to slow inactivation was measured with a sequential entry protocol (Figure 4, *inset*). A conditioning pulse to 0 mV was applied for a variable duration to inactivate Na$^+$ channels. Next, a brief recovery period at –120 mV for 20 msec was applied to allow complete recovery from fast inactivation. Finally, the membrane voltage was stepped to -10 mV to measure the available Na current (fraction non-slow inactivated). Peak current during the test pulse was normalized to the maximal current observed when the conditioning pulse was omitted and averaged data are shown in Figure 4 for each of the β1 constructs. Solid lines show monoexponential fits to the data. The rate of entry to slow inactivation was not affected by coexpression of WT β1 or the β1 C-terminal deletion

(β1/CTdel) in comparison to the data for the α-subunit alone. The β1 N-terminal mutant (β1/C121W), however, prolonged the entry rate by 1.4-fold ($p < 0.05$). Estimated values for the entry time constants were: α 1780 ± 193 msec, $n = 5$; α + β1: 1640 ± 121 msec, $n = 6$; α + β1/C121W: 2470 ± 208 msec, $n = 5$; α + β1/CTdel: 1740 ± 132 msec, $n = 5$.

3.4.4 Recovery from slow inactivation. The time course for recovery of sodium channel availability upon repolarization after prolonged depolarization is the critical defining feature that distinguishes among the multiple components of inactivation described for sodium channels. We measured recovery following conditioning pulses to 0 mV of either 3 s or 30 s duration. This strategy was designed to optimize the sensitivity of examining the two most prominent components: recovery from intermediate inactivation, I_M, with a time course on the order of 200 msec; recovery from slow inactivation, I_S, with a time course on the order of 3 s.

Recovery from slow inactivation at -120 mV was measured with a sequential recovery protocol, in which a series of brief test pulses (3 msec, -10 mV) were applied at progressively longer times after a long conditioning pulse to 0 mV (either 3 s or 30 s). Control experiments verified that the brief repeated excursions to -10 mV did not alter the time course of recovery in comparison to the more laborious technique of measuring a single point along the recovery trajectory and then reapplying the conditioning pulse to reset the level of inactivation before the next test pulse. After a 3 s conditioning pulse (Fig. 5 A), about 75% of channels were slow inactivated, consistent with the entry data shown in Figure 4. Recovery at -120 mV after the initial 20 msec had a dominant exponential component with a time constant of ~200 msec, indicating that channels were in the intermediate state of slow inactivation (I_M). The recovery data were tightly clustered and there was no statistical difference in recovery time constant from

WT (Table 2). Following a 30 s conditioning pulse (Fig. 5 *B*), the recovery after the initial 20 msec had two clearly distinguishable components. The faster component recovered with a time constant of ~200 msec which we interpret as recovery from I_M, and the slower component recovered with a time constant on the order of 15 s which we interpret as channels recovering from the I_S state. The maximal extent of slow inactivation (I_M plus I_S) at the end of the 30 s conditioning pulse was comparable for all β1 constructs tested, as shown by the overlap of data for the initial recovery point at 20 msec in Figure 5B. Similarly, the time constants were not affected by co-expression of the β1 subunit (Table 2). The large difference in recovery behavior was attributable to partitioning of channels among I_M and I_S states. Co-expression of WT β1 or the C-terminal deletion mutation β1/CTdel impeded entry to I_S within the 30 s conditioning pulse. Figure 5C shows the fraction of channels partitioned into I_S, as determined from the bi-exponential fits, was about 0.3 for these constructs, whereas in the absence of β1 co-expression or for the β1/C121W mutation the fraction in I_S was 0.43 (Table 2).

3.4.5   Removal of fast inactivation does not abolish the β1 effect on slow inactivation.   The possibility that the β1 effect on slow inactivation may occur through coupling of fast and slow inactivation was tested with a mutant α-subunit construct that abolished fast-inactivation. The rationale is based on prior observations of negative coupling between fast and slow inactivation. The initial observation was made in squid giant axon internally perfused with pronase, which abolished fast inactivation but slow inactivation persisted and the onset was two-fold faster [18]. Disruption of fast inactivation by mutating the IFM → QQQ motif in the III-IV linker increases the maximal extent of slow inactivation and accelerates the rate of onset for Nav1.4 or Nav1.5 expressed in oocytes [17, 21]. Conversely, the β1 subunit enhances fast

inactivation for many expression systems, especially frog oocytes [9, 10], although this effect was not apparent for the HEK cell studies herein. Nevertheless, the fact that coupling between fast and slow inactivation is firmly established raises the question of whether the β1 impediment of slow inactivation observed herein is dependent upon intact fast inactivation. To test this possibility, we disrupted the sodium channel III-IV loop fast inactivation gate and measured the effects of coexpression of WT β1 on steady-state slow inactivation. Nav1.4 channels with the IFM→QQQ mutation express poorly in HEK cells, and therefore we used an F1311C mutant that expresses reasonably well and has a complete loss of fast inactivation upon intracellular exposure to the thiol cross-linking reagent MTS-ET.

Peak Na current amplitudes were reduced ~10-fold in HEK cells transfected with α/F1311C compared to WT. Addition of 5 μM MTS-ET to the pipette solution produced a dramatic loss of fast inactivation, as shown in Figure 6A. The voltage-dependence of steady-state slow inactivation in MTS-ET modified F1311C channels, with and without co-expression of WT β1, was measured with a 30 s conditioning pulse as described for above. Co-expression of the WT β1 subunit impeded slow inactivation, even in the absence of fast inactivation, as shown by the +8 mV rightward shift ($p < 0.005$) of the data for F1311C + WT β1 channels in Figure 6B. The $V_{1/2}$ and k values for the Boltzmann fits were: F1311C : $V_{1/2} = -59.3 \pm 1.3$ mV, $k = 6.98 \pm 1.54$ mV, $n = 4$; F1311C + β1 $V_{1/2} = -51.0 \pm 1.1$ mV, $k = 4.89 \pm 0.34$, $n = 4$.

3.5   *Discussion*

Webb et al.

A widely-accepted conceptual model of the mechanism by which voltage-gated sodium channels undergo slow inactivation has not yet emerged, despite much effort and the use of a wide variety of experimental approaches. Several lines of evidence implicate the pore, in the region of the selectivity filter [4, 6, 11] or adjacent areas in S6 segments [7, 22], as the critical region that undergoes a conformational change resulting in a non-conducting slow-inactivated state(s). These observations have led to speculation that slow inactivation of sodium channels shares mechanistic features in common with C-type inactivation of Kv channels, for which several lines of evidence are consistent with a model wherein constriction at the outer vestibule of the pore prevents conduction [23, 24], although the inner cavity between the selectivity filter and activation gate also undergoes structural changes [25]. There are some glaring differences for C-type inactivation, however, compared to the properties of slow inactivation for NaV channels, which suggest the molecular mechanisms may share little in common between the two channel types. First, unlike C-type inactivation for Kv channels, there is little evidence for an external foot-in-the door effect that impedes slow inactivation for WT NaV channels (but see [26]). Second, sites in the external vestibule within one residue of the DEKA selectivity filter are accessible to modification by MTS-ET in the (intermediate) slow-inactivated state [27]. Third, manipulations from the internal side of the NaV selectivity filter may have large effects on slow inactivation; such as batrachotoxin binding [28] which is the only modification known to completely remove slow inactivation, mutations in S6 segments [7, 22], or lidocaine acting as an internal foot-in-the door to impede ultra-slow inactivation of K1237E mutant Nav1.4 channels [29].

Given the uncertainty surrounding the mechanism of slow inactivation for NaV channels, we designed the present study to address the more focused question of whether the accessory β1

subunit has a role in slow inactivation of Nav1.4 channels, and if so what domain of β1 is critical for this effect? Several prior studies have characterized the effects of the accessory β1 subunit expression on activation and fast inactivation, [9, 10, 30, 31], and to a lesser extent on slow inactivation [4, 6, 11]. These studies on β1 and slow inactivation were all performed in the oocyte expression system, where the effects of β1 co-expression on fast gating are very prominent. A serious limitation of these studies is that sodium channels comprised of the α subunit only, when expressed in oocytes, have an anomalous slow mode of fast inactivation gating that has kinetic features similar to the "intermediate" form of slow inactivation (I_M), but bears an uncertain relation to true slow inactivation. The anomalous slow mode and I_M are clearly different, as can be distinguished for example with trains of brief test depolarizations which cause a modal shift in gating (from slow to fast) for α-subunit only channels expressed in oocytes, but not α/β1 heteromeric channels. In our view, while studies of slow inactivation on α/β1 heteromeric NaV channels can be performed in the oocyte expression system, the observations on slow gating for α-subunit homomeric channels are difficult, if not impossible, to interpret. Therefore, we used a mammalian expression system (transient transfection in HEK cells) to characterize the effects of β1 subunit co-expression on slow inactivation.

The primary finding of this study is that co-expression of the β1 accessory subunit mildly impedes slow inactivation of Nav1.4 channels expressed in a mammalian cell background. The disruption of slow inactivation by the β1 subunit is manifest by a +10 mV rightward shift in steady-state voltage dependence (Figure 3) and a reduced propensity to partition into the slow-inactivated (I_S) state during a 30 s conditioning pulse (Figure 5B). Notice that a less comprehensive test of slow inactivation recovery would have missed the difference produced by co-expression of the β1 subunit, as shown by the similarity of the responses following a 3 s

conditioning pulse (Figure 5A). Aside from the caveats listed above for the interpretation of NaV slow gating in oocytes, our results in HEK cells are in agreement with two previous oocyte studies showing that co-expression of β1 impedes slow inactivation [4, 11]; whereas a third study concluded just the opposite [6].

Mutational analysis has provided additional insights on the domain of the β1 subunit that was required to modulate slow inactivation. Prior studies on β1 function, based on assays of fast inactivation in the oocyte system, have shown that the cytoplasmic carboxyl tail (residues 185-218) is not required [10], whereas the large extracellular amino terminus has a critical Ig-like fold that when disrupted by mutation causes a total loss of the β1 enhancement of fast inactivation [10, 19]. The present studies on modulation of slow inactivation in HEK cells are precisely concordant with the studies on modulation of fast inactivation: deletion of the entire cytoplasmic terminus does not alter modulation of slow inactivation (β1/CTdel impedes slow inactivation to the same extent as WT β1), whereas the β1/C121W mutation that disrupts a critical disulfide bond in the extracellular Ig-like fold caused a loss of modulatory function. These concordant observations suggested that the effect of β1 on slow inactivation may operate through coupling to fast inactivation. To explore this possibility, we introduced an α-subunit mutation to abolish fast inactivation and then examined the ability of β1 expression to still modulate slow inactivation. Figure 6 shows that even in the absence of fast inactivation, co-expression of the β1 subunit still disrupts slow inactivation. We interpret these data as supportive evidence for a model in which the β1 subunit modulates slow inactivation by impeding occupancy of the I_S state, through α/β interactions in the transmembrane or extracellular domains, and that is independent of β1 effects on fast inactivation. Studies of β1 subunit effects

on gating properties of Nav1.4 / Nav1.5 chimeras expressed in oocytes have suggested an interaction between the extracellular amino terminus of β1 and the α subunit pore loops [6, 32], perhaps through the effect of negative charge on the A/A' strand of the Ig-like fold [19]. This observation fits well with the notion that conformational changes in the pore region are critical for slow inactivation [4, 6, 11], and therefore this interaction site may be the mechanism by which the β1 subunit modulates slow inactivation gating.

The C121W mutation of β1 subunit is a cause of generalized epilepsy with febrile seizures plus, GEFS(+) [12]. Expression studies to explore the pathomechanism in this disorder have revealed a loss of function defect for fast inactivation in that C121W fails to promote the fast mode of inactivation in oocytes [12], despite intact dimerization of the mutant β1 subunit with neuronal α subunits [33]. Our studies herein have identified another functional defect, failure to modulate slow inactivation, which should also be considered to be a contributing factor to the pathogenesis of GESF(+).

Webb et al.

3.6   References

1.   Schauf, C.L., T.L. Pencek, and F.A. Davis, *Slow sodium inactivation in Myxicola axons. Evidence for a second inactive state.* Biophys J, 1976. **16**(7): p. 771-8.
2.   Rudy, B., *Inactivation in Myxicola giant axons responsible for slow and accumulative adaptation phenomena.* J Physiol, 1981. **312**: p. 531-49.
3.   Cannon, S.C., *Slow inactivation of sodium channels: more than just a laboratory curiosity.* Biophys J, 1996. **71**(1): p. 5-7.
4.   Balser, J.R., et al., *External pore residue mediates slow inactivation in mu 1 rat skeletal muscle sodium channels.* J Physiol (Lond), 1996. **494**(Pt 2): p. 431-42.
5.   Vilin, Y.Y., E. Fujimoto, and P.C. Ruben, *A single residue differentiates between human cardiac and skeletal muscle Na+ channel slow inactivation.* Biophys J, 2001. **80**(5): p. 2221-30.
6.   Vilin, Y.Y., et al., *Structural determinants of slow inactivation in human cardiac and skeletal muscle sodium channels.* Biophys J, 1999. **77**(3): p. 1384-93.
7.   Vedantham, V. and S.C. Cannon, *Rapid and slow voltage-dependent conformational changes in segment IVS6 of voltage-gated Na(+) channels.* Biophys J, 2000. **78**(6): p. 2943-58.
8.   Kontis, K.J. and A.L. Goldin, *Sodium channel inactivation is altered by substitution of voltage sensor positive charges.* J Gen Physiol, 1997. **110**(4): p. 403-13.
9.   Isom, L.L., et al., *Primary structure and functional expression of the beta 1 subunit of the rat brain sodium channel.* Science, 1992. **256**(5058): p. 839-42.
10.   Chen, C.F. and S.C. Cannon, *Modulation of Na$^+$ channel inactivation by the β_1 subunit: a deletion analysis.* Pflügers Archiv, 1995. **431**: p. 186-195.
11.   Todt, H., et al., *Ultra-slow inactivation in mu1 Na+ channels is produced by a structural rearrangement of the outer vestibule.* Biophys J, 1999. **76**(3): p. 1335-45.
12.   Wallace, R.H., et al., *Febrile seizures and generalized epilepsy associated with a mutation in the Na+-channel beta1 subunit gene SCN1B.* Nat Genet, 1998. **19**(4): p. 366-70.
13.   Chahine, M., et al., *Functional expression and properties of the human skeletal muscle sodium channel.* Pflugers Archiv - European Journal of Physiology, 1994. **427**(1-2): p. 136-42.
14.   McClatchey, A.I., et al., *The cloning and expression of a sodium channel beta 1-subunit cDNA from human brain.* Human Molecular Genetics, 1993. **2**(6): p. 745-9.
15.   Hayward, L.J., R.H. Brown, Jr., and S.C. Cannon, *Inactivation defects caused by myotonia-associated mutations in the sodium channel III-IV linker.* J Gen Physiol, 1996. **107**(5): p. 559-76.
16.   Jurman, M.E., et al., *Visual identification of individual transfected cells for electrophysiology using antibody-coated beads.* Biotechniques, 1994. **17**(5): p. 876-81.
17.   Featherstone, D.E., J.E. Richmond, and P.C. Ruben, *Interaction between fast and slow inactivation in SkM1 sodium channels.* Biophysical Journal, 1996. **71**: p. 3098-3109.
18.   Rudy, B., *Slow Inactivation of the sodium conductance in squid giant axons. Pronase resistance.* Journal of Physiology, 1978. **283**: p. 1-21.

19.   McCormick, K.A., et al., *Molecular determinants of Na+ channel function in the extracellular domain of the beta1 subunit.* J Biol Chem, 1998. **273**(7): p. 3954-62.

20.   Moran, O., M. Nizzari, and F. Conti, *Endogenous expression of the beta1A sodium channel subunit in HEK-293 cells.* FEBS Lett, 2000. **473**(2): p. 132-4.

21.   Richmond, J.E., et al., *Slow Inactivation in Human Cardiac Sodium Channels.* Biophysical Journal, 1998. **74**: p. 2945-2952.

22.   O'Reilly, J.P., S.Y. Wang, and G.K. Wang, *Residue-specific effects on slow inactivation at V787 in D2-S6 of Na(v)1.4 sodium channels.* Biophys J, 2001. **81**(4): p. 2100-11.

23.   Liu, Y., M.E. Jurman, and G. Yellen, *Dynamic rearrangement of the outer mouth of a K+ channel during gating.* Neuron, 1996. **16**(4): p. 859-67.

24.   Choi, K.L., R.W. Aldrich, and G. Yellen, *Tetraethylammonium blockade distinguishes two inactivation mechanisms in voltage-activated K+ channels.* Proc Natl Acad Sci U S A, 1991. **88**(12): p. 5092-5.

25.   Panyi, G. and C. Deutsch, *Probing the cavity of the slow inactivated conformation of shaker potassium channels.* J Gen Physiol, 2007. **129**(5): p. 403-18.

26.   Townsend, C. and R. Horn, *Effect of alkali metal cations on slow inactivation of cardiac Na$^+$ channels.* Journal of General Physiology, 1997. **110**: p. 23-33.

27.   Struyk, A.F. and S.C. Cannon, *Slow inactivation does not block the aqueous accessibility to the outer pore of voltage-gated Na channels.* J Gen Physiol, 2002. **120**(4): p. 509-16.

28.   Wang, S.Y. and G.K. Wang, *Point mutations in segment I-S6 render voltage-gated Na+ channels resistant to batrachotoxin.* Proc Natl Acad Sci U S A, 1998. **95**(5): p. 2653-8.

29.   Sandtner, W., et al., *Lidocaine: a foot in the door of the inner vestibule prevents ultra-slow inactivation of a voltage-gated sodium channel.* Mol Pharmacol, 2004. **66**(3): p. 648-57.

30.   Isom, L.L., et al., *Functional co-expression of the beta 1 and type IIA alpha subunits of sodium channels in a mammalian cell line.* Journal of Biological Chemistry, 1995. **270**(7): p. 3306-12.

31.   Patton, D.E., et al., *The adult rat brain beta 1 subunit modifies activation and inactivation gating of multiple sodium channel alpha subunits.* Journal of Biological Chemistry, 1994. **269**(26): p. 17649-55.

32.   Makita, N., P.B. Bennett, and A.L. George, Jr., *Molecular determinants of beta 1 subunit-induced gating modulation in voltage-dependent Na+ channels.* J Neurosci, 1996. **16**(22): p. 7117-27.

33.   Meadows, L.S., et al., *Functional and biochemical analysis of a sodium channel beta1 subunit mutation responsible for generalized epilepsy with febrile seizures plus type 1.* J Neurosci, 2002. **22**(24): p. 10699-709.

3.7   Tables and Figures (below)

Table 1. Fast Inactivation Gating Parameters

Channel Subunit	$V_{\frac{1}{2}}$ mV	k mV	$\tau_{Recovery}$ msec
α	-76.4 ± 1.0 (12)	5.2 ± 0.20 (12)	2.0 ± 0.10 (10)
α + β1	-70.8 ± 0.61 (6)**	4.5 ± 0.09 (6)	1.9 ± 0.07 (6)
α + β1C121W	-73.1 ± 1.2 (6)	6.2 ± 0.34 (6)*	2.0 ± 0.15 (5)
α + β1/CTdel	-71.1 ± 0.91 (6)*	4.6 ± 0.08 (6)	2.0 ± 0.08 (4)

Values are means ± SEM with the number of observations in parentheses. *Statistically different from α-subunit only at $p < 0.05$. **Statistically different from α-subunit only at $p < 0.005$

Table 2. Kinetics of Recovery from Slow Inactivation

Channel Subunit	3 – second conditioning pulse		30 – second conditioning pulse			
	τ_M msec	I_M	τ_M msec	I_M	τ_S sec	I_S
α	210 ± 15	0.73 ± 0.02	230 ± 50	0.55 ± 0.03	15 ± 1.6	0.40 ± 0.03
$\alpha + \beta 1$	180 ± 5.5	0.77 ± 0.02	220 ± 32	$0.70 \pm 0.03*$	19 ± 4.0	$0.28 \pm 0.02**$
$\alpha + \beta 1C121W$	240 ± 11	0.74 ± 0.04	180 ± 20	0.50 ± 0.02	14 ± 1.6	0.47 ± 0.03
$\alpha + \beta 1/CTdel$	180 ± 11	0.71 ± 0.03	230 ± 25	$0.67 \pm 0.03*$	17 ± 2.9	$0.30 \pm 0.02*$

Values are means $\pm$ SEM; N = 5 for all channel types except for $\alpha + \beta 1$ in which N = 6.
*Statistically different from α-subunit only at $p < 0.05$. **Statistically different from α-subunit only at $p < 0.01$. I_M = Intermediate Inactivation, and I_S = Slow Inactivation.
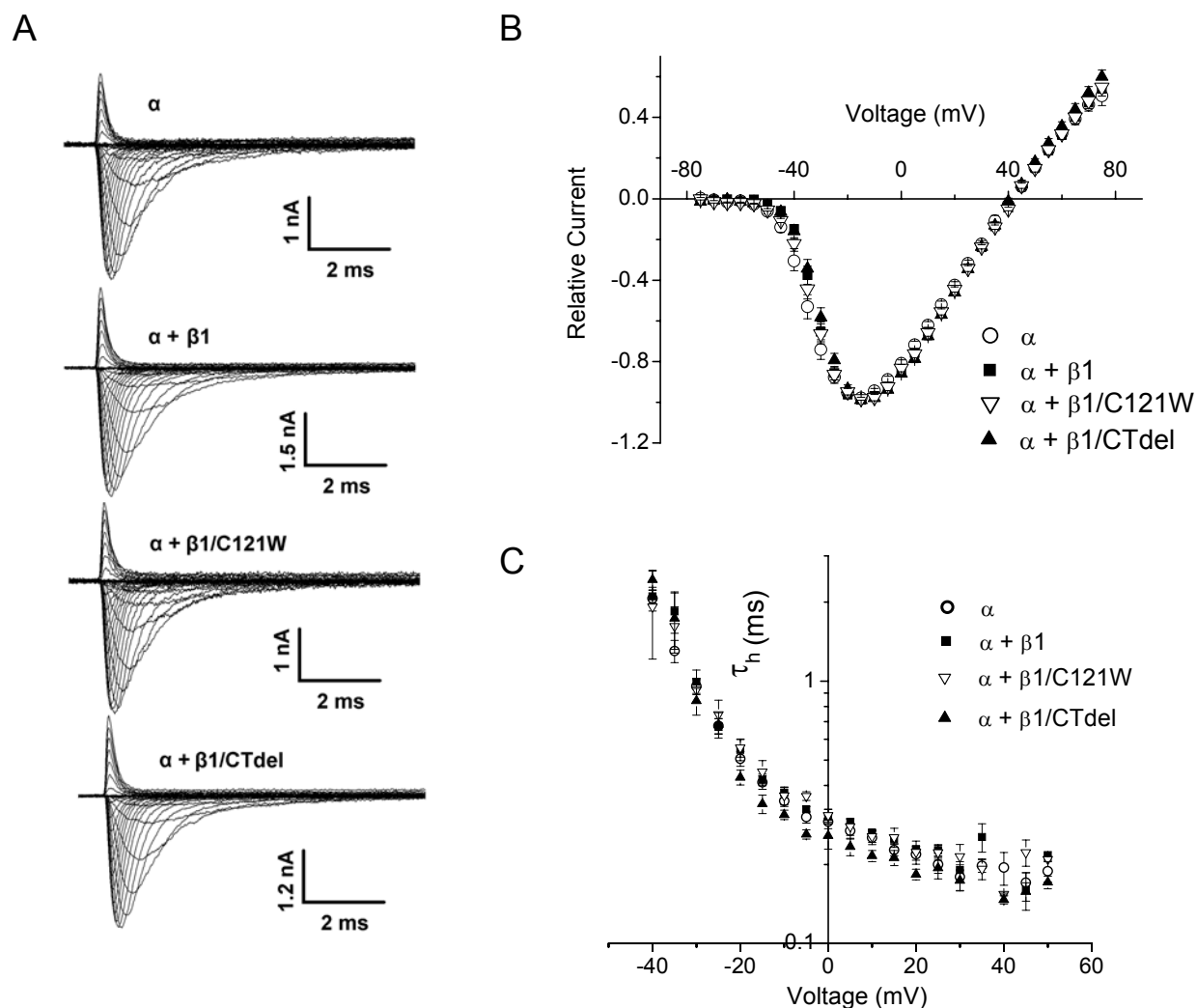
A

B

C

FIGURE 1   Sodium channel activation was not altered by co-expression of wild-type or mutant sodium channel $\beta 1$ subunits. Sodium currents were elicited by a series of voltage steps from a holding potential of -120 mV to voltages ranging from -75 to $+75$ mV. (*A*) Representative current traces from cells expressing Nav1.4 α-subunit alone (α); α plus wild-type $\beta 1$ ($\alpha + \beta 1$); α plus $\beta 1$ N-terminal mutant C121W ($\alpha + \beta 1$/C121W); and α plus $\beta 1$ C-terminal deletion ($\alpha + \beta 1$/CTdel). (*B*) Normalized peak I-V curves show that the voltage-dependence of activation was not affected by coexpression of wild-type or mutant $\beta 1$ subunits. (C) Time constant of entry to fast inactivation was not affected by coexpression of wild-type or mutant $\beta 1$ subunits.
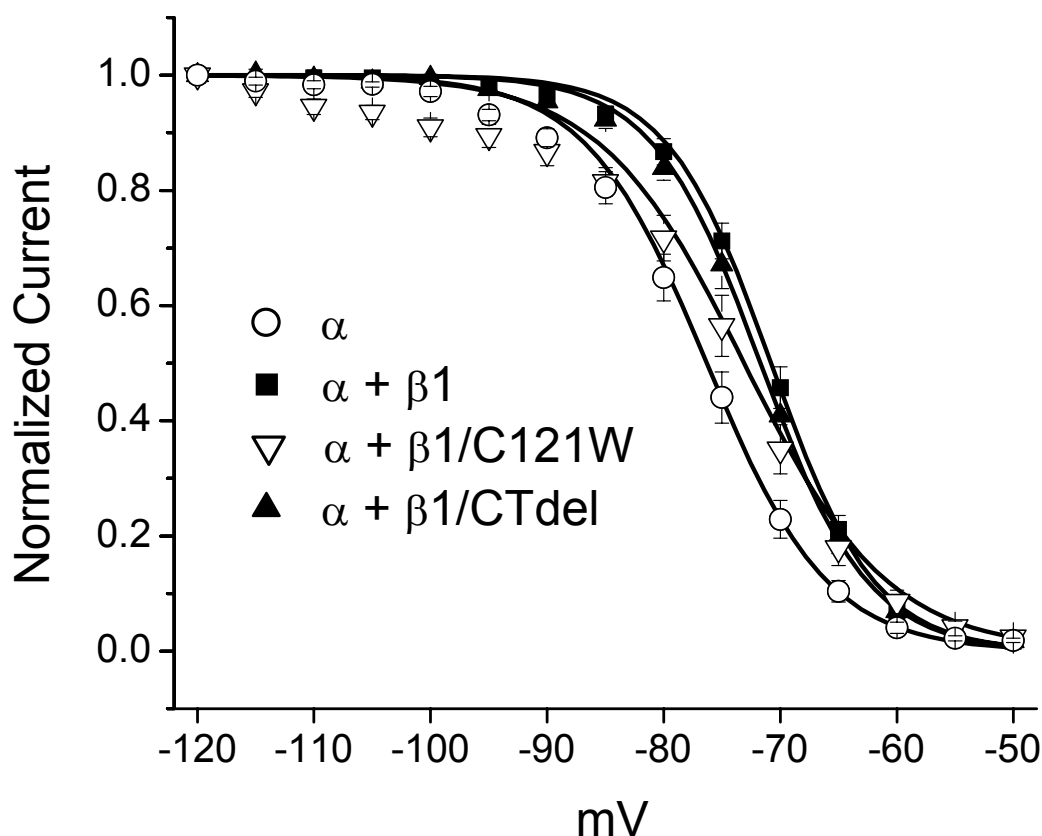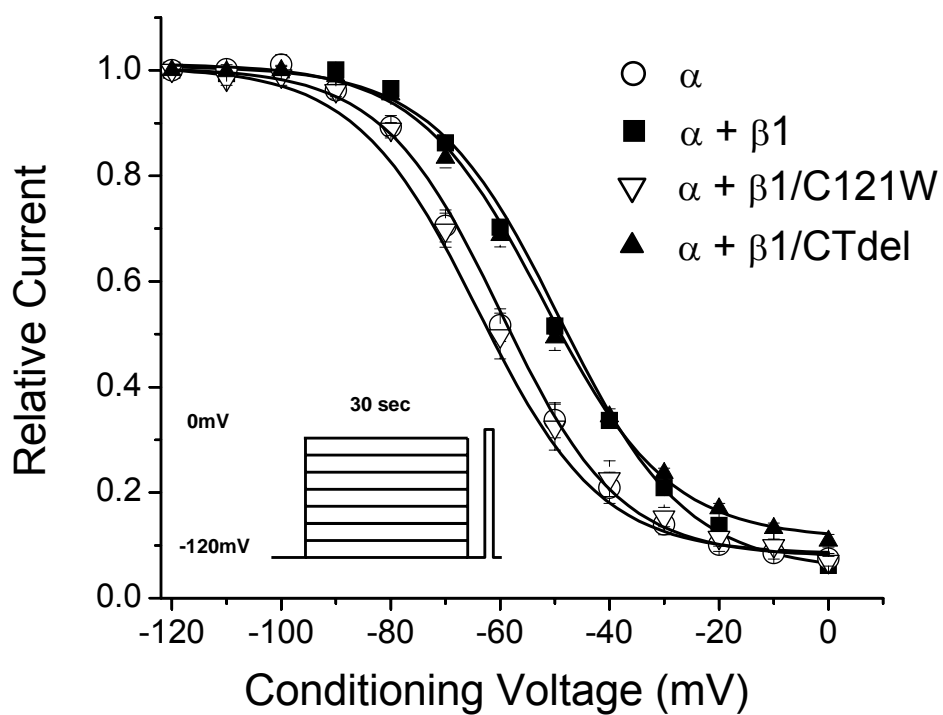
FIGURE 2 Voltage-dependence of fast inactivation was mildly disrupted by coexpression of β1. Voltage-dependence of fast inactivation was determined from test depolarizations to −10 mV immediately after a 300-msec conditioning pulse at potentials ranging from −120 to −50 mV. Coexpression of wild-type β1 (α + β1, ■) caused a 5.5–mV rightward shift in $V_{1/2}$ of fast inactivation compared to α subunit alone (α, ○) ($p < 0.005$), and modestly decreased the slope factor (Table 1). β1 C-terminal deletion mutant (α + β1/CTdel, ▲) effects were similar to wild-type β1 (α + β1, ■). The N-terminal mutant (α + β1/C121W, ▽) had an intermediate effect with a 3.2 mv shift of $V_{1/2}$, and an increased the slope factor compared to wild-type β1 ($p < 0.05$).
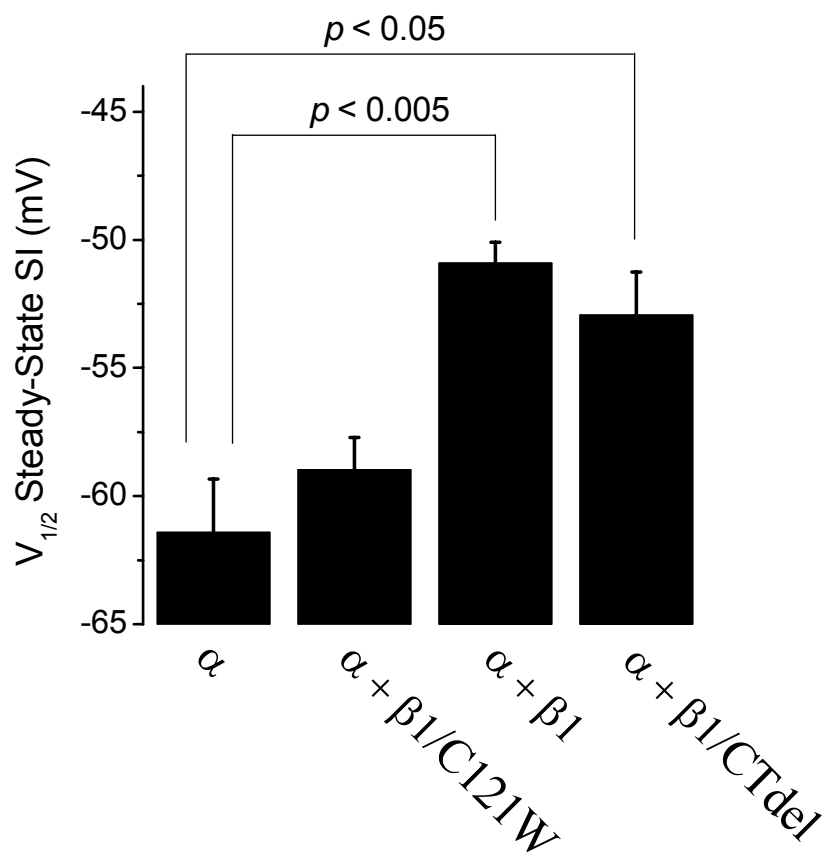
A

B

Figure 3

FIGURE 3   The β1 subunit mildly impedes steady-state slow inactivation. The voltage dependence of slow inactivation was measured as the peak current elicited by a test depolarization to −10 mV after 30-s conditioning pulses ranging from −120 to 0 mV (*inset*). Conditioning and test pulses were separated by a 20-msec recovery gap at −120 mV to remove fast inactivation. (*A*) Coexpression of the wild-type β1 subunit (α + β1, ■) or the β1 C-terminal deletion (α + β1/CTdel, ▲) depolarized (right-shifted) the voltage-dependence of steady-state slow inactivation compared to expression of α-subunit alone (α, ○) or coexpressed with the β1 N-terminal mutation C121W (α + β1/C121W, ∇). (*B*) Voltage of half-inactivation ($V_{1/2}$) for steady-state slow inactivation was depolarized by ~10mV upon coexpression of wild-type β1 (*p* < 0.005), and β1/CTdel (*p* < 0.05) compared to α-subunit alone, while $V_{1/2}$ for β1/C121W was not significantly different.
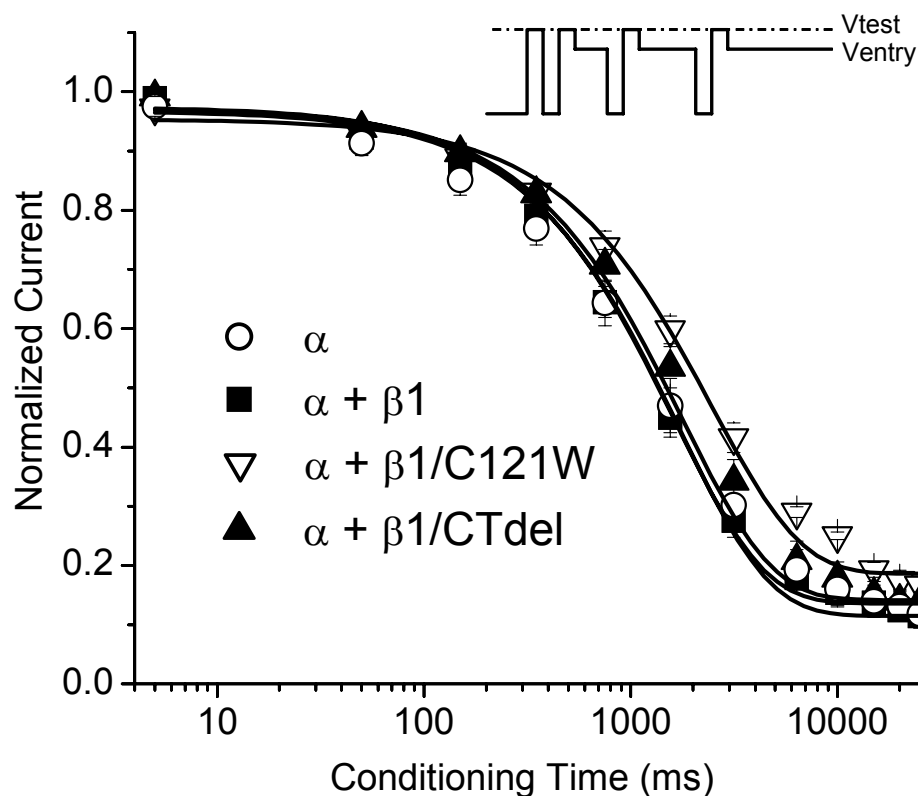
FIGURE 4 The rate of entry to slow inactivation was not affected by coexpression of WT β1, but was slightly prolonged by coexpression of β1/C121W. Entry to slow inactivation at 0 mV was measured using a sequential entry protocol (*inset*). Expression of wild-type β1 (α + β1, ■) or α and β1 C-terminal deletion mutant (α + β1/CTdel, ▲) did not affect the rate of entry to slow inactivation, as compared to coexpression of α subunit alone (α, ○). The β1 N-terminal mutation C121W (α + β1/C121W, ∇) prolonged the rate of entry to slow inactivation by 1.4-fold ($p < 0.05$).
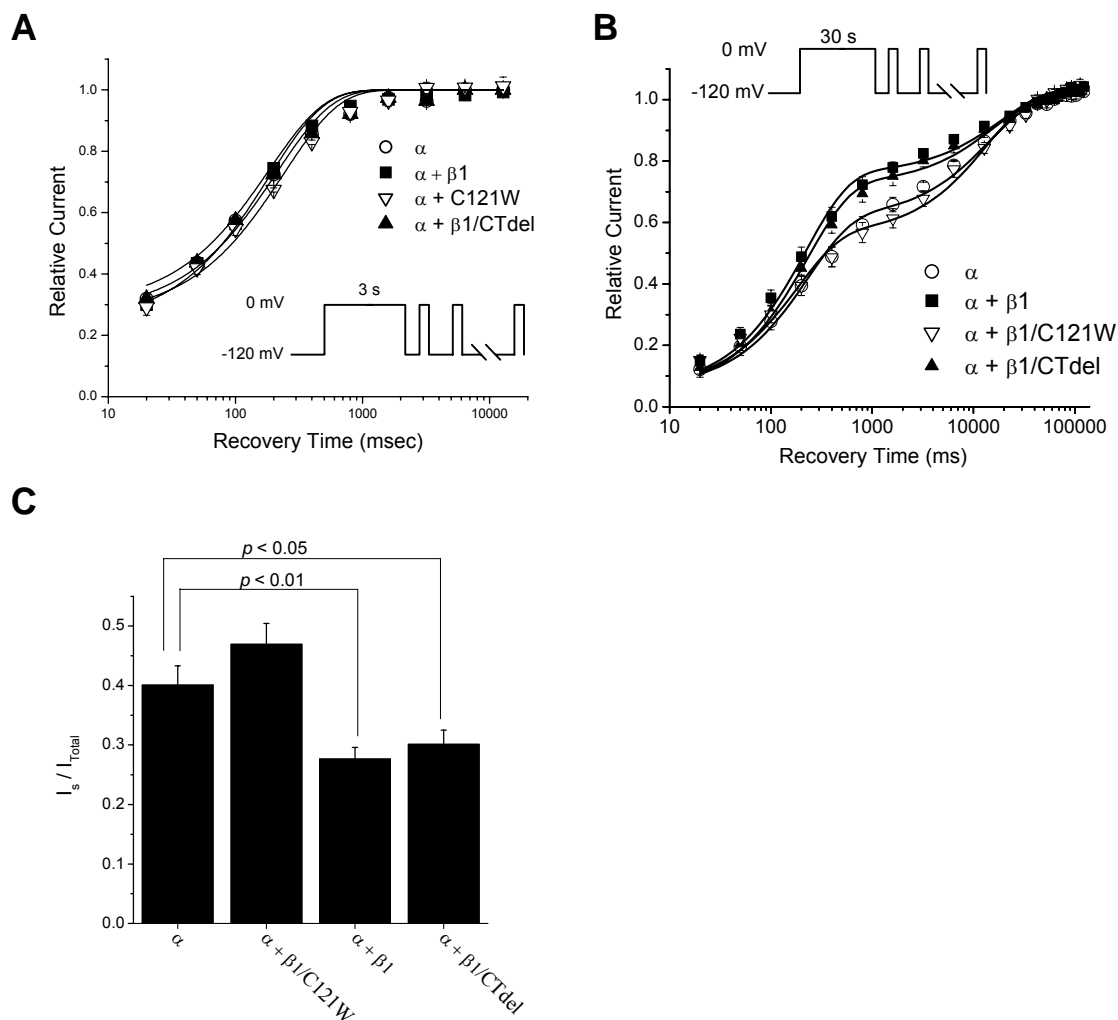
FIGURE 5 The β1 subunit preferentially disrupted the I_S component of slow inactivation. Recovery from slow inactivation at -120 mV was determined by applying a series of brief test depolarizations to -10 mV at progressively longer times after returning to -120 mV from either a 3 or 30-s conditioning pulse to 0 mV. (*A*) After a short (3-s) conditioning pulse recovery from slow inactivation was monoexponential with a time constant of ~200 msec, reflecting recovery from the intermediate inactivated (I_M) state. Coexpression of WT β1 (α + β1, ■) or either β1 subunit mutation (α + β1/CTdel, ▲ ; α + β1/C121W, ∇) did not affect the magnitude or the

kinetics of recovery from the I_M state, relative to expression of α subunit alone (α, $\circ$). Smooth curves show bi-exponential fits with the fast time constant set at a fixed value equal to that determined from the fast inactivation recovery protocol (Table 1). (*B*) Recovery after a longer (30-s) conditioning pulse showed two distinct kinetic components that reflected recovery from both the I_M and I_S states. Coexpression of wild-type $\beta1$ did not alter recovery kinetics of either state, but decreased the relative proportion of channels partitioned into the I_S state compared to α-subunit alone ($p < 0.01$) (Table 2). The $\beta1$ C-terminal deletion mutant yielded I_S results similar to WT $\beta1$, while the $\beta1$/C121W mutant disrupted the $\beta1$ effect on I_S, yielding results similar to expression of α-subunit alone. (*C*) Quantification of the percentage of channels recovering from the slow (I_S) component after 30-s conditioning pulses. Coexpression of α plus WT $\beta1$ or $\beta1$/CTdel caused an ~25% reduction in channels occupying the I_S state relative to expression of α-subunit alone or $\alpha + \beta1$/C121W ($p < 0.05$).

A

WT

F1311C + MTS-ET

B
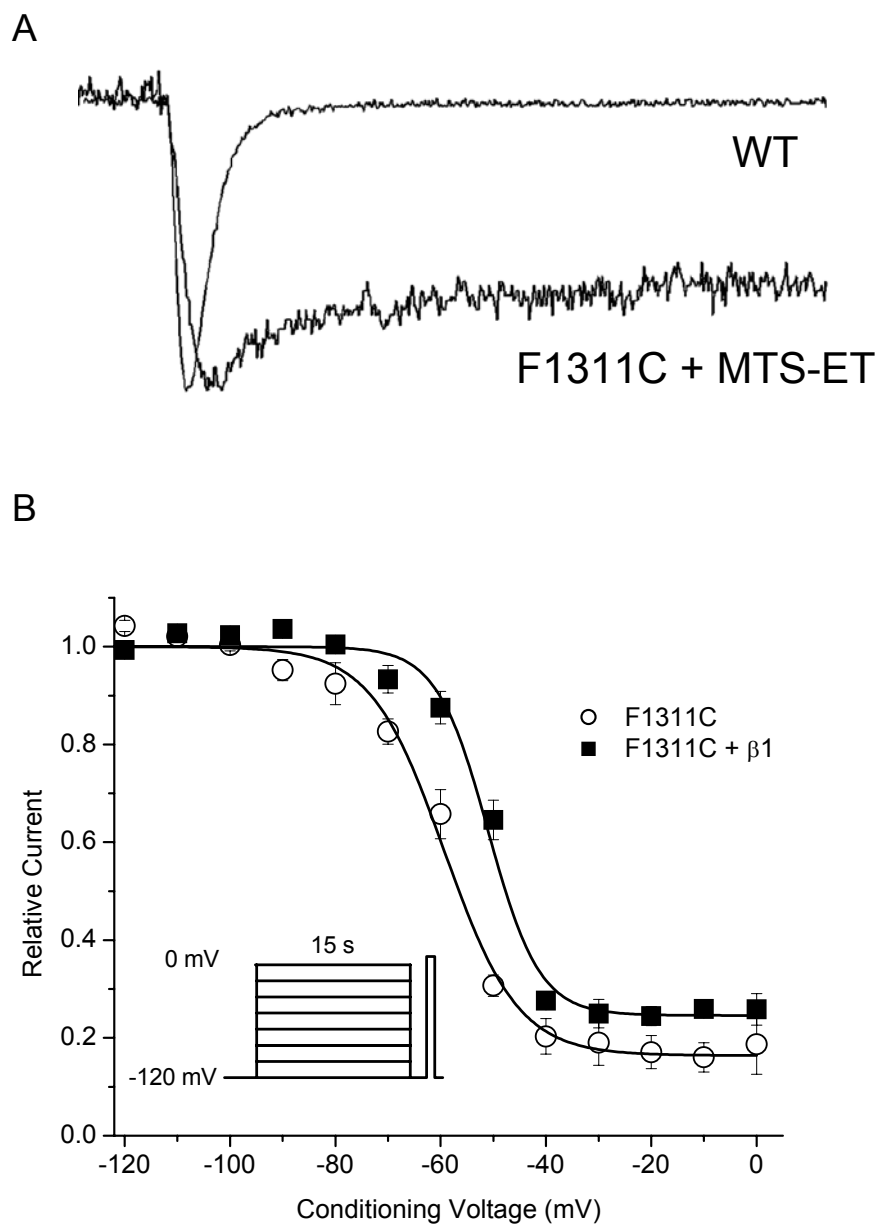
FIGURE 6 Disruption of fast inactivation did not abolish β1 modulation of slow inactivation. Fast inactivation was severely disrupted by the α-subunit F1311C mutant when channels were exposed to 500 μM internal MTS-ET. (*A*) Raw traces demonstrate the profound disruption of fast inactivation in the F1311C mutant exposed to internal MTS-ET. (*B*) In the absence of fast

inactivation, coexpression of β1 (F1311C + β1, ■) caused an +11 mV depolarization (right-shift)

in half-inactivation ($V_{1/2}$) of slow inactivation compared to expression of mutant α-subunit alone

/F1311C, ○), $p < 0.005$. Steady-state slow inactivation was measured as described in Fig 5.

Webb et al.

CHAPTER 4

ALKALI CATIONS IMPEDE SODIUM CHANNEL SLOW INACTIVATION AT OR NEAR THE SELECTIVITY FILTER.

Jadon Webb and Stephen C. Cannon

(Adapted from a paper being submitted to *Journal of General Physiology*)

4.1 Abstract

Upon membrane depolarization, voltage-gated sodium channels are driven into non-conducting states that are termed 'fast' and 'slow' inactivation, as distinguished by the time courses of recovery. Fast inactivation is thought to result from occlusion of the inner mouth of the channel by the III-IV loop, while the mechanism of slow inactivation remains unclear. Alkali metal cations in the external bath have been shown to influence slow inactivation, but little is known about the location and mechanism of this interaction. To address this, we examined the interaction of Group IA alkali metal cations with slow inactivation in human

Nav1.4 channels expressed in HEK293t cells. Slow inactivation was significantly impeded by external, but not internal Na^+ and Li^+. External K^+, Rb^+, and Cs^+, on the other hand, caused little effect compared to sucrose (cation-free) solution. Cation effects on slow inactivation were found to be very low affinity and were not dependent on the ability of cations to permeate deep into the channel. Indeed, the effect on slow inactivation occurred at a shallow apparent electrical distance (δ) of 0.15 relative to the outside of the channel, and was affected by mutations in the outer pore. Overall, these results suggest that external cations modulate slow inactivation at a selective interaction site located in the outer entrance of the pore region, external to the channel selectivity filter.

4.2   *Introduction*

Fast and slow inactivation are mechanistically distinct gating events that terminate the flow of cations through the sodium channel [1]. The mechanism of fast inactivation has been extensively characterized, and appears to involve occlusion of the inner pore of the channel by the III-IV intracellular loop [2]. Slow inactivation remains intact after complete disruption of fast inactivation [3], but despite decades of study its mechanism remains a mystery.

Slow inactivation appears to be a complex process involving a wide variety of channel structures from all four domains. Disease mutations in the transmembrane segments [4], the small loops connecting these segments [5, 6], and even the large domain-connecting intracellular loops of the channel [7] modestly disrupt slow inactivation, underscoring the difficulty in localizing where this process occurs. More directed attempts to characterize the mechanism of

Webb et al.

slow inactivation, however, suggest that the pore region of the channel is a particularly important place to consider [8].

The pore region of the sodium channel is thought to be comprised of the S5-S6 loops on the external side, with the S6 transmembrane segments lining the internal side [9]. In addition to providing the permeation pathway for ion conduction through the channel, the pore region is also critically important for slow inactivation. Mutations in the pore-forming region can cause dramatic effects on slow inactivation [10-14]. Cross-linking experiments also showed that residues in the outer pore move significantly during slow inactivation [15, 16], and that inhibiting these movements correspondingly impedes slow inactivation. Finally, alteration of charged amino acids in the outer pore caused dramatic enhancement of slow inactivation, leading to speculation that electrostatic interaction in the outer pore stabilizes the channel against the slow inactivated state(s) [17-19]. Based on these results, it is reasonable to speculate that slow inactivation involves a conformational change at or near the selectivity region of the pore. [20] showed that, unlike in K^+ channels [21], outright occlusion of the outer vestibule of the pore external to the selectivity filter is unlikely to occur.

In K^+ channels, external alkali metal cations impede slow, C-type inactivation [22, 23]. This "foot in the door" effect of external cations is strong evidence that C-type inactivation involves a collapse of the outer vestibule and pore of the K channel [23-25]. External cations were also noted to affect sodium channel slow inactivation [16, 26-29]. But unlike the situation for K^+ channels, far less is known about where and how cations interact with sodium channels to modulate slow inactivation. To address this question, we characterized the effects of the Group IA alkali metal cations on slow inactivation of human skeletal muscle Nav1.4 channels. A cation

effect on slow inactivation was observed exclusively on the extracellular face of the channel, at a shallow electrical depth in the external pore. This interaction site was distinct from, and external to, the selectivity filter. Furthermore, this interaction site appeared to be highly selective, and may be the same or at least overlap with the TTX binding site.

4.3   *Methods*

4.3.1   Site-directed mutagenesis.   The QuikChange site-directed mutagenesis kit (Stratagene, La Jolla, CA) was used to introduce specific mutations into the human skeletal muscle sodium channel (Nav1.4), which was subcloned into the mammalian expression construct pRc/CMV-hSkM1 (provided by A. L. George, Vanderbilt University, Nashville, TN). The point mutations and flanking regions were sequenced to confirm the presence of the mutation and exclude spurious changes.

4.3.2 Expression of sodium channels. Human embryonic kidney cells (HEK293t) were transiently transfected using the calcium phosphate method [30]. In brief, normal WT or mutant sodium channel α-subunit plasmid (0.6 μg per 35-mm dish) was cotransfected at two-fold molar excess with the p-hβ1-IRES2-CD8 plasmid (provided by Fen-fen Wu), a bicistronic plasmid containing human sodium channel β1 and CD8 marker coding sequences. After 24–72 h, cells were trypsinized briefly and passaged to 12-mm round glass cover slips for electrophysiological recording. Individual transfection-positive cells were identified by labeling with anti-CD8 antibody cross-linked to microbeads [31] (Dynal, Great Neck, NY).

4.3.3 Whole-cell recording. Na^+ currents were measured using conventional whole-cell recording techniques as previously described [30]. Recordings were made with an Axopatch 200A amplifier (Axon Instruments, Union City, CA). The output was filtered at 5 kHz and digitally sampled at 50 kHz using a DigiData 1200 interface (Axon Instruments). Data were stored to a Pentium-based (Intel, Santa Clara, CA) computer using Clampex 8.2 software (Axon Instruments). More than 70% of the series resistance was compensated by the analog circuitry of the amplifier and leakage conductance was corrected by digital scaling and subtraction of the passive current elicited by several small depolarizations from the holding potential. After initially establishing whole-cell access, we often observed a slow increase in the size of the peak current over time. To compensate for this, we waited until peak currents reached a steady state level before recording, which typically took several minutes after gaining whole cell access.

Patch electrodes were fabricated from borosilicate capillary tubes with a multi-stage puller (Sutter, Novato, CA). The shank of the pipette was coated with Sylgard and the tip was heat-polished to a final tip resistance (in bath solution) of 0.5–2.0 MΩ. Various external (bath) and internal (pipette) solutions were made, each containing a different alkali cation salt (labeled as 'Cation'). The internal solution consisted of (mM): (Cation)F 100, (Cation)Cl 40, Hepes 10; pH 7.4. Fluoride was used in the pipette to prolong seal stability. The bath solution contained (mM): (Cation)Cl 140, Hepes 10, Glucose 2, $CaCl_2$ 2; pH 7.4. External sucrose bath contained: Sucrose 280, Hepes 10, Glucose 2, $CaCl_2$ 2; pH 7.4. Recordings were made at room temperature (21–23°C).

4.3.4 Data analysis. Raw current traces were analyzed manually off-line using pClamp 9.0 (Axon Instruments) or Origin 6.0 (Microcal, Northampton, MA). In some experiments,

Webb et al.

permeant ions were present on only one side of the membrane, and so the Goldman-Hodgkin-Katz current equation for a monovalent cation was used to compute relative permeability as a measure of channel activation:

where I is the measured peak current; V_m is the membrane potential; C_{in} and C_{out} are the concentrations of internal and external cation; T is the absolute temperature, and the constants F and R have their conventional meanings. Plots of relative permeability versus membrane potentials were fitted to a Boltzmann calculated as $P = P_{MAX}/(1 + \exp((V_m - V_{1/2})/k)$, where P_{MAX} is the maximum permeability, $V_{1/2}$ is the half-maximum voltage and k is the slope factor. Steady-state fast and slow inactivation were fitted to a Boltzmann function with a non-zero pedestal (I_0) calculated as $I/I_{MAX} = (1 - I_0)/[1 + \exp((V - V_{1/2})/k)] + I_0$, where $V_{1/2}$ is the half-maximum voltage and k is the slope factor. Symbols with error bars indicate means $\pm$ SEM. Statistical significance was determined by the Student's unpaired t test with P-values noted in the text.

4.4   Results

4.4.1   External, but not internal, cations impede slow inactivation. Extracellular cations have been reported to affect sodium channel slow inactivation in a variety of different preparations and experimental paradigms [16, 28, 29, 32, 33]. We sought to clarify our

Webb et al.

understanding of how cations modulate slow inactivation by performing a more comprehensive series of studies on the effects of both extracellular (OUT) and intracellular (IN) alkali metal cations on human skeletal muscle (Nav1.4) sodium channels, expressed in HEK293t cells.

Figure 1 shows a comparison of the effects of varying the external (left column) or internal (right column) cation on slow inactivation. Steady-state slow inactivation was measured using a series of 15-s conditioning pulses to voltages ranging from −120 to 0 mV. Each conditioning pulse was followed by a 20-msec gap at −120 mV to allow full recovery from fast inactivation before a test depolarization was applied to measure slow inactivation as the reduction in peak current (Figure 1 *A*, *inset*). Peak currents elicited by the test pulses were normalized to the maximum available current from a holding potential of −120 mV. Data from a series of conditioning depolarizations were then fitted with a Boltzmann function plus a non-zero pedestal. Sodium channels exposed to 140 mM external Na^+ were much more resistant to slow inactivation than channels exposed to 140 mM external Rb^+ (Fig. 1 *A*, *left*), as demonstrated by a right-shift in the voltage of half-inactivation ($V_{1/2}$) by 20.8 mV ($P < 0.0001$). The slope factor (k) was also slightly decreased ($P < 0.05$). In contrast, replacing the internal Na^+ with internal Rb^+ (Fig. 1 *A*, right) did not affect any of the steady-state parameters when recorded in external Na^+ bath (*Table 1*).

Entry to slow inactivation was also measured in response to varying the external cation (Fig. 1 *B*, *left*), or the internal cation (*right*). Entry rate was measured by using a sequential entry protocol (Fig. 1 *B*, *inset*). A 0 mV conditioning pulse was applied to inactivate the Na^+ channels. Brief recovery gaps to −120 mV for 20 msec were given to allow full recovery from fast inactivation, followed by a test pulse to evaluate remaining (i.e. non-slow inactivated) current. Peak current declined with lengthening conditioning time in an exponential manner towards a

non-zero pedestal, as progressively more channels became slow inactivated. The rate of entry to slow inactivation was approximately two-fold slower in cells exposed to external Na^+ compared to external Rb^+ ($P < 0.0001$, *Table 1*). Additionally, the remaining non-slow inactivated current was approximately two-fold larger in external Na^+ compared to Rb^+ ($P < 0.005$). Entry rate and maximal extent of slow inactivation was the same for internal Na^+ or internal Rb^+ in the presence of external Na^+ (Fig. 1 *B*, *right*).

Recovery from slow inactivation at -120 mV was determined by applying a series of brief (5-msec) test pulses at progressively longer times after returning to -120 mV from a single 15-s conditioning pulse to 0 mV (Fig. 1 *C*, inset). Recovery from slow inactivation was 1.6-fold faster in external Na^+ versus external Rb^+ (Fig. 1 *C*, *left*, *Table 1*). In contrast, recovery from slow inactivation was identical for internal Na^+ and internal Rb^+ (Fig. 1 *C*, *right*).

All three measures showed that slow inactivation was impeded by external Na^+ as compared to Rb^+. In external Na^+, recovery from slow inactivation was accelerated, the entry rate was slower, the voltage-dependence was shifted toward depolarized potentials, and the maximal extent was reduced. In contrast, slow inactivation was not affected by varying the internal cation from Na^+ to Rb^+, in the background of high external Na^+.

4.4.2 The lack of an internal cation effect is not due to fast inactivation. In WT sodium channels the fast inactivation gate quickly renders the sodium channel non-conductive, and likely does so by occlusion of the inner pore of the channel [34]. It is possible, then, that the fast gate could prevent internal cations from accessing a slow-inactivation modulatory site located in the inner pore. To test this possibility, we disrupted fast inactivation by mutating a pair of residues thought to be the docking site of the fast gate (L437C/A438W), as was done

previously [35]. The extent to which L437C/A438W disrupted fast inactivation is shown by the superposition of the amplitude-normalized traces in Fig. 2 A. First, we verified that for the mutant channel steady-state slow inactivation remained sensitive to external Na^+ compared to Rb^+ in the presence of internal Na^+ (Fig. 2 B, *filled black symbols are right-shifted compared to open black circles*), similar to the effect on WT channels in Figure 1 A. We then measured the effects of 140 mM internal Na^+ or K^+, to test whether slow inactivation was now sensitive to internal cations in the absence of fast inactivation.   The impediment of slow inactivation by external Na^+ was independent of whether the internal cation was Na^+ or K^+, (Figure 2 B, *filled symbols*). The voltage of half-inactivation ($V_{1/2}$) and the slope factor (k) were not significantly different when the internal cation was varied ($P > 0.05$). Na_{In}: $V_{1/2} = -60.3 \pm 1.7$ mV, $k = 6.58 \pm 0.52$ mV, $n = 3$; K_{In}: $V_{1/2} = -57.4 \pm .6$ mV, $k = 7.31 \pm .14$ mV, $n = 3$.

4.4.3 Impediment of slow inactivation by external Na^+ does not obscure an internal cation effect. Since external Na^+ impedes slow inactivation relative to Rb^+, it is possible that using Na^+ as the external cation might obscure or prevent effects on slow inactivation caused by internal cations. To test this possibility, we measured steady-state slow inactivation using 140 mM Rb^+ as the external cation with either 140 mM Na^+ (*black, open symbols*) or K^+ (*blue, open symbols*) as the internal cation (Fig. 2 B). The $V_{1/2}$ of slow inactivation was still insensitive to internal cations, although the slope factor (k) was slightly increased in Na^+ compared to Rb^+ ($P < 0.001$). Na_{In}: $V_{1/2}$, -74.5 ± 1.4 mV; k, 6.44 ± 0.16 mV; $n = 4$; K_{In}: $V_{1/2}$, $-72.7 \pm .8$ mV; k, 8.09 ± 0.06 mV; $n = 3$. We used K^+ instead of Rb^+ as the intracellular cation in these experiments because internal K^+ was sufficiently permeable through the channel to produce measurable

outward currents in external Rb^+ and because K^+ had a comparable effect to Rb^+ on slow inactivation (see Fig. 5).

Taken together, the four ionic conditions tested in Fig. 2 B show that even in the absence of fast inactivation, the internal cation does not modify slow inactivation parameters, whereas the external cation has a potent inhibitory effect.

4.4.4 External cation modulation of fast gating. Prior reports give conflicting results on the extent to which alkali cations affect activation and fast inactivation of sodium channels [32, 33, 36, 37]. Furthermore, these fast gating transitions, and fast inactivation in particular, are partially coupled to slow inactivation [3, 38]. Therefore it is possible that the changes in slow inactivation that we observed may be a consequence of external cation effects on fast gating. To test this possibility, we measured the effects of 140 mM external Na^+ or Rb^+ on fast gating parameters with a constant internal solution of Na^+ (Fig. 3).

The voltage-dependence of activation (Fig. 3 *A*) was measured by applying step depolarizations from a holding potential of −120 mV. Peak Na^+ current was normalized by the driving force predicted from the Goldman-Hodgkin-Katz equation to determine peak permeability at each test potential (METHODS). The permeability data were then fit with a Boltzmann function. Channels exposed to external Na^+ had a −4.8 mV left shift in the activation midpoint relative to external Rb^+, which was not statistically significant ($P > 0.05$), whereas the a two-fold decreased slope factor was ($P < 0.0001$). Na_{Out}: $V_{1/2} = -28.5 \pm 2.4$ mV, $k = 6.31 \pm 0.36$ mV, $n = 5$; Rb_{Out}: $V_{1/2} = -23.8 \pm 3.7$ mV, $k = 11.9 \pm 0.88$ mV, $n = 6$.

Webb et al.

The kinetics of fast inactivation (Fig. 3 *B*) was measured over a voltage range from −40 to +75 mV by fitting the decay of macroscopic current with a single exponential. Data between -10 and +10 mV are missing for external Na$^+$ because the reversal potential is within this range and the Na$^+$ currents were too small to reliably determine a time constant. Overall, fast inactivation kinetics were roughly similar in Na$^+$ and Rb$^+$ over a voltage range from −40 through +55 mV.

The voltage-dependence of steady-state fast inactivation (Fig. 3 *C*) was measured as the peak current elicited following a 300-msec conditioning prepulse over a range of voltages from −120 to 0 mV. The voltage of half-inactivation ($V_{1/2}$) was right-shifted by 6.8 mV in external Na$^+$ compared to external Rb$^+$ ($P < 0.001$), while the slope factor was not affected. Na$_{Out}$: $V_{1/2}$ = −66.8 ± 1.8 mV, $k = 4.70 ± 0.19$ mV, $n = 5$; Rb$_{Out}$: $V_{1/2}$ = −73.6 ± 1.4 mV, $k = 4.73 ± 0.08$ mV, $n = 6$.

The changes in fast gating properties are not sufficient to have caused the external cation effects on slow inactivation. For example, a complete disruption of fast inactivation is known to cause only a 2-fold increase in the rate of entry ([3]) But more importantly, these changes are in the wrong direction. External Rb$^+$ impeded activation (Fig. 3 *A*) and enhanced fast inactivation (Fig. 3 *C*). Both of these changes would tend to impede slow inactivation, but just the opposite was observed. Slow inactivation is enhanced in external Rb$^+$ compared to Na$^+$ (Fig. 1).

4.4.5 External cation modulation of slow inactivation in Nav1.5. External cations have been reported to affect slow inactivation in other sodium channel isoforms [26-28].

Because the changes we observed for slow inactivation were more pronounced than these prior reports, we wanted to test whether the large effects that we observed were specific to the Nav1.4 isoform, or whether these effects are applicable to other Na^+ channel isoforms as well. The heart isoform Nav1.5 is distinctly different from the skeletal muscle or neuronal isoforms in that Nav1.5 is much less prone to slow inactivation [39]. We therefore chose Nav1.5 to test whether the external cation effects we observed were a general feature of Nav channels. We measured the effects of extracellular Na^+ or Rb^+ on steady-state slow inactivation (Fig. 4). The pulse protocol for these measurements is identical to that in Fig. 1 A. The midpoint of steady-state slow inactivation was right-shifted by 17.8 mV ($P < 0.05$) in channels exposed to external Na^+ compared to Rb^+, and thereby confirms that impediment of slow inactivation by external Na^+ is a common feature of Na^+ channels. Na_{Out}: $V_{1/2} = -46.6 \pm 10.5$ mV; $k = -15.80 \pm 3.95$ mV; $I0 = 0.17 \pm 0.05$; $n = 4$; Rb_{Out}: $V_{1/2} = -71.0 \pm 2.7$ mV; $k = -16.70 \pm 2.13$ mV; $I0 = 0.15 \pm 0.01$; $n = 3$.

4.4.6 Selectivity of the external cation effect on slow inactivation. Early reports showed that external Na^+ impeded slow inactivation more so than K^+ [26, 28], although a later report did not notice a difference among the alkali cations [27]. To test whether the effect of external cations on slow inactivation is selective, we tested all of the Group IA alkali metal cations on the voltage-dependence of steady-state slow inactivation (Fig. 5). In addition, we also measured the effect of 140 mM external sucrose as a cation-free control. Slow inactivation in the presence of 140mM external K^+, Rb^+, and Cs^+ was very similar to that observed in the absence of an alkali cation (140 mM sucrose), although the slope factor (k) and the fraction of non-slow inactivating channels (S_0) in sucrose were slightly less than the cations (*Table 2*). Na^+ and Li^+, on the other hand, both strongly impeded slow inactivation to a similar degree. The

comparison to the control condition of no external cation (140 mM sucrose) suggests that Na^+ and Li^+ impede slow inactivation, rather than the alternative interpretation that Rb^+, K^+, and Cs^+ enhance it.

4.4.7 Selectivity of the pore is not the determinant of whether a cation disrupts slow inactivation. The two cations (Na^+ and Li^+) which caused significant impediment of slow inactivation (Fig. 5) are both highly permeable through the channel, while the other three cations (K^+, Rb^+, and Cs^+) that had little effect on slow inactivation are relatively impermeable. It is possible, then, that the site of cation interaction that modulates slow inactivation is at or internal to the selectivity filter, such that only highly permeable cations have access to this site. To test this hypothesis, we constructed a mutation in the selectivity filter, K1237C, which virtually abolishes selectivity among the monovalent cations and allows robust Rb^+ permeation through the channel [40]. Fig. 6 A illustrates an example of the inward Rb^+ currents observed in K1237C compared to WT. Steady-state slow inactivation was assessed in the K1237C mutant channels with external Na^+, Rb^+, or sucrose (Fig. 6 *B*). External Rb^+ caused a minimal (3.5mV, $P < 0.05$) right-shift in the voltage of half-inactivation ($V_{1/2}$) compared to sucrose. The right-shift caused by external Na^+ was still much greater than Rb^+ (10.5 mV shift, $P < 0.001$), although it was reduced compared to the shift seen in WT channels. Steady-state slow inactivation values for K1237C were: Sucrose$_{Out}$: $V_{1/2}$, -68.1 ± 0.8 mV; k, 4.67 ± 0.17 mV; $n = 4$; Rb$_{Out}$: $V_{1/2}$, -64.6 ± 0.7 mV; k, 5.76 ± 0.07 mV; $n = 3$; Na$_{Out}$: $V_{1/2}$, -57.6 ± 1.7 mV; k, 6.93 ± 1.15 mV; $n = 4$.

These data refute the notion that permeability is a major determinant by which external cations are able to impede slow inactivation; otherwise Rb^+ should have shifted the voltage-dependence rightward to an extent similar to Na^+.

4.4.8 Dose response of external cation effect. The concentration dependence of the external cation effect on slow inactivation has not been previously established. To test this, we measured a dose-response of the effect of external Na^+ on steady-state slow inactivation (Fig. 7). Steady-state slow inactivation was measured with a pulse protocol identical to that described for Fig. 1. Half-inactivation voltages ($V_{1/2}$) of channels exposed to varying concentrations of external Na^+ are shown as the mean ± SEM for several concentrations of external Na^+. Rb^+ was used to replace Na^+ to maintain constant ionic strength. Increasing concentrations of Na^+ caused an approximately linear shift in the $V_{1/2}$ (linear regression (r^2) > 0.99), at a rate of +1 mV per 6.4 mM of external Na^+. This effect showed no signs of saturation at the highest concentration tested (140 mM), which implies that this is a very low affinity interaction.

4.4.9 Apparent electrical distance of external cation interaction site. Charged particles acting within a transmembrane electric field sense a fraction of the voltage drop proportional to their distance through the field [41]. Because of this, a charged ligand can change its apparent affinity depending upon the fractional electrical distance of the interaction site and the applied transmembrane voltage. We measured the entry rate to slow inactivation (voltage protocol as described in Fig. 1) at a series of conditioning pulse voltages ranging from 0 to +100 mV, and exposed the channels to variable concentrations of external Na^+. Sucrose was

used to maintain the osmolality of the solutions at 280 mM. The sensitivity of changes in the rate of entry to slow inactivation, relative to the change in concentration of external Na^+, was plotted on a natural log scale as a family of tau entry curves, each at a different conditioning voltage (Fig. 8 *A*). A voltage effect for the external Na^+ interaction with slow inactivation is clearly apparent, because the slope of the tau entry – $[Na^+]$ curve is shallower at more strongly depolarized conditioning voltages. At these more positive potentials, the local concentration of Na^+ in the external vestibule would be reduced due to the driving force of the transmembrane electric field. The fraction of the membrane field sensed by the cation while it interacts at this site (i.e. apparent electric distance δ) can be calculated according to the Woodhull model where $\tau_{entry}(V) = \tau_{entry}(V = 0)\, e^{z\delta FV/RT}$, where $\tau_{entry}(V = 0)$ represents the entry rate to slow inactivation in the absence of an electric field, z represents the cation charge (+1), V is the conditioning voltage, and F, R, and T have their conventional meanings [41]. A plot of the relative sensitivity of $\Delta\tau_{Entry}$ / $\Delta[Na^+]$ for different conditioning voltages yielded a δ value of 0.15 ± 0.02, or approximately 15% of the distance through the electrical field relative to the outside of the channel. In Fig. 8C this electrical distance is compared to δ values previously determined for various outer pore amino acids [42]. Based on this comparison, Na^+ and Li^+ appear to bind within the outer pore region, external to the selectivity filter. The approximate location of the outer EEDD ring (comprised of amino acids E403, E758, D1241, D1532), the ring of tryptophans (W402, W756, W1240, W1531), and the DEKA selectivity filter (D400, E755, K1237, A1532) are shown on the right hand side of Fig. 8 C in boxes.

4.4.10 Mutational analysis of external pore residues as potential candidates for the cation interaction site. The data presented thus far are consistent with a model wherein cation

interaction with a low affinity site external to the selectivity filter impedes slow inactivation. We sought to refine this mapping further by making site-directed mutations at residues that were likely candidates for the interaction site in the external vestibule: residues in the outer ring of charge (EEDD), the ring of tryptophans, and the DEKA selectivity filter. We then measured the ability of Na^+ to impede steady-state slow inactivation compared to the behavior observed in the absence of external alkali cation (sucrose). Shifts in $V_{1/2}$ relative to sucrose are shown for each mutation in Fig. 9 and Table 3. The color code denotes the magnitude of the shift in $V_{1/2}$ ($V_{1/2}$Na $- V_{1/2}$sucrose) for each mutant channel compared to the shift observed for WT. A value of 0 mV (*white*) represents a Na-sucrose shift identical to WT channels (about 18 mV) whereas blue indicates a greater rightward shift and red indicates a reduced shift. Disruption of an external cation interaction site (or its allosteric effects) would be expected to reduce the shift (*red*). Apparently, residues from all four domains at various depths in the pore can affect the cation interaction with slow inactivation. Most mutations reduced the ability of Na^+ to impede slow inactivation, although some residues (e.g. D400N) enhanced this effect.

4.5   Discussion

Based on the overall results of this study, we propose that alkali metal cations interact with slow inactivation at a low-affinity but highly selective binding site in the outer pore of the sodium channel, located externally to the selectivity filter mechanism. The location of this site may be the same or at least overlap the TTX binding site.

Webb et al.

4.5.1 External, but not internal alkali cations impede slow inactivation in Nav1.4 channels. Previous reports observed that cations in the external bath solution can affect sodium channel slow inactivation, while the role of internal cations in modulating slow inactivation is not known [16, 26-29]. In our experiments, external Na^+ (Fig. 1) slowed entry and sped recovery from slow inactivation, right-shifted the half-inactivation voltage of steady-state slow inactivation, and increased the proportion of channels that did not slow inactivate at highly depolarized potentials. In striking contrast, we found that internal Na^+ did not affect any of the slow inactivation parameters tested.

4.5.2 The fast inactivation gate does not block cation access to an inner pore slow inactivation modulatory site. Slow inactivation in wild-type channels is clearly insensitive to internal Na^+. This observation alone, however, does not necessarily rule out the presence of internal cation binding sites that might influence slow inactivation. For example, the channel fast gate closes and blocks current flow almost immediately after depolarization, and this event might also block cation access to any internal site(s). To account for this, we examined internal Na^+ effects on slow inactivation with fast inactivation removed. Removal of fast inactivation provided an extended opportunity for intracellular sodium to permeate the inner pore and interact with any potential binding sites that might be inaccessible in Wt channels. Even in the mutant channels, however, intracellular Na^+ caused no discernible changes to slow inactivation (Fig. 2).

4.5.3 Extracellular Na^+ does not prevent internal cation effects on slow inactivation. In the experiments discussed thus far, we examined the effect of internal cations on slow inactivation with external Na^+ always present. External Na^+ clearly impedes slow inactivation,

and so might be inducing allosteric or other changes in the channel that prevent the detection of an internal cation effect. When the external buffer was switched from Na^+ to Rb^+, however, internal Na^+ still showed minimal effects, causing no change in the half-inactivation voltage of steady-state slow inactivation, and causing a small change in the slope (*k*). This, again, is in stark contrast to the large effects caused by external cations. Overall, these results suggest that alkali cations interact with slow inactivation exclusively on the external side of the channel.

4.5.4 Cation effect on slow inactivation is not due to coupling with fast gating changes. Extracellular cations are known to affect channel fast gating, although the extent of these effects is not completely defined [32, 33, 36, 37]. Some changes in fast gating, such as disruption of fast inactivation, are coupled with changes in slow inactivation [38, 39]. Therefore, we measured cation effects on fast gating to determine whether significant coupling to slow inactivation was likely. External Na^+ did not affect the half-voltage of activation and modestly disrupted fast inactivation relative to external Rb^+ (Fig. 3). Such relatively minor changes are very unlikely to be coupled to changes in slow inactivation. Notably, however, Na^+ reduced the steepness of voltage-dependence of channel activation (Fig. 3 *A*). While this was the most significant fast gating change observed, activation was still insignificant at voltages lower than $-50mV$. Extracellular cations, however, are still able to cause dramatic changes to slow inactivation at far more negative potentials than this. Moreover, the changes in activation are in the wrong direction to be coupled with impairment of slow inactivation by external Na^+. We conclude, then, that cation-induced changes in fast gating are not sufficient to explain the significant effects on slow inactivation. Instead, external cations are likely to directly interact with the slow inactivation mechanism.

4.5.5   Extracellular cations affect cardiac Nav1.5 channels. Skeletal muscle Nav1.4 and heart Nav1.5 channels show significant differences in slow inactivation gating and in binding affinity for a variety of cationic toxins and metals [39, 43, 44]. Although extracellular cations are known to modulate slow inactivation in other Na^+ channel isoforms [27, 28, 32], we wanted to ensure that the large effects that we observed in our expression system and with our voltage protocols applied to other channel isoforms as well. Extracellular Na^+ impeded (right-shifted) steady-state slow inactivation in heart Nav1.5 channels (Fig. 5). This shift was very similar in direction and magnitude to that observed in Nav1.4 (+17.8 mV for Nav1.5, compared to +20.8 mV for Nav1.4). The cation effect that we observed, then, is not specific to just one channel isoform. Instead, it is likely to be more generally applicable to other sodium channels, and is probably the same effect previously observed in other preparations [26-28].

4.5.6   The cation interaction site with slow inactivation is highly selective. We examined the effects of all of the Group IA alkali metal cations on slow inactivation (Fig. 5), and found that Na^+ and Li^+ both significantly impeded it compared to sucrose buffer. In contrast, K^+, Rb^+, and Cs^+ had much less effect. These results are consistent with either a highly selective slow inactivation binding site, or with other selectivity mechanism(s) elsewhere in the channel preventing the impermeable metal cations from reaching a non-selective binding site. Some of the original work that first identified sodium channel slow inactivation similarly observed selectivity in cation effects, finding that slow inactivation was impeded by extracellular Na^+ versus K^+ [28, 32]. Later work by Townsend and Horn [27] also showed that extracellular cations could influence slow inactivation, although in contrast to us and others they did not

report a difference among the various alkali metals. This discrepancy may arise at least in part because their protocols focused primarily on examining the maximum extent of slow inactivation (I_0) among metal cations in Nav1.5, a test which we found to be less sensitive for discriminating these large cation differences, especially for Nav1.5 (Fig. 5). Furthermore, they examined these effects in channels with fast inactivation removed, a condition which clearly affects slow inactivation. This might have further obscured any differences between the cations in their system, although we still observed clear differences between external Rb^+ and Na^+ after removing fast inactivation (Fig. 2).

4.5.7 Cation interaction with slow inactivation is not dependent on permeability through the selectivity filter of the channel. We noticed that alkali cations which were highly permeable through the channel (Na^+, Li^+) dramatically altered slow inactivation, while the impermeable cations had no effect (Fig. 5). Based on these observations, we wondered if the site of cation interaction with slow inactivation is located deep in the permeation pathway, such that the selectivity filter prevented impermeable cations from reaching the interaction site. The K1237C mutation virtually abolishes selectivity among the alkali cations and promotes robust Rb^+ movement through the channel (Fig. 6 *A*). If cation access to a deep site in the channel is sufficient to promote interaction with slow inactivation, then Rb^+ should impede slow inactivation similarly to Na^+ in the K1237C channels. We found, however, that the K1237C only mildly promoted the ability of Rb^+ to impede slow inactivation (3.5 mV right-shift), while decreasing the ability of Na^+ to do so compared to Wt (10.5 mV right-shift in K1237C,

Webb et al.

compared to the 20.8mV right-shift in Wt). Apparently, a dramatic increase in cation permeability is not sufficient to promote cation interaction with slow inactivation.

4.5.8 External cation interaction with slow inactivation is low affinity. Our results showed that increases in external Na^+ linearly right-shifted the voltage of half-inactivation of slow inactivation over a range of $0 - 140$ mM, suggesting that Na^+ interaction with the slow inactivation modulatory site is very weak. Two other lines of evidence agree with this assertion. First, numerous other groups have investigated Na^+ affinity for the permeation pathway of the sodium channel by measuring current flow saturation and competition with channel pore blockers, and they similarly found that Na^+ affinity for the channel is weak [45-51]. These groups reported an apparent Kd ranging from tens to hundreds of millimolar, with an average of over 300 mM. Second, if Na^+ interacts with slow inactivation within the permeation pathway, then interaction of the cation with the channel must be very fast (weak) to support the high rate of current flow through the channel. Therefore, the weak cation binding affinity that we describe here is consistent with our proposal that cation interaction with slow inactivation occurs in the permeation pathway.

4.5.9 Na^+ interacts with slow inactivation at a shallow electrical distance within the membrane electrical field. A novel finding of this study is that the interaction of Na^+ with slow inactivation occurs at an apparent electrical distance (δ) of 0.15, relative to the external side of the channel. Comparison of this measurement to the δ of various outer pore amino acid residues (Fig. 8 *B*) suggests that the interaction occurs at a relatively shallow location in the outer pore, between the external EEDD charged ring and the inner DEKA selectivity filter.

125

Webb et al.

Prior work has established that the shallow outer pore region above the selectivity filter interacts with a wide variety of extracellular cations. For instance, charged toxins (TTX, STX), hydrogen ions, and multivalent metal cations (Ca^{+2}, Mg^{+2}) are known to block sodium current when applied externally, and both voltage-dependent and voltage-independent blocking modes have been observed [41, 52-56]. On average, block of the channel by these various cations showed low voltage-dependence (avg. $\delta = 0.23 \pm 0.08$, $n = 19$) relative to the outside of the channel, consistent with shallow outer pore block. Our measurement of δ for Na^+ with slow inactivation reported in this study is in good general agreement with the average values reported for these outer pore blockers. This may indicate a common region that mediates both channel block and interaction with slow inactivation.

Other evidence suggesting a common region of cation interaction is that external alkali cations appear to directly compete for binding with other outer pore blockers such as divalent cations [57, 58] and guanidinium toxins [47-49, 59-61]. Of particular interest is the interaction of Na^+ and TTX. Numerous mutagenesis studies have established that TTX binds in the outer pore region, coordinating primarily with amino acids at or near to the EEDD and DEKA rings [62-65]. TTX binding is also clearly voltage dependent, yielding a δ of 0.16 [53], which is very similar to our results for Na^+ interaction with slow inactivation. Moczydlowski et al. further showed that Na^+ interacts via simple competition with TTX when applied from the external side [47]. Notably, however, internal Na^+ did not compete with TTX binding, even when outward Na^+ currents were elicited. This closely parallels our observation that Na^+ only interacts with the slow inactivation site when it is applied to the external side of the channel (Figs. 1, 2). It has also been repeatedly shown that Na^+ and Li^+ are more effective at competing with TTX binding than are K^+, Rb^+, and Cs^+ [47-49, 59-61]. This sequence corresponds to our observation that

Webb et al.

Na$^+$ and Li$^+$ are much more effective at impeding slow inactivation in wild-type sodium channels than are the others (Figs. 5, 8). Together, these observations suggest that Na$^+$ interacts with slow inactivation either at or very close to the TTX binding site.

4.5.10 Mutagenesis in the channel pore region affected cation interaction with slow inactivation. We mutated residues in the outer pore and assessed the impact of these changes on cation interaction with slow inactivation. Our results showed that residues at various depths from all four domains in the channel contribute to this effect. This complex array of participating residues, coupled with the stringent selectivity of this interaction site, suggest that cation-mediated impediment of slow inactivation is a complex, highly coordinated process involving cation interaction with many parts of the outer pore. This is in contrast to a simple foot-in-the-door model in which any non-specific cation can simply occupy the outer pore and prevent closure of a slow inactivation gate. It also contrasts to the idea of simple outer pore charge neutralization. A newly proposed model of slow inactivation [66] suggests the many negative charges in the outer pore, especially in the EEDD ring, oppose each other and create a driving force for the outer pore to open wider. This outer pore opening is proposed to allosterically cause channel closure deeper within the permeation pathway via a pivoting motion, leading to slow inactivation and block of current flow. In this model, Na$^+$ ions were proposed to enter the pore and partially neutralize the negative charge, thereby reducing the repulsive driving force to open the outer pore (i.e. slow inactivate). Our results, however, suggest that the cation effect on slow inactivation is more complex than this. For one, positively charged cations such as Rb$^+$ are highly accessible to the pore in mutations such as K1237C (Fig. 6), but still do not cause a large change to slow inactivation. This again indicates that the simple presence of

positive charges in the outer pore is insufficient to impede slow inactivation. Also, mutagenesis of uncharged (tryptophan) residues that do not affect the electrostatic potential of the pore can still profoundly affect cation interaction with slow inactivation. Finally, neutralization of negatively charged residues in the outer pore were shown to cause a wide range of effects, from no effect to disruption or even enhancement of the cation effect on slow inactivation. Such observations are inconsistent with a simple electrostatic interaction between a cation and a negatively charged outer pore. They instead argue that cation interaction with slow inactivation is a very precise process in which only certain cations (e.g. Na^+ and Li^+) can appropriately interact with multiple residues to impede this process.

Webb et al.

4.6 References

1. Schauf, C.L., T.L. Pencek, and F.A. Davis, *Slow sodium inactivation in Myxicola axons. Evidence for a second inactive state.* Biophys J, 1976. **16**(7): p. 771-8.
2. West, J.W., et al., *A cluster of hydrophobic amino acid residues required for fast Na(+)-channel inactivation.* Proc Natl Acad Sci U S A, 1992. **89**(22): p. 10910-4.
3. Rudy, B., *Slow inactivation of the sodium conductance in squid giant axons. Pronase resistance.* J Physiol, 1978. **283**: p. 1-21.
4. Takahashi, M.P. and S.C. Cannon, *Enhanced slow inactivation by V445M: a sodium channel mutation associated with myotonia.* Biophys J, 1999. **76**(2): p. 861-8.
5. Cummins, T.R. and F.J. Sigworth, *Impaired slow inactivation in mutant sodium channels.* Biophys J, 1996. **71**(1): p. 227-36.
6. Hayward, L.J., G.M. Sandoval, and S.C. Cannon, *Defective slow inactivation of sodium channels contributes to familial periodic paralysis.* Neurology, 1999. **52**(7): p. 1447-53.
7. Kuzmenkin, A., et al., *Impaired slow inactivation due to a polymorphism and substitutions of Ser-906 in the II-III loop of the human Nav1.4 channel.* Pflugers Arch, 2003. **447**(1): p. 71-7.
8. Ulbricht, W., *Sodium channel inactivation: molecular determinants and modulation.* Physiol Rev, 2005. **85**(4): p. 1271-301.
9. Lipkind, G.M. and H.A. Fozzard, *KcsA crystal structure as framework for a molecular model of the Na(+) channel pore.* Biochemistry, 2000. **39**(28): p. 8161-70.
10. Balser, J.R., et al., *External pore residue mediates slow inactivation in mu 1 rat skeletal muscle sodium channels.* J Physiol, 1996. **494 (Pt 2)**: p. 431-42.
11. McNulty, M.M., et al., *An inner pore residue (Asn406) in the Nav1.5 channel controls slow inactivation and enhances mibefradil block to T-type Ca2+ channel levels.* Mol Pharmacol, 2006. **70**(5): p. 1514-23.
12. O'Reilly, J.P., S.Y. Wang, and G.K. Wang, *Residue-specific effects on slow inactivation at V787 in D2-S6 of Na(v)1.4 sodium channels.* Biophys J, 2001. **81**(4): p. 2100-11.
13. Wang, S.Y. and G.K. Wang, *A mutation in segment I-S6 alters slow inactivation of sodium channels.* Biophys J, 1997. **72**(4): p. 1633-40.
14. Wang, S.Y., C. Russell, and G.K. Wang, *Tryptophan substitution of a putative D4S6 gating hinge alters slow inactivation in cardiac sodium channels.* Biophys J, 2005. **88**(6): p. 3991-9.
15. Xiong, W., et al., *Molecular motions of the outer ring of charge of the sodium channel: do they couple to slow inactivation?* J Gen Physiol, 2003. **122**(3): p. 323-32.

16. Benitah, J.P., et al., *Molecular dynamics of the sodium channel pore vary with gating: interactions between P-segment motions and inactivation.* J Neurosci, 1999. **19**(5): p. 1577-85.

17. Xiong, W., et al., *A conserved ring of charge in mammalian Na+ channels: a molecular regulator of the outer pore conformation during slow inactivation.* J Physiol, 2006. **576**(Pt 3): p. 739-54.

18. Zhang, Z., et al., *A negatively charged residue in the outer mouth of rat sodium channel determines the gating kinetics of the channel.* Am J Physiol Cell Physiol, 2003. **284**(5): p. C1247-54.

19. Todt, H., et al., *Ultra-slow inactivation in mu1 Na+ channels is produced by a structural rearrangement of the outer vestibule.* Biophys J, 1999. **76**(3): p. 1335-45.

20. Struyk, A.F. and S.C. Cannon, *Slow inactivation does not block the aqueous accessibility to the outer pore of voltage-gated Na channels.* J Gen Physiol, 2002. **120**(4): p. 509-16.

21. Liu, Y., M.E. Jurman, and G. Yellen, *Dynamic rearrangement of the outer mouth of a K+ channel during gating.* Neuron, 1996. **16**(4): p. 859-67.

22. Baukrowitz, T. and G. Yellen, *Modulation of K+ current by frequency and external [K+]: a tale of two inactivation mechanisms.* Neuron, 1995. **15**(4): p. 951-60.

23. Lopez-Barneo, J., et al., *Effects of external cations and mutations in the pore region on C-type inactivation of Shaker potassium channels.* Receptors Channels, 1993. **1**(1): p. 61-71.

24. Berneche, S. and B. Roux, *A gate in the selectivity filter of potassium channels.* Structure, 2005. **13**(4): p. 591-600.

25. Kiss, L., J. LoTurco, and S.J. Korn, *Contribution of the selectivity filter to inactivation in potassium channels.* Biophys J, 1999. **76**(1 Pt 1): p. 253-63.

26. Adelman, W.J., Jr. and Y. Palti, *The effects of external potassium and long duration voltage conditioning on the amplitude of sodium currents in the giant axon of the squid, Loligo pealei.* J Gen Physiol, 1969. **54**(5): p. 589-606.

27. Townsend, C. and R. Horn, *Effect of alkali metal cations on slow inactivation of cardiac Na+ channels.* J Gen Physiol, 1997. **110**(1): p. 23-33.

28. Peganov, E.M., B.I. Khodorov, and L.D. Shishkova, *[Slow sodium inactivation in Ranvier's node membrane. Role of external potassium].* Biull Eksp Biol Med, 1973. **76**(9): p. 15-9.

29. Chen, Z., et al., *Lidocaine induces a slow inactivated state in rat skeletal muscle sodium channels.* J Physiol, 2000. **524 Pt 1**: p. 37-49.

30. Hayward, L.J., R.H. Brown, Jr., and S.C. Cannon, *Inactivation defects caused by myotonia-associated mutations in the sodium channel III-IV linker.* J Gen Physiol, 1996. **107**(5): p. 559-76.

31. Jurman, M.E., et al., *Visual identification of individual transfected cells for electrophysiology using antibody-coated beads.* Biotechniques, 1994. **17**(5): p. 876-81.

32. Adelman, W.J., Jr. and Y. Palti, *The influence of external potassium on the inactivation of sodium currents in the giant axon of the squid, Loligo pealei.* J Gen Physiol, 1969. **53**(6): p. 685-703.

33. Townsend, C., H.A. Hartmann, and R. Horn, *Anomalous effect of permeant ion concentration on peak open probability of cardiac Na+ channels.* J Gen Physiol, 1997. **110**(1): p. 11-21.

34.   Catterall, W.A., *From ionic currents to molecular mechanisms: the structure and function of voltage-gated sodium channels.* Neuron, 2000. **26**(1): p. 13-25.

35.   Wang, S.Y., et al., *Tryptophan scanning of D1S6 and D4S6 C-termini in voltage-gated sodium channels.* Biophys J, 2003. **85**(2): p. 911-20.

36.   Wright, S.N., *Comparison of aconitine-modified human heart (hH1) and rat skeletal (mu1) muscle Na+ channels: an important role for external Na+ ions.* J Physiol, 2002. **538**(Pt 3): p. 759-71.

37.   Keynes, R.D., N.G. Greeff, and I.C. Forster, *Activation, inactivation and recovery in the sodium channels of the squid giant axon dialysed with different solutions.* Philos Trans R Soc Lond B Biol Sci, 1992. **337**(1282): p. 471-84.

38.   Nuss, H.B., et al., *Coupling between fast and slow inactivation revealed by analysis of a point mutation (F1304Q) in mu 1 rat skeletal muscle sodium channels.* J Physiol, 1996. **494 (Pt 2)**: p. 411-29.

39.   Richmond, J.E., et al., *Slow inactivation in human cardiac sodium channels.* Biophys J, 1998. **74**(6): p. 2945-52.

40.   Tsushima, R.G., R.A. Li, and P.H. Backx, *Altered ionic selectivity of the sodium channel revealed by cysteine mutations within the pore.* J Gen Physiol, 1997. **109**(4): p. 463-75.

41.   Woodhull, A.M., *Ionic blockage of sodium channels in nerve.* J Gen Physiol, 1973. **61**(6): p. 687-708.

42.   Chiamvimonvat, N., et al., *Depth asymmetries of the pore-lining segments of the Na+ channel revealed by cysteine mutagenesis.* Neuron, 1996. **16**(5): p. 1037-47.

43.   Rogart, R.B., et al., *Molecular cloning of a putative tetrodotoxin-resistant rat heart Na+ channel isoform.* Proc Natl Acad Sci U S A, 1989. **86**(20): p. 8170-4.

44.   Ravindran, A., L. Schild, and E. Moczydlowski, *Divalent cation selectivity for external block of voltage-dependent Na+ channels prolonged by batrachotoxin. Zn2+ induces discrete substates in cardiac Na+ channels.* J Gen Physiol, 1991. **97**(1): p. 89-115.

45.   Begenisich, T.B. and M.D. Cahalan, *Sodium channel permeation in squid axons. II: Non-independence and current-voltage relations.* J Physiol, 1980. **307**: p. 243-57.

46.   Hille, B., *Ionic selectivity, saturation, and block in sodium channels. A four-barrier model.* J Gen Physiol, 1975. **66**(5): p. 535-60.

47.   Moczydlowski, E., S.S. Garber, and C. Miller, *Batrachotoxin-activated Na+ channels in planar lipid bilayers. Competition of tetrodotoxin block by Na+.* J Gen Physiol, 1984. **84**(5): p. 665-86.

48.   Henderson, R., J.M. Ritchie, and G.R. Strichartz, *Evidence that tetrodotoxin and saxitoxin act at a metal cation binding site in the sodium channels of nerve membrane.* Proc Natl Acad Sci U S A, 1974. **71**(10): p. 3936-40.

49.   Reed, J.K. and M.A. Raftery, *Properties of the tetrodotoxin binding component in plasma membranes isolated from Electrophorus electricus.* Biochemistry, 1976. **15**(5): p. 944-53.

50.   Weigele, J.B. and R.L. Barchi, *Analysis of saxitoxin binding in isolated rat synaptosomes using a rapid filtration assay.* FEBS Lett, 1978. **91**(2): p. 310-4.

51.   Yamamoto, D., J.Z. Yeh, and T. Narahashi, *Interactions of permeant cations with sodium channels of squid axon membranes.* Biophys J, 1985. **48**(3): p. 361-8.

52.   Yamamoto, D., J.Z. Yeh, and T. Narahashi, *Voltage-dependent calcium block of normal and tetramethrin-modified single sodium channels.* Biophys J, 1984. **45**(1): p. 337-44.

53.   Satin, J., et al., *The saxitoxin/tetrodotoxin binding site on cloned rat brain IIa Na channels is in the transmembrane electric field.* Biophys J, 1994. **67**(3): p. 1007-14.

54. Daumas, P. and O.S. Andersen, *Proton block of rat brain sodium channels. Evidence for two proton binding sites and multiple occupancy.* J Gen Physiol, 1993. **101**(1): p. 27-43.

55. Sheets, M.F. and D.A. Hanck, *Mechanisms of extracellular divalent and trivalent cation block of the sodium current in canine cardiac Purkinje cells.* J Physiol, 1992. **454**: p. 299-320.

56. Green, W.N., L.B. Weiss, and O.S. Andersen, *Batrachotoxin-modified sodium channels in planar lipid bilayers. Ion permeation and block.* J Gen Physiol, 1987. **89**(6): p. 841-72.

57. Visentin, S., et al., *Sodium current block caused by group IIb cations in calf Purkinje fibres and in guinea-pig ventricular myocytes.* Pflugers Arch, 1990. **417**(2): p. 213-22.

58. French, R.J., et al., *Ion permeation, divalent ion block, and chemical modification of single sodium channels. Description by single- and double-occupancy rate-theory models.* J Gen Physiol, 1994. **103**(3): p. 447-70.

59. Barchi, R.L. and J.B. Weigele, *Characteristics of saxitoxin binding to the sodium channel of sarcolemma isolated from rat skeletal muscle.* J Physiol, 1979. **295**: p. 383-96.

60. Lonnendonker, U., B. Neumcke, and R. Stampfli, *Interaction of monovalent cations with tetrodotoxin and saxitoxin binding at sodium channels of frog myelinated nerve.* Pflugers Arch, 1990. **416**(6): p. 750-7.

61. Weigele, J.B. and R.L. Barchi, *Saxitoxin binding to the mammalian sodium channel. Competition by monovalent and divalent cations.* FEBS Lett, 1978. **95**(1): p. 49-53.

62. Terlau, H., et al., *Mapping the site of block by tetrodotoxin and saxitoxin of sodium channel II.* FEBS Lett, 1991. **293**(1-2): p. 93-6.

63. Noda, M., et al., *A single point mutation confers tetrodotoxin and saxitoxin insensitivity on the sodium channel II.* FEBS Lett, 1989. **259**(1): p. 213-6.

64. Satin, J., et al., *A mutant of TTX-resistant cardiac sodium channels with TTX-sensitive properties.* Science, 1992. **256**(5060): p. 1202-5.

65. Kontis, K.J. and A.L. Goldin, *Site-directed mutagenesis of the putative pore region of the rat IIA sodium channel.* Mol Pharmacol, 1993. **43**(4): p. 635-44.

66. Tikhonov, B.S.Z., *Molecular Modeling of Slow Inactivation and State-Dependent Drug Binding in Sodium Channels.* Biophysical Society Abstract, 2007.

4.7   Tables and Figures

Table I Slow inactivation gating parameters for channels exposed to external or internal Na$^+$ or Rb$^+$

| OUT / IN | Steady State | | | Entry | Recovery |
	V1/2 (mV)	k (mV)	I$_0$	T (msec)	T (msec)
Na / Na	-52.2 ± 0.3 (4)	7.63 ± .28 (4)	0.19 ± .04 (6)	1554 ± 152 (6)	125 ± 13 (6)
Na / Rb	-51.0 ± 0.8 (4)	7.82 ± 1.2 (4)	0.22 ± .01 (5)	1390 ± 261 (5)	119 ± 15 (4)
Rb / Na	-73.0 ± 2.8** (5)	6.55 ± .43* (5)	0.12 ± .01* (6)	769 ± 109** (6)	199 ± 11** (5)

Values are means ± S.E.M. with number of experiments in parantheses *Significantly different from NaOut / NaIn, $P < 0.05$; **Significantly different from NaOut / NaIn, $P < 0.001$

Table II Steady state slow inactivation parameters for various external cation buffers

Ext.Cation	$V_{1/2}$ (mV)	k (mV)	I_0
Li$^+$	-52.1 ± 2.1** (4)	6.50 ± 0.32**	0.21 ± .02**
Na$^+$	-52.2 ± 0.3** (4)	7.63 ± 0.28**	0.19 ± .02**
K$^+$	-71.3 ± 1.4 (6)	5.86 ± 0.16**	0.11 ± .01**
Rb$^+$	-73.0 ± 1.2 (5)	6.55 ± 0.43**	0.09 ± .01**
Cs$^+$	-71.9 ± 0.6 (3)	5.98 ± 0.62*	0.10 ± .01**
Sucrose	-71.8 ± 3.5 (6)	4.44 ± 0.25	0.05 ± .02

Values are means ± SEM with number of experiments in parentheses. * Significantly different from Sucrose, $P < 0.05$; ** Significantly different from Sucrose, $P < 0.005$

Table III Voltages of half inactivation ($V_{1/2}$) of steady state slow inactivation in various outer pore mutants exposed to external sucrose or Na+.

	Sucrose	Na+	Shift
Wt	-71.8 ± 3.5 (6)	-52.3 ± 0.4 (5)	19.5
E403Q	-69.5 ± 4.6 (4)	-54.7 ± 2.0 (5)	14.8
E758Q	-63.6 ± 7.2 (7)	-54.5 ± 0.7 (4)	9.1
D1241N	-71.8 ± 1.1 (3)	-53.1 ± 2.6 (4)	18.7
D1532N	-76.5 ± 2.7 (3)	-54.7 ± 3.2 (6)	21.8
W402C	-62.8 ± 12.3 (7)	-47.1 ± 9.3 (5)	15.8
W756C	-56.1 ± 4.3 (4)	-35.6 ± 2.1 (3)	20.5
W1239C	-78.4 ± 4.9 (6)	-65.4 ± 1.0 (3)	13
W1531C	-93.9 ± 1.6 (3)	-79.6 ± 1.8 (4)	14.3
D400N	-85.2 ± 4.1 (4)	-57.1 ± 2.5 (5)	28.1
E755Q	-72.7 ± 0.8 (3)	-59.5 ± 1.0 (4)	13.2
K1237C	-68.1 ± 0.8 (4)	-57.6 ± 1.7 (4)	10.5
A1529D	-75.3 ± 1.6 (3)	-57.8 ± 3.4 (5)	17.5

Values are means ± SEM with number of experiments in parentheses. The cation induced shift was calculated by subtracting the $V_{1/2}$ of cells exposed to external Na+ from those exposed to sucrose.
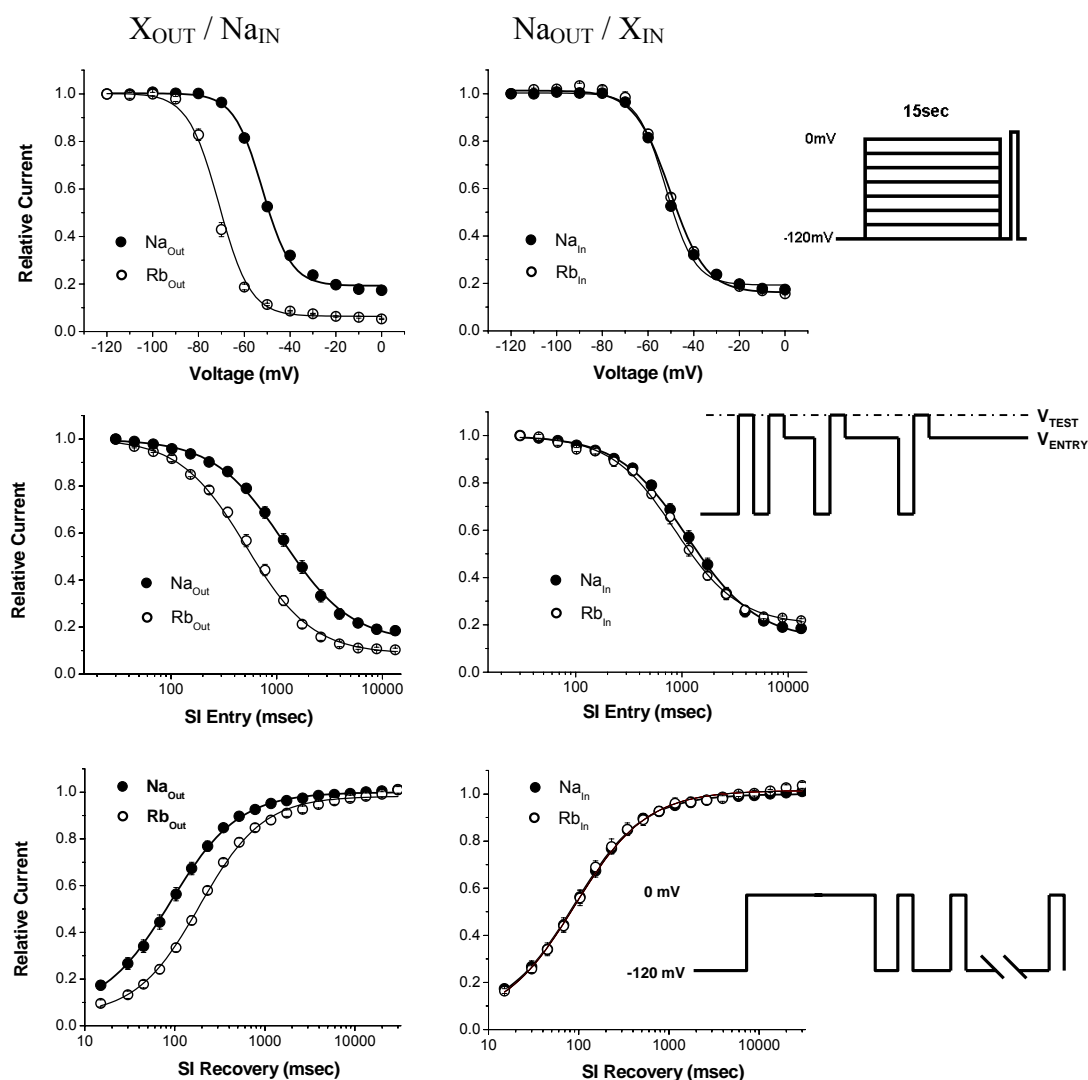
FIGURE 1 External, but not internal, monovalent cations affected the kinetics and voltage-dependence of slow inactivation. Data points are mean ± SEM of four to six measurements. Left column (X_{OUT} / Na_{IN}) shows the behavior of slow inactivation in the presence of 140 mM external Na^+ or Rb^+, with 140 mM Na^+ as the internal cation in both cases. Right column (Na_{OUT} / X_{IN}) shows the behavior of slow inactivation in response to 140 mM internal Na^+ or Rb^+, with 140 mM Na^+ as the external cation in both cases. Pulse protocols are shown in the insets; see text for details. **(A)** Voltage-dependence of steady-state slow inactivation was right-shifted (impeded) by +20.8 mV in external Na^+ versus external Rb^+ (*left column*), whereas the voltage-

dependence was identical with either Na^+ or Rb^+ as the internal cation (*right column*). **(B)** Rate of entry to slow inactivation was two-fold slower in Na_{Out} versus Rb_{Out}, and the proportion of non-slow inactivating current (I_0) was also three-fold less in Na_{Out} (*left column*). In contrast, the rate of entry to slow inactivation was the same for Na_{In} versus Rb_{In}. (*right column*) **(C)** Recovery from slow inactivation was 1.6-fold faster for Na_{Out} versus Rb_{Out} (*left column*) but was the same for Na_{In} versus Rb_{In} (*right column*).
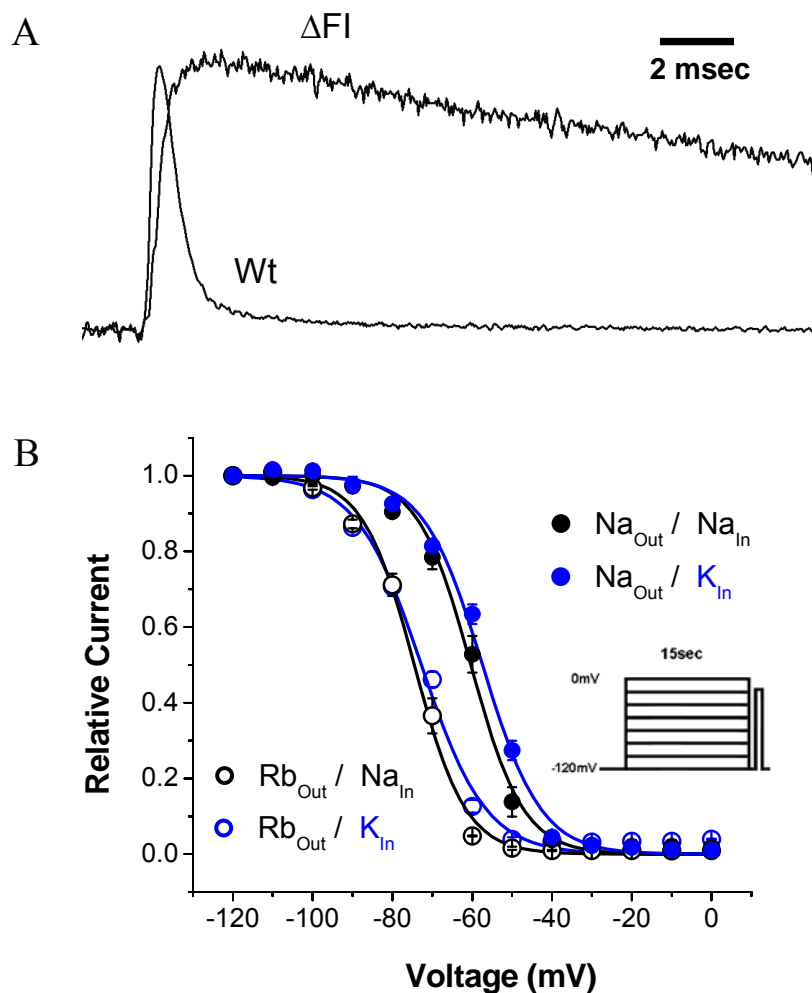
FIGURE 2 The lack of an internal cation effect on slow inactivation was not due to interference from the fast inactivation gate, nor due to the influence of external cations. **(A)** The L437C/A438W double mutation caused a profound disruption of fast inactivation (ΔFI). Currents elicited by a step depolarization were normalized to peak amplitude and superimposed **(B)** Varying the internal cation between 140 mM Na^+ or K^+ in the ΔFI mutant did not affect the voltage of half-inactivation ($V_{1/2}$) in the background of external Na^+ or Rb^+. This contrasts to the large (~15 mV) shift in $V_{1/2}$ caused by varying the external cation. Data points are mean ± SEM for three to four measurements.
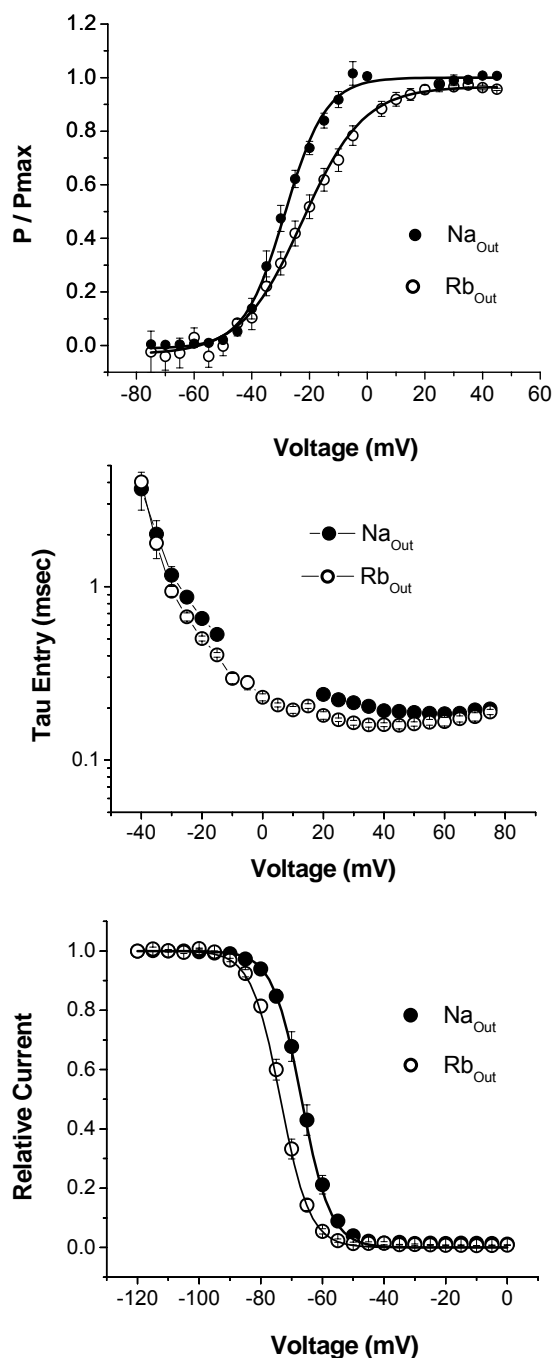
FIGURE 3 External cations affected sodium channel fast gating. Data points are mean ± SEM of four to six measurements. Pulse protocols are described in RESULTS. **(A)** External Na^+ (Na_{Out}) decreased the slope factor (k) of channel activation by two-fold relative to external Rb^+ (Rb_{Out}) ($P < 0.0001$). The voltage of half-activation ($V_{1/2}$) was not significantly affected. **(B)**

Kinetics of fast inactivation was largely unaffected by external Na$^+$ compared to external Rb$^+$.

(C) Voltage-dependence of steady-state fast inactivation was right-shifted (impeded) by 6.8 mV in external Na$^+$ compared to external Rb$^+$ ($P < 0.0005$).
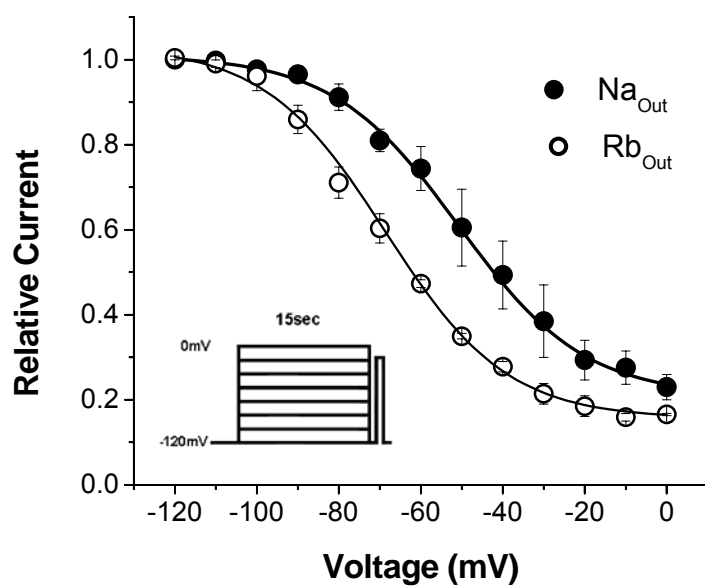
+

FIGURE 4 External cations affected slow inactivation in the Nav1.5 heart channel isoform. Steady-state slow inactivation was measured for channels exposed to 140 mM external Na^+ or Rb^+. The pulse protocol (*inset*) is identical that in Fig. 1 A. External Na^+ right-shifts the half-inactivation ($V_{1/2}$) of steady-state slow inactivation by 17.8 mV relative to external Rb^+. Data points are mean ± SEM of three to four measurements.
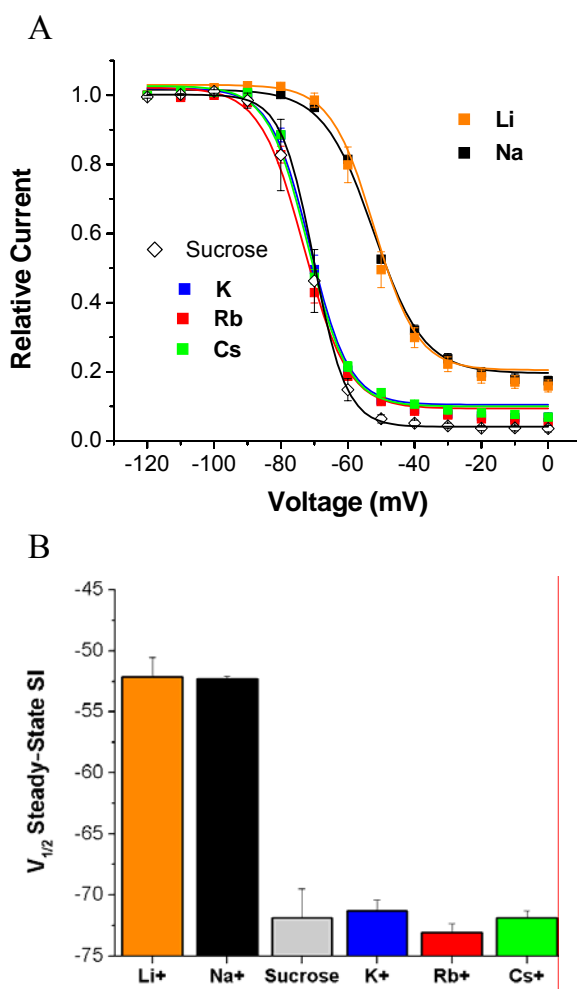
A

B

FIGURE 5 Slow inactivation was impeded by external Na^+ and Li^+, but was not affected by external K^+, Rb^+, and Cs^+. (A) Steady-state slow inactivation curves for cells exposed to various external alkali metal cations or sucrose. All cation and sucrose concentrations were 140 mM, and 140 mM Na^+ was always used as the internal cation. (B) Bar plot of the half-inactivation voltages ($V_{1/2}$) for channels exposed to the various external alkali metal cations. Slow inactivation behavior in the presence of K^+, Rb^+, and Cs^+ ions is nearly identical to that in 140 mM sucrose, while Na^+ and Li^+ both right-shift the steady state curves by ~20 mV. Data points are mean ± SEM of three to six measurements.
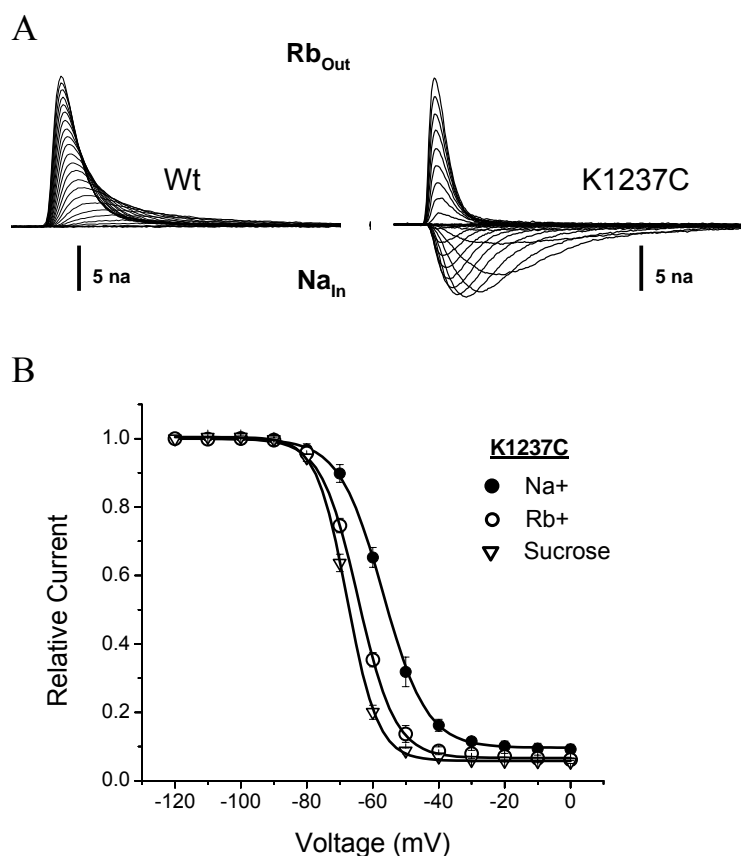
A

B

FIGURE 6 The cation effect on slow inactivation does not require permeability through the channel. (A) Currents recorded from WT and K1237C channels were normalized to peak amplitude to facilitate a comparison of the response in external Rb^+ and internal Na^+. Rb^+ was not measurably permeable in WT (*left traces*), as shown from the lack of inward currents. The K1237C mutation (*right traces*) abolished selectivity of Na^+ over Rb^+ and had a reversal potential near 0 mV. (B) Rb^+ permeability of K1237C mutant channels does not result in an impediment of slow inactivation comparable to that produced by external Na^+. Steady-state slow inactivation was measured in external Na^+, Rb^+ or sucrose. External Na^+ induced a 10.5 mV right-shift compared to sucrose, whereas Rb^+ caused very little shift of slow inactivation relative to sucrose (3.5 mV right shift, $P < 0.05$). Data points are mean ± SEM for three to six measurements.

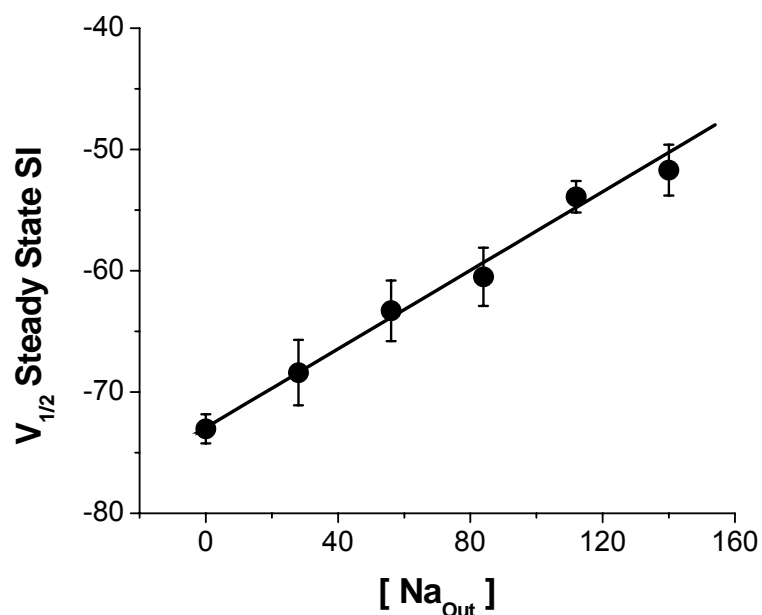**FIGURE 7** Dose-response of shift in steady-state slow inactivation caused by external Na^+. Data points are mean ± SEM of four to nine measurements. The half-inactivation ($V_{1/2}$) of steady-state slow inactivation was measured as a function of various concentrations of external Na^+ ($[Na_{Out}]$) ranging from 0 to 140 mM. Increasing concentration of external Na^+ caused an approximately linear right-shift (depolarization) of $V_{1/2}$, and no saturation of this effect was seen even at 140mM. This indicates that interaction of Na^+ and slow inactivation is very weak.
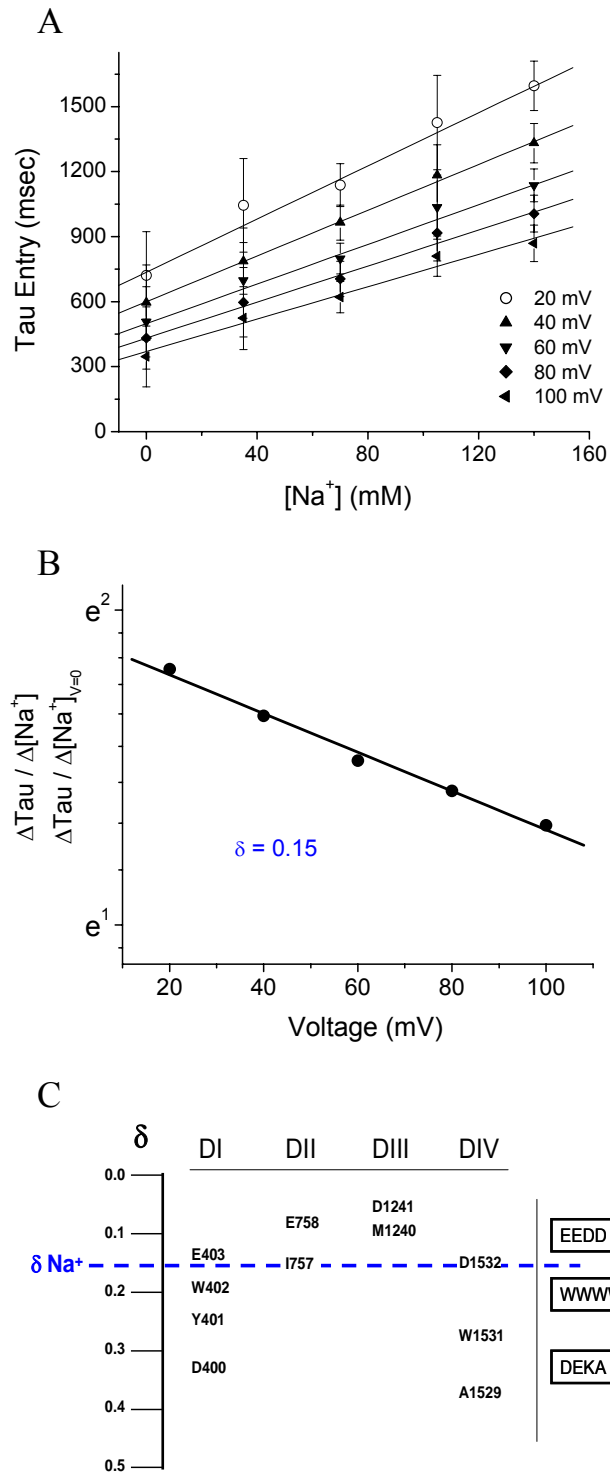
Webb et al.

FIGURE 8 Apparent electrical distance (δ) of the site of Na$^+$ interaction with slow inactivation is in the outer pore region of the sodium channel, external to the selectivity filter. **(A)** Tau entry

rates at entry conditioning potentials ranging from +20 through +100mV are plotted at different

concentrations of external Na$^+$ (n = 29 cells). The rate of change in tau entry versus [Na$^+$] was

linear at each voltage. **(B)** The slopes of the linear rate of change in Tau entry (ΔTau) relative to

the change in concentration of external Na$^+$ ($\Delta[Na^+]$) are plotted as a function of the various

entry conditioning voltages. Results are displayed on a natural log scale, with values of *e*-fold

change given for reference on the Y-axis. The rate of entry to slow inactivation (Tau entry) was

less sensitive to changes in the concentration of external cation at higher conditioning potentials,

indicating a voltage effect at the slow inactivation/cation interaction site. The apparent electrical

distance (δ) calculated from the voltage effect according to the Woodhull model [41] indicates

that Na$^+$ senses about 0.15 of the transmembrane electric field when interacting with slow

inactivation, relative to the outside of the channel. **(C)** The apparent electrical distance (δ) of

Na$^+$ interaction with slow inactivation (broken blue line) is compared to previously measured δ

values of outer pore amino acids from domains I – IV (adapted from [42]). For convenience, the

approximate locations of the outer ring of charge (EEDD), the ring of tryptophans (WWWW),

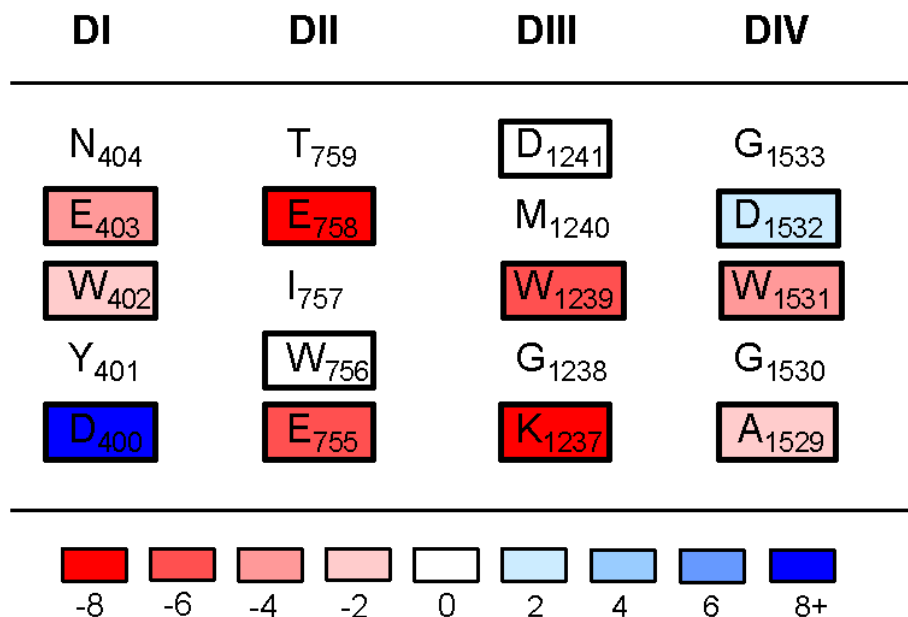and the selectivity filter (DEKA) are shown in boxes next to the chart.

FIGURE 9 Mutagenesis of outer pore residues affects the interaction of external Na^+ with slow inactivation. The voltage-dependence of steady-state slow inactivation was measured as described in Fig. 1 for various mutations exposed to either 140 mM external sucrose or Na^+. The resulting shift in the voltage of half-inactivation ($V_{1/2}$) caused by external Na^+ was then compared to the shift (19.5 mV) seen in Wt channels. Residues from the outer pore region are shown, and mutations that were tested are enclosed in colored boxes. Colors represent the difference in mV of the $V_{1/2}$ shift observed in the mutant compared to Wt, according to the color key at the bottom. Red boxes indicate a disruption of the cation effect in the mutant (smaller shift in $V_{1/2}$ compared to Wt), while blue boxes represent an enhancement of the cation effect. The steady-state slow inactivation values for each mutation are also shown in Table 3.

CHAPTER 5   CONCLUSIONS AND FUTURE DIRECTIONS

5.1 Molecular Mechanism of Slow Inactivation

The primary aim of the experiments in this thesis was to assist a larger effort to characterize where and how sodium channel slow inactivation occurs. This was accomplished by examining the manner in which external factors (i.e. the β1 subunit and alkali cations) influence slow inactivation. Our results demonstrate an interaction with the outer pore of the channel, and suggest in agreement with a growing body of work that the outer pore is an essential component for this gating process. Additionally, the contribution of slow inactivation to human disease was explored, and our data support a link between defective slow inactivation and a predisposition to muscle periodic paralysis. This chapter further summarizes what was learned, and proposes future directions for the field.

5.2 Slow Inactivation and Periodic Paralysis

Chapter 2 presented the biophysical properties of a novel sodium channel missense mutation associated with periodic paralysis. Defects in Nav1.4 fast

gating have long been known to associate with a spectrum of muscle disease, which can be broadly classified into myotonias (stiffness) and periodic paralysis (weakness). Cannon (Cannon, 2006) and others noticed that defects in slow inactivation always associated with weakness and not myotonia, and so they proposed that defective slow inactivation is a strong risk factor for paralysis. But this model is continuing to be developed, since these diseases are very rare and therefore the number of opportunities to observe additional mutations is small. The P1158S mutation, then, offered another rare chance to test this model. Even more striking, the symptoms were provoked by temperature, a novel feature that allowed me to test whether temperature would also provoke biophysical defects in slow inactivation.

The results of these experiments were clear: a defect in slow inactivation was found, and cold temperature provoked this channel defect. Such data provides strong support for a defect in slow inactivation as a risk factor for depolarization-induced attacks of weakness. For future direction, models are currently being built to more fully characterize the effects of channel gating defects on specific electrical behavior in the muscle. Key to refining this will be to test these point mutations in more physiological backgrounds, such as mouse models.

During these experiments, I also observed that the Q_{10} (or temperature sensitivity) of entry to slow inactivation in WT channels was over 10. This is

quite high, since typical values for channel gating transitions are around 3. The temperature dependence of slow inactivation has thus far received little attention, and this is the first known report of this unusual Q_{10} value in sodium channels. Given that a number of sodium channel-linked diseases have strong temperature dependence, this area deserves more scrutiny from a disease standpoint.

From a mechanistic standpoint, this high Q10 value provides a number of interesting experimental possibilities. As a starting point for future direction, it would be highly informative to measure temperature dependence of the kinetics of both I_M and I_S, since only I_M was tested in our study. If this Q_{10} is vastly different for the two states, this might provide a useful marker to distinguish them in mutant channels where the identity of the slow inactivated state(s) being observed is not always clear.

The mechanism of this exquisite slow inactivation temperature dependence also deserves examination in its own right, as this may help yield insights into the overall mechanism of slow inactivation. A starting point for testing this would be to measure how things that modify slow inactivation also modify its temperature dependence. For instance, the temperature dependence of slow inactivation could be assessed when fast inactivation is removed, when β-subunits are introduced, and in the context of the various external alkali cations. Perhaps this temperature sensitivity relies on one of these factors, and finding this

would assist in separating voltage-dependent and enthalpic components of movement in slow inactivation.

5.3 $\beta 1$ Subunit and Slow Inactivation

The β1 subunit has long been know to modulate channel fast gating, and it is increasingly believed that the N-terminal (external) region of β1 interacts with the channel pore region to mediate these effects. Interaction of β1 and slow inactivation, however, is poorly understood especially in mammalian cells, and the region(s) of β1 that mediate this interaction were not known. I examined the effects of adding β1 on slow inactivation gating, and which region(s) of it were responsible for these effects. The hope in doing this was to find clear, pronounced effects and then use the β1 as a tool to probe the mechanism of slow inactivation.

The results of these experiments were unequivocal, but were not as dramatic as we had hoped. I was able to establish that the N-terminus, but not the C-terminus of β1 was necessary for the disruptive effects on slow inactivation. This observation is similar to other studies showing the requirement of an intact N-terminus for modulation of fast gating. I further refined this observation by showing that the I_S component was the most affected of the two slow inactivation states. Finally, I also showed that β1 can act even in the absence of a functioning

fast gate. This indicates that the action of β1 on slow inactivation is more likely to be direct, rather than secondarily caused by coupling to other fast gating changes.

These observations add to our understanding of how β1 works, and join a large body of other evidence, including the alkali cation experiments in Chapter 4, in suggesting that the channel outer pore region is an important modulator of slow inactivation.

There were limitations to this investigation, however. Primarily, we felt that the effects on slow inactivation were too small in this case for β1 to serve as a tool for detailed probing of the slow inactivation mechanism. Had the effect been more pronounced, it might have been a useful tool to further investigate which regions of the β1 N-terminus were responsible for this effect. Other studies have shown that N-terminus of β1 may act on the sodium channel by presenting negative charges to the outer pore and altering the local electrostatic environment. It is quite possible that interaction with slow inactivation also occurs in this manner. To test this, groups of negatively charged amino acids on the surface of the N-terminus that are suspected to affect fast gating could have been neutralized to see which, if any, of these can account for this effect. Alternatively, some have proposed that β1 sialic acids may be at least partly responsible for the fast gating effects, and so removing the sialic acids and testing effects on slow inactivation

may yield additional insights. It is possible that β1 effects on slow inactivation will be more pronounced in other model systems, such as frog oocytes. There is certainly precedence for this with regard to fast gating effects. In that case, β1 may well serve as a useful tool to probe slow inactivation. But again, for our purposes of focusing on channel behavior in mammalian systems, the effect was not strong enough in this case, especially in light of the fact that we concurrently observed a much stronger effect caused by the alkali cations.

5.4 Alkali Cations and Slow Inactivation

The most insightful experiments from my work were directed at understanding the interaction between the alkali metal cations and slow inactivation. The effects of external alkali cations have served as a fundamental tool for probing the mechanism of C-type inactivation in K+ channels, and have been instrumental in identifying the likely location of the C-type gate (although this subject still remains under debate). Even though a cation effect on sodium slow inactivation was reported decades ago, surprisingly little is known about it. For the most part, the effect has simply been reported as a phenomenon, with no follow up as to where or how this effect is occurring.   In Nav1.4 channels, I initially noticed a profound effect when switching the external solutions with different alkali cations.

The results of these our studies on external cation effects suggest a highly selective slow inactivation modulatory site in the outer pore region that is above and distinct from the selectivity filter. These results again underscore the importance of the outer pore region in modulating slow inactivation. It is hoped that this initial characterization will serve as a foundation for future experiments detailing the nature of this binding site and how it mechanistically relates to the slow inactivation process.

For future work, it would be of great interest to examine the cation effect on specifically on the I_S component, since this work focused on the I_M state. Measuring I_S will certainly be more difficult, as it takes much longer duration conditioning pulses to induce this state. It would be highly informative, however, to know whether both slow inactivated states respond to alkali cations in this manner. If the response is different, this would be another tool to mechanistically separate the two states.

It would also be of great interest to expand the investigation of external cations to include the numerous organic cations. This may potentially add additional insight because of the sheer number and diversity of these molecules. A more comprehensive analysis of a large number of these compounds will define the selectivity of this slow inactivation modulatory site, in a similar strategy to the older experiments that surveyed these compounds to define the inner and outer vestibule as well as the channel selectivity filter.

Mutational analysis of the outer pore showed that numerous residues from all four channel domains can alter the influence of external cations on slow inactivation. This suggests that the interaction between cations and slow inactivation may involve coordinated actions from multiple domains, and not a simply binding event to a specific residue. Moreover, given the stringent selectivity of this interaction site, it seems likely that this binding is not the result of a simple electrostatic interaction with a charged residue in the pore, but is a highly interactive process much like ion selectivity through the pore.

It has taken many years and many laboratories to characterize the interaction of alkali cations and K^+ channels, and the work is far from over. It is probable that the road ahead in sodium channels is equally long, but certainly equally interesting.

5.3   *References:*

Cannon, S.C. 2006. Pathomechanisms in channelopathies of skeletal muscle and brain. *Annual review of neuroscience*. 29:387-415.